Dissertation zur Erlangung des Doktorgrades

der Fakultät für Chemie und Pharmazie

der Ludwig-Maximilians-Universität München

Stress inducible glycosyltransferases in *Arabidopsis thaliana* and their impact on plant metabolism and defense mechanisms

Veronica von Saint Paul

aus

Bad Harzburg

2010

Erklärung

Diese Dissertation wurde im Sinne von § 13 Abs. 3 bzw. 4 der Promotionsordnung vom 29. Januar 1998 von PD Dr. Anton R. Schäffner betreut.

Ehrenwörtliche Versicherung

Diese Dissertation wurde selbstständig, ohne unerlaubte Hilfe erarbeitet

München, am 10.10.2010

(Veronica v. Saint Paul)

Dissertation eingereicht am 21.10.2010

1. Gutacher PD Dr. Anton R. Schäffner

2. Gutachter Prof. Dr. Patrick Cramer

Mündliche Prüfung am 20.12.2010

ABSTRACT

Small molecule glycosylation in plants is crucial for the biosynthesis of secondary metabolites and the regulation of the activity of several signaling molecules and defense compounds. One hundred and twenty-two different UDP-dependent glycosyltransferases (UGTs) catalyzing these conjugations exist in the model plant *Arabidopsis thaliana*. Despite major advances in plant biology due to genome annotations and 'omics' approaches, the vast majority are still uncharacterized enzymes without known specific substrates and physiological roles. In this project, the role of UGTs in plant stress response was investigated focusing on top stress responsive candidate genes. Transcriptional responsiveness of all UGT members of *Arabidopsis* was analyzed using publicly available expression data of plants exposed to several abiotic and biotic stress cues. A clear clustering of stress-dependent inductions was observed highlighting several highly responsive *UGT* genes with yet unknown function. The two top-ranking stress-induced and previously uncharacterized glucosyltransferases *UGT76B1* and *UGT87A2* were selected for further functional characterization. Both are broadly up-regulated by abiotic as well as biotic cues, suggesting an important stress related role. Using a reverse genetics approach (knockout and overexpression lines) metabolic and phenotypic changes correlating with the expression of the corresponding *UGT* gene were analyzed.

In the case of *UGT87A2*, plants with altered *UGT* expression did not reveal any obvious phenotypes even when several stress cues were applied. Non-targeted FT-ICR-MS analyses in the negative mode of two knockout lines did not reveal significant metabolic changes, whereas independent overexpression lines showed several m/z peaks indicating up-regulated metabolites. Further characterization of these compounds led to the identification of a new metabolite in *Arabidopsis*, ascorbic acid 2-O-ß-glucoside. Together with the upregulation of other putative compounds, the results suggest potential roles for *UGT87A2* in ascorbic acid homeostasis or cell wall biosynthesis.

UGT76B1 was identified as a novel player in plant defense affecting the antagonistic salicylic acid and jasmonate-dependent signaling pathways. Loss of the *UGT76B1* function led to enhanced resistance to hemibiotrophic pathogens and accelerated senescence. This was accompanied by constitutively elevated SA levels and SA-related marker gene expression and repression of JA-dependent marker genes. The overexpression caused the opposite phenotypes. UGT76B1 therefore attenuates SA-dependent plant defense in the absence of infection, promotes JA response and suppresses the onset of senescence. Non-targeted metabolomic analyses of *ugt76b1* knockout and *UGT76B1*-OE lines using ultra-high

resolution Fourier-transform ion cyclotron mass spectrometry led to an unprecedented *ab initio* substrate identification. *In vitro* assays employing the recombinant enzyme confirmed isoleucic acid (2-hydroxy-3-methyl-pentanoic acid) as the UGT76B1 substrate. The findings indicate a novel link of amino acid-related molecules to plant pathogen defense pathways via small-molecule glucosylation.

Together these findings emphasize the importance of plant secondary metabolite UGTs in plant defense mechanisms and provide a foundation for a detailed understanding of their role in plant stress response. Further, the results presented highlight the great potential of using high resolution metabolomic analysis for non-targeted screening plant mutants to identify new metabolites and reveal novel gene functions without any other prior knowledge.

CONTENTS

ABBREVIATIONS

ABA	Abscisic acid
A. thaliana	*Arabidopsis thaliana*
AA	Ascorbic acid
AA-2G	Ascorbic acid-2-O-α-glucoside
AGI	*Arabidopsis* Genome Initiative
CAZy database	Carbohydrate-Active Enzyme database
cDNA	complementary DNA
CTAB	Cetyltrimethylammonium bromide
d	day
ddH2O	double distilled water
DEPC	Diethylpyrocarbonate
DMSO	Dimethyl sulfoxide
DNA	Deoxyribonucleic Acid
dNTPs	Deoxynucleotide-5'-triphosphates
DTT	Dithiothreitol
E. coli	*Escherichia coli*
EDTA	Ethylene Diamine Tetra-acetic Acid
FT-ICR-MS	Fourier transform ion cyclotron resonance mass spectrometry
GFP	Green Fluorescent Protein
GST	Glutathione-S-transferase
GT	glycosyltransferase
GUS	β-Glucuronidase
h	hour
ILA	Isoleucic acid
ILE	Isoleucine
JA	Jasmonic acid
kb	Kilo base pair
kDa	KiloDalton

MeJA	Methyl jasmonate
min	minute
MS	Murashige and Skoog
NASC	Nottingham *Arabidopsis* Stock Center
NDP	nucleoside diphosphate
OE	overexpression
PCR	Polymerase chain reaction
Ps-vir	*Pseudomonas syringae pv tomato* DC3000
Ps-avir	*Pseudomonas syringae* (avrRpt2)
PSPG-Box	Plant Secondary Product Glycosyltransferase (PSPG)-Box
RNA	Ribonucleic Acid
rpm	revolutions per minute
RT-PCR	Reverse Transcription-PCR
RT-qPCR	Real-time quantitative PCR
SA	Salicylic acid
SAG	Salicylic acid 2-O-β-D-glucose
SD	Standard Deviation
SDS	Sodium Dodecyl Sulfate
SE	Standard Error
SGE	SA glucose ester
TAE	Tris-Acetate-EDTA
T-DNA	Transfer-DNA
UDP	Uridine diphosphate
UGT	UDP-dependent glycosyltransferase
v/v	volume per volume
w/v	weight per volume
wt	wild type
X-Gluc	5-Bromo-4-chloro-3-indolyl-β-D-glucuronic acid

FIGURES AND TABLES

FIGURES

TABLES

SUPPLEMENTAL MATERIAL

Supplemental Figures

Supplemental Tables (Non-targeted metabolome analyses)

1. INTRODUCTION

1.1.   PLANT SECONDARY METABOLITE GLYCOSYLTRANSFERASES

1.1.1.   General overview and importance

Approximately two-thirds of the carbon in the biosphere exists as carbohydrate (Sinnot, 1990) and the transfer of glucose is quantitatively the most important biotransformation on earth (Campbell et al., 1997). Glycosyltransferases, which catalyze the transfer of a sugar residue from an activated donor to an acceptor molecule, are found in all living organisms. Since plants, in contrast to animals, are sessile organisms and cannot move away from adverse environmental conditions they need to adapt themselves to environmental stresses. Therefore they have evolved distinct mechanisms by which tolerance against these stresses can be achieved, including a huge range of small molecule compounds active in defense and signaling. Plant secondary metabolite glycosyltransferases (UGTs) play an important role in this adaptation (Figure 1), as glycosylation changes the stability, solubility and biological activity of such small molecules and creates a high diversity of different kinds of plant metabolites. They are crucial for the biosynthesis of secondary metabolites and the regulation of the activity of several signaling molecules and defense compounds and they also play a significant role in the detoxification and compartmentation of endogenous compounds and xenobiotics (Jones and Vogt, 2001). The huge diversity of plant secondary metabolites is especially attractive for human exploitation. Several pharmaceuticals and food additives are based on plant chemical structures because of the antimicrobial, antioxidative and anticancerigenic nature of several of these natural compounds. The use of recombinant glycosyltransferases could also have interesting industrial applications, providing a unique toolbox for the specific design of modified natural products. Finally, UGTs are suitable candidates to improve food or crop quality and a better understanding of their *in vivo* function could have interesting prospects for plant metabolic engineering. Despite major advances in plant biology due to genome annotations and omics approaches, only a few plant UGT functions could be deciphered to date. The vast majority are still orphan enzymes without known specific substrates and physiological roles, thus providing a high, still unexplored potential.

The following sections of this chapter will give a more detailed introduction on all important aspects regarding plant secondary metabolite glycosyltransferases mentioned in this short overview.

Plant glycosyltransferases

Organism and plant cell

signaling molecules and defense compounds

(Lairson 2008) *

detoxification and compartimentation

transfer of carbohydrates to **small organic metabolites**

secondary metabolites

Development and stress responses
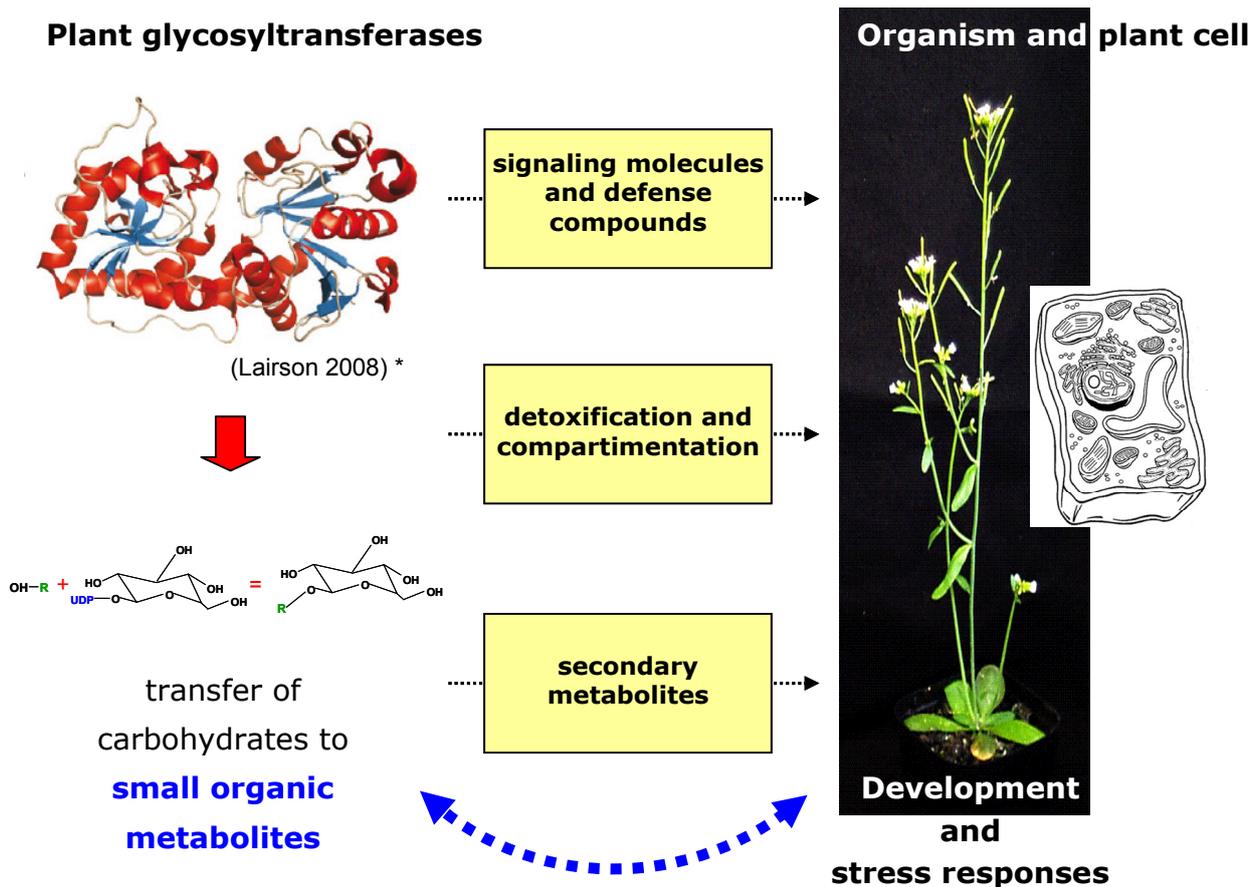
Figure 1. Functional importance of plant glycosyltransferases.

UGTs catalyze the transfer of a sugar residue from an activated donor to small organic metabolites. This glycosylation changes the stability, solubility and biological activity of such molecules, being crucial for the biosynthesis of secondary metabolites, the regulation of several small molecule compounds active in defense and signaling as well as for the detoxification and compartmentation of endogenous compounds and xenobiotics. UGT substrates are ubiquitous and have diverse functions or activities. Their glycosylation has several consequences at single cell level and for the whole plant.

*The GT-B fold UGT structure model (Lairson et al., 2008) was reprinted, with permission, from the Annual Review of Biochemistry, Volume 77 ©2008 by Annual Reviews (www.annualreviews.org)

1.1.2.   Classification

According to the International Union of Biochemistry and Molecular Biology (IUBMB) nomenclature, glycosyltransferases (GTs) belong to class EC 2.4.x.y. (Campbell et al., 1997). But there are several limitations applying this classification on GTs, as for most of these enzymes biological functions are still unknown and many of them are known to have broad substrate specificities. Therefore they are characterized into different families according to their degree of primary sequence identity (Campbell et al., 1997; Coutinho et al., 2003). To

2

date there are 92 glycosyltransferase families listed in the Carbohydrate-Active Enzyme (CAZy) database [(Cantarel et al., 2009), http://afmb.cnrs-mrs.fr/CAZY/]. This study focuses on family 1 GTs, and among these enzymes on those, which utilize a uridine diphosphate (UDP) activated sugar as donor in the glycosylation reaction, and are therefore referred to as UDP-dependent glycosyltransferases or UGTs (Mackenzie et al., 1997; Lim and Bowles, 2004). 122 different UGTs exist in the model plant *Arabidopsis thaliana*, which are classified in 14 different phylogenetic groups (Li et al., 2001; Ross et al., 2001). A UGT nomenclature was developed based on divergent evolution (Mackenzie et al., 1997). Enzymes which show more than 40% amino acid identity are grouped within the same family designed by a number, plant UGTs belong to families 71-100. Each family is further divided into different subfamilies, each of them comprising UGTs with 60% or more sequence identity described by a letter which is followed by an Arabic number assigning each single gene (Figure 2). A second nomenclature exists which is based on secondary and tertiary structure of GTs and their mechanism of catalysis (Coutinho et al., 2003). In this work the UGT nomenclature based on Mackenzie et al. (1997) was used.
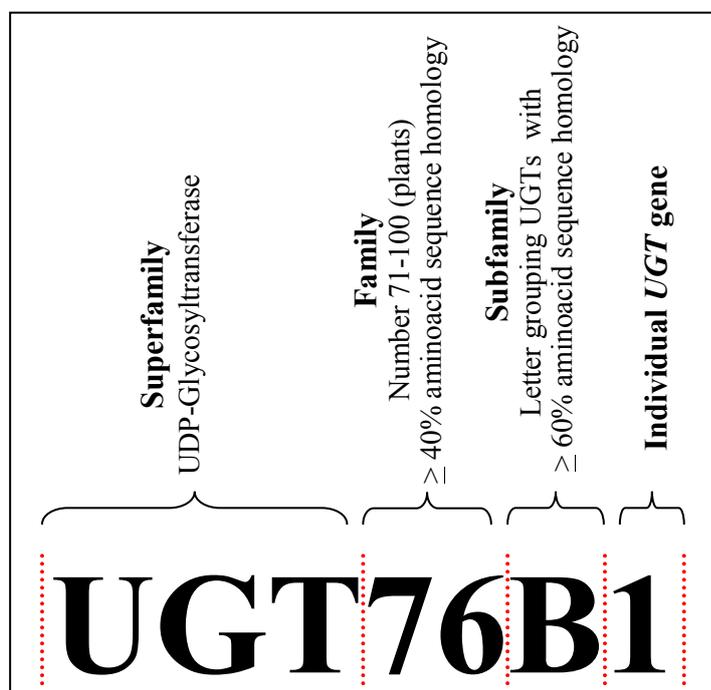
Figure 2. UGT superfamily nomenclature based on divergent evolution.

The scheme shows the current system used for UGT nomenclature based on divergent evolution (Mackenzie et al., 1997)

1.1.3. Sequence homology

Plant glycosyltransferases in general show only little sequence similarity (Vogt and Jones, 2000). However, their amino-terminal regions are more variable than the carboxy-terminal regions, which supports the suggestion that this domain might be involved in the recognition and binding of the diverse aglycon substrates. The carboxy-terminal region in contrast shows more sequence homology and was thought to be involved in binding the nucleotide sugar substrate (Lim et al., 2003). This assumption could later be confirmed by analysis of the crystal structure (Li et al., 2007) and site directed mutagenesis (Osmani et al., 2008). A highly conserved sequence was found in the C-terminal region of UGTs involved in secondary plant metabolism called Plant Secondary Product Glycosyltransferase (PSPG)-Box (Hughes, 1994). This 44 amino acid long box contains an N-terminal extension compared to the originally proposed consensus sequence for UDP-glycosyltransferases (Mackenzie et al., 1997). Database searches for sequence similarity with the PSPG motif led to the identification of more than 100 different plant GTs. In the *Arabidopsis* GT family 1, most of the GTs are UGTs, carrying the C-terminal consensus sequence except for three GTs. *UGT80A2*, *UGT81A1* and *UGT81B1* have incorporated additional residues in their PSPG motif and therefore show higher similarity to non-plant UGT sequences. They are more conserved and catalyze housekeeping functions. The UGT families containing the PSPG motif are less stable than the ones without it, since PSPG containing UGTs are putatively involved in secondary metabolism and thus subjected to recruitment for novel functions (Paquette et al., 2003).

1.1.4. Reactions catalyzed by UGTs and substrate specificity

Glycosyltransferases catalyze the transfer of a sugar residue from a donor molecule to an acceptor molecule by the formation of a glycosidic bond. They are generally perceived as unidirectional catalysts, but GTs which catalyze the reverse reaction producing the NDP-sugar, have also been characterized (Miller et al., 1999; Zhang et al., 2006; Modolo et al., 2007). Most of the sugar-transferring enzymes need an activated carbohydrate molecule as cosubstrate. This activation can be via a free phosphate, a lipid phosphate or a nucleoside phosphate (Charnock et al., 2001). NDP (Nucleosidediphosphate)-glycosyltransferases (NDP-GT) [EC 2.4.x.y.] catalyze the transfer of a sugar moiety from an activated nucleosidediphosphate to an aglycon. Nucleotide sugar-dependent glycosyltransferases are often also referred to as Leloir enzymes. Luis F. Leloir was awarded the Nobel Prize in chemistry in 1970 for discovering the first sugar nucleotide and for his enormous

contributions to our understanding of glycoside biosynthesis and sugar metabolism. UDP-glucose is the most commonly used nucleotidic sugar in plants (Ross et al., 2001). But plant UGTs also recognize other sugars or derivatives including UDP-galactose (Miller et al., 1999), UDP-xylose (Martin et al., 1999a), UDP-rhamnose (Jones et al., 2003; Frydman et al., 2004), UDP-arabinose (Yonekura-Sakakibara et al., 2008) and UDP-glucuronic acid (Sawada et al., 2005). UDP-glucuronic acid is the most common sugar derivative donor used by the mammalian UGTs (Ross et al., 2001). In general, UGTs show very high specificity for the sugar donor (Sawada et al., 2005; Shao et al., 2005; Yonekura-Sakakibara et al., 2007; Osmani et al., 2008).

The acceptor molecule can be a protein (glycoprotein), a lipid (glycolipid), a sugar (oligo-, polysaccharide) or small organic molecules. UGTs can transfer a sugar moiety to O- (OH- or COOH-), N-, S- or C atoms of the acceptor molecule, but hydroxylated forms are the most common ones (Jones and Vogt, 2001). Additionally, a broad range of different carbohydrate moieties can be transferred to one acceptor molecule leading to mono-, di-, triglycosides, etc., or bis-glycosides, which leads to a broad spectrum of possible glycosidic structures for a given aglycon.

Considering the huge number of different glycosides found in plants, high specificity would indicate the requirement for many more UGTs than actually identified (Lim and Bowles, 2004). As observed by *in vitro* glycosylation tests, most UGTs are indeed regiospecific rather than substrate-specific. Broad substrate specificity is a general characteristic of enzymes involved in ultimate steps of the biosynthesis of natural products, such as UGTs, P450s (Chapple, 1998) and methyltransferases (Frick and Kutchan, 1999). It confers plants a certain degree of flexibility and enables them to respond to rapidly changing environmental conditions or evolutionary tendencies (Vogt and Jones, 2000). Low substrate specificity could lead to problems with respect to undesired side reactions like inactivation of plant hormones. The UGT activity should therefore be under a tight control. This regulation is proposed to involve transcriptional control (Tohge et al., 2005), and incorporation of the UGTs as part of metabolons (Jorgensen et al., 2005; Nielsen et al., 2008). Both mechanisms could contribute to regulate the available set of UGTs in a spatial and temporal manner.

1.1.5.   Reaction mechanism

According to the mechanism of the catalytic reaction, which is generally conserved within a CAZy family, GTs were divided into two classes (Figure 3). The catalysis can lead either to an inversion or to the retention of the anomeric configuration of the sugar donor. In retaining

GTs (α-group), the stereochemistry of the glycosidic bond is identical with the one of the sugar donor (α→α), whereas inverting GTs (β-group) create a glycosidic bond with opposite stereochemistry to that of the sugar donor (α→β) (Coutinho et al., 2003).
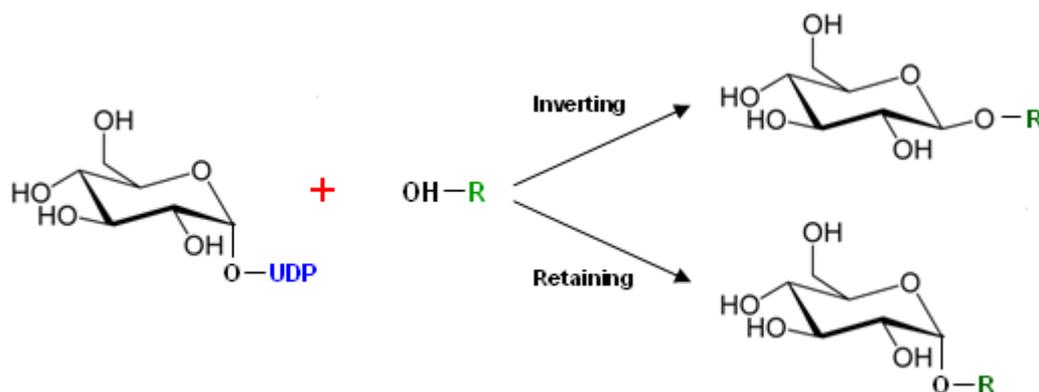
Figure 3. Reactions catalyzed by glycosyltransferases.

Glycosyltransferases catalyze the transfer of a glycosyl group with either inversion or retention of the anomeric stereochemistry with respect to the donor sugar. Plant secondary metabolite GTs (UGTs) are inverting enzymes.

1.1.6. Functions of plant secondary metabolite glycosyltransferases

1.1.6.1. Glycosylation of secondary metabolites

Plants are capable of synthesizing several thousands of different low molecular weight compounds or so called "secondary metabolites". These are organic compounds that are not directly involved in the normal growth, development, or reproduction of organisms and that are not absolutely required for the survival of the organism. The extremely high diversity of secondary metabolites found to date might be necessary for the plants to be able to respond to a continuously changing environment to which they are exposed due to their sedentary life style (Bowles et al., 2006).

Each plant family, genus, and species produces a characteristic mix of secondary metabolites which can therefore sometimes also be a useful taxonomic tool. Glycosylation is a prominent modification reaction and is often the last step in the biosynthesis of natural compounds. Other modifications which contribute to the high variety and complexity of plant secondary metabolites are carboxylation, methylation and hydroxylation (Jones and Vogt, 2001). Glycosides of a huge group of secondary metabolites such as phenolics, terpenoids, alkaloids (e.g. betalains), thiohydroximates (glucosinolate precursors), cyanohydrins (cyanogenic

6

glycoside precursors) and steroids could be identified (Vogt and Jones, 2000). Flavonoids, for example, are a huge and diverse group of plant natural products which often exist in glycosylated forms. Approximately 9000 different flavonoids have already been reported from plant sources (Williams and Grayer, 2004). In addition to their UV-protective function, evidence suggests that flavonoids are also involved in plant development such as for example pollen fertility in petunia and maize (Mo et al., 1992) or auxin transport (Peer and Murphy, 2007). Among the flavonoids, anthocyanins, the glucosides of anthocyanidins, are the major flower pigments in higher plants. They are water-soluble and may appear red, purple, or blue according to the vacuolar pH (Mol et al., 1998). 1-O-sinapoylglucose, a compound derived from the phenylpropanoid pathway (in members of the Brassicaceae family), is an intermediate in the synthesis of sinapoylmalate, a putative ultraviolet protectant in foliar tissue (Bowles et al., 2006). Glucosinolates, which are found almost exclusively in the Brassicaceae family, are compounds derived from glucose and an amino acid. They are stored in the plant vacuole, upon tissue damage they come in contact with enzymes which convert them to compounds responsible for the bitter or sharp taste of many common foods. In addition to their roles in plant defense against herbivores they have also been shown to have fungicidal and bactericidal as well as cancer chemoprotective attributes (Fahey et al., 2001). These are only few examples of the huge array of glycosidic secondary metabolites synthesized by plants.

Glycosylation not only plays an important role in the biosynthesis of secondary metabolites, it also alters the physical and chemical properties of the small acceptor molecules and their movement within the cell. The covalent bonding of sugar residues to the nucleophilic parts of organic molecules leads to reduced reactivity, toxicity and/or higher stability of the acceptor molecules or converts them into more stable storage forms (Jones and Vogt, 2001). The addition of sugar moieties to small hydrophobic molecules also increases the polarity and thereby the water solubility of the resulting compound. This inhibits the free diffusion through lipidic membranes thereby influencing cellular compartmentation and regulating the local concentration of metabolites (Lim and Bowles, 2004). Aromatic compounds such as for example vanillin are stored as a bitter glycoside in the vacuole and released through the action of endogenous glycosidases during the ripening process (Prince and Gunson, 1994). Glycosylation of cyanogenic compounds avoids their spontaneous hydrolysis which releases toxic hydrogen cyanide (Poulton, 1988; Jones et al., 1999). Saponins are terpene glucosides with antifungal properties. Removal of their sugar residues results in loss of bioactivity

(Osbourn, 2003). Another example is the reduced toxicity of the glycosylated form of the alkaloid solanidin from *Solanum tuberosom* (Moehs et al., 1997).

Glycosylation usually leads to stabilization and inactivation, but cases are known, where addition of the sugar residue also leads to activated conjugates which are highly energetic compounds and biosynthetic intermediates. This has primarily been demonstrated with 1-O-sinapoylglucose, a high-energy glucose ester, which is used as an activated sinapate donor in the synthesis of sinapoylmalate and sinapoylcholine in the Brassicaceae family (Bowles et al., 2006).

In addition to sugar conjugation, hydrolysis is another important and complementary part of glycoside metabolism (Warzecha et al., 1999; Cicek et al., 2000). The hydrolysis of the glycosides by beta-glucosidases leads to the fast delivery of the (usually active) aglycon.

1.1.6.2.   Regulation of plant hormones

Control of hormone homeostasis is crucial to enable rapid adaptation of plants to continuously changing external environments. Therefore, a wide range of mechanisms, including glycosylation, have evolved to precisely control the levels and compartmentation of different active hormones in plant cells and tissues.

Depending on the individual hormone, glycosylation can be either reversible (most hormone glycosides) or irreversible [e.g. 7-N- and 9-N-glucosilation of cytokinins (Hou et al., 2004)] and glycoside conjugates have bioactivities different from the free forms of the hormones. Glycosylation of plant hormones or their precursors is an important issue in the regulation of related defense pathways. All classical hormones with the exception of ethylene occur as glycosides *in planta* (Bowles et al., 2006). Many other mechanisms regulating hormone activity exist and also other conjugation forms including for example amides or fatty acid esters.

The first glycosyltransferase glucosylating the plant hormone indole acetic acid (IAA) was cloned from maize (Szerszen et al., 1994). Later *UGT84B1*, showing high IAA glucosylating activity, was isolated from *Arabidopsis* (Jackson et al., 2001).

Glycosylation of cytokinins involves O-glucosylation, O-xylosylation, and N-glucosylation (Mok and Mok, 2001). Zeatin is the most common cytokinin, its glucosides are transport and storage forms which are protected from enzymatic digestion. Zeatin glycosylating enzymes have been identified from several plant species (Martin et al., 1999a, b; Mok et al., 2000; Martin et al., 2001). UGT76C1 and UGT76C2 from *Arabidopsis* are able to form N- and O-

glucoside conjugates *in vitro*. UGT76C1 function towards cytokinins *in vivo* was confirmed in transgenic plants with constitutive overexpression (Hou et al., 2004).

Abscisic acid glucose ester is the most abundant conjugate of the plant hormone abscisic acid (ABA), but several other glycosides of ABA have been identified in many plant species (Nambara and Marion-Poll, 2005). The *Arabidopsis thaliana* genome contains eight sequences coding for UGTs able to glycosylate abscicic acid. One of them, UGT71B6, showed enantioselective glucosylation only towards the naturally occurring cis-S-(+)-ABA *in vitro* (Lim et al., 2005). The same protein was also shown to be able to glucosylate a wide range of ABA analogues *in vitro* (Priest et al., 2005).

Several brassinosteroid glycosides have also been identified in plants (Fujioka and Yokota, 2003; Bajguz, 2007). The only glycosyltransferase able to glycosylate brassinosteroids was found in *Arabidopsis thaliana* (Poppenberger et al., 2005). *UGT73C5* catalyzes 23-O-glucosylation of the brassinosteroid brassinolide and its biosynthetic precursor castasterone. Studies using overexpression and knockout lines confirmed that *UGT73C5* is involved in brassinolide glucosylation *in planta*. Interestingly the same gene has been shown to be able to glycosylate a fungal toxin (Poppenberger et al., 2003), which suggests that *UGT73C5* may play a dual role in the plant glycosylating endogenous and exogenous acceptors.

Salicylic as well as jasmonic acid are two other important plant hormones, the activity of which seems to be regulated by conjugation. As both are key players in plant defense reactions, they will be further described in the next section.

1.1.6.3.   Involvement in plant defense and detoxification of endogenous and exogenous compounds

Plants have to defend themselves continuously against a host of different unfavorable environmental conditions. These can be abiotic stress cues such as drought, heat, cold or oxidative stress as well as biotic stress factors such as herbivore attack, bacterial or fungal infections. Several UGTs are highly inducible by both abiotic as well as biotic stress factors (Mazel and Levine, 2002; Langlois-Meurinne et al., 2005; Meissner et al., 2008), indicating an important stress related function.

Accordingly, changed expression of candidate *UGT* genes led to an altered defense response in several cases. Langlois-Meurinne et al. (2005), for example, reported two *ugt* knockout mutants with decreased resistance towards the hemibiotrophic pathogen *Pseudomonas syringae*. Scopoletin is a phytoalexin that accumulates in abundance during the hypersensitive response to block the spreading of tobacco mosaic virus; it is known to be glycosylated in

tobacco through the UGT TOGT. Downregulation of TOGT led to increased oxidative stress, whereas overexpression in plants resulted in precocious lesion formation during the hypersensitive response to tobacco mosaic virus (Chong et al., 2002; Gachon et al., 2004). Overexpression of *UGT74F2* led to increased susceptibility to the hemibiotrophic pathogen *Pseudomonas syringae,* caused by reduced salicylic acid and its glucoside levels (Song et al., 2008).

Salicylic acid (2-O-hydroxybenzoic acid) is an important signal molecule in plant development and defense. Two glucosylated forms have been identified in plant species: the glucose ester and the 2-O-glucoside (reviewed in Vlot et al. (2009)). Both the conjugated and the free form are increased upon pathogen infection. An *in vitro* screening of several recombinant UGTs from *Arabidopsis* revealed two proteins which were active against salicylic acid (SA) and benzoic acid (Lim et al., 2002). UGT74F1 formed only SA 2-O-β-D-glucose (SAG), while UGT74F2 forms both SAG and the SA glucose ester (SGE). Using mutant *Arabidopsis* plants it could be shown that changes in the activity of either *UGT74F1* or *UGT74F2* can have a dramatic effect on the *in vivo* metabolism of exogenously supplied SA (Dean and Delaney, 2008).

Jasmonic acid is another important plant hormone involved in plant defense against herbivores (wounding) and necrotrophic pathogens (Wasternack, 2007). One *Arabidopsis* GT (UGT74D1) recognized JA *in vitro*, but it also showed significant activity towards other substrates (Song, 2005). Additionally, a jasmonic acid glucoside was found to accumulate in wounded leaf extracts of *Arabidopsis thaliana* (Glauser et al., 2010). This further supports the importance of plant UGTs in hormone regulation and plant pathogen interactions.

As already mentioned in section 1.1.6.1, glycosides can also serve as storage forms of for example toxic antimicrobial compounds or insect repellents which can be rapidly delivered by the plant in case of pathogen attack (Chong et al., 2002). Plants are not only able to glycosylate their own endogenous compounds but also a broad range of foreign compounds originating from other organisms or man-made chemicals, known as xenobiotics (Pflugmacher and Sandermann, 1998; Jones and Vogt, 2001). After inactivation and solubilization through glycosylation, toxic compounds are stored and accumulated in the vacuole and apoplastic space with a low turnover rate (Bowles et al., 2006).

Invading pests and pathogens use a wide repertoire of mechanisms in their struggle to overcome plant defenses, including the production and secretion of toxins into the cells of the plant being invaded (Jones and Dangl, 2006). Glycosylation is a crucial defense mechanism of plants to protect themselves against the huge range of toxic compounds released by their

attackers. The relatively low substrate specificity of UGTs is an important point in order to offer a flexible repertoire of defenses against rapidly evolving invading mechanisms. Several publications showed clear evidence that several fungal toxins can be modified and inactivated *in planta* (Karlovsky, 1999; Pedras et al., 2001). *Sinapis alba* for example is able to hydroxylate and glycosylate destructin B, a toxin produced by *Alternaria brassicae*, and simultaneously activate the production of phytoalexins which makes the plant species resistant to the blackspot fungus (Pedras et al., 2001). Plant pathogenic fungi of the genus *Fusarium* cause agriculturally important diseases of small grain cereals and maize. It produces trichothecene deoxynivalenol (DON), a harmful mycotoxin, if present in food or feed products. *UGT73C5* from *Arabidopsis thaliana* has been shown to recognize and detoxify this fungal toxin (Poppenberger et al., 2003). The recombinant UGT catalyzed the formation of DON-3-O-glucoside in yeast cells and, when overexpressed in transgenic *Arabidopsis*, conferred enhanced tolerance to DON.

Extensive literature is also available on the ability of plants to detoxify non-natural chemical compounds in their environments. Screens of recombinant UGT activities revealed several exogenous chemical compounds which were shown to be glycosylated by plant UGTs (Taguchi et al., 2001; Hefner et al., 2002; Messner et al., 2003), and partial purification of UGT activities towards several xenobiotics has also been described (Brazier et al., 2002, 2003; Lao et al., 2003; Loutre et al., 2003). Finally, the conjugating activity of one enzyme, UGT72B1, towards 3,4-dichloroaniline could also be confirmed *in vivo* using a reverse genetics approach (Brazier-Hicks and Edwards, 2005).

In addition to their functions during plant pathogen interactions and detoxification, resistance towards several abiotic stressors is also influenced by *UGT* expression. Ectopic overexpression of *UGT74E2* for example, led to improved survival during drought and salt stress in *Arabidopsis* through its activity toward the auxin indole-3-butyric acid (Tognetti et al., 2010). Loss-of-function mutations in *UGT73B1*, *UGT73B2*, or *UGT73B3* (tandemly clustered flavonoid *UGT*s) enhanced plant resistance to oxidative stress (Lim et al., 2006). Loss of *UGT71C1* function in *Arabidopsis* led to increased tolerance to methyl viologen, also indicating a role in oxidative stress response (Lim 2008).

1.1.7. Potential applications of plant glycosyltransferases

1.1.7.1. Industrial applications

By stabilizing and solubilizing compounds and improving the pharmacological properties of drug molecules, such as absorption, distribution, metabolism as well as excretion (ADME properties), glycosylation has important implementation in the pharmaceutical as well as in the food industry (Weymouth-Wilson, 1997; Ahmed et al., 2006). Ascorbic acid-2-O-α-glucoside (AA-2G), for example, is widely used in both the pharmaceutical and the food industry as a stable antioxidant additive compared to its free form which is rapidly oxidized (Mandai et al., 1992). Pure chemical synthesis of complex sugar-containing natural products is still a difficult and costly task. Stepwise chemical glycosylation involves long synthetic schemes and appropriate blocking reagents to protect other reactive sites on the molecule which must be removed afterwards. The use of UGTs for direct glycosylation of natural compounds is therefore an attractive and simple alternative. Especially their ability to accept a wide range of acceptors and to glycosylate them in a regioselective manner makes them attractive candidates for industrial use in addition to their *in planta* function.

Additionally, the stereoselectivity of GTs is a valuable attribute which has been exploited in the chiral separation of (+)-ABA from (±)-ABA using a whole-cell biocatalysis system (Lim et al., 2005). The ability of some UGTs to catalyze both glycosylation and deglycosylation reactions (Zhang et al., 2006; Modolo et al., 2007) can also have interesting applications for the synthesis of activated sugars.

1.1.7.2. Plant metabolic engineering

In addition to their applications in the field of biocatalysis, a deeper understanding of plant UGT functions can be of great interest for metabolic engineering of crop plants. The ability of UGTs to conjugate toxic xenobiotics such as herbicides or human drugs in addition makes them suitable targets for phytoremediation purposes. Enzymes involved in mechanisms that help the plant to protect itself against abiotic and biotic stress factors could be targets for genetic engineering to improve plant tolerance to unfavorable conditions and product yield. Several *UGT*-encoding genes could as well be suitable candidates to be inserted into a variety of plants with the aim of improving food or crop quality. Dhurrin for example is a tyrosine-derived cyanogenic glucoside from *Sorghum bicolor* which confers resistance to the flea beetle *Phyllotreta nemorum*, a natural pest of several members of the crucifer group. Inserting

12

the entire pathway for dhurrin biosynthesis (*CYP79A1*, *CYP71E1* and *UGT85B1*) from *Sorghum bicolor* into *Arabidopsis thaliana* led to increased *Phyllotreta* resistance (Tattersall et al., 2001). Further work demonstrated that dhurrin accumulation could be achieved with only marginal inadvertent effects on plant morphology, free amino acid pools, transcriptome, and metabolome (Kristensen et al., 2005). Insertion of the glycosyltransferase from *Sorghum* was essential, as none of the *UGT*s from *A. thaliana* was capable of converting the aglycon p-hydroxymandelonitrile into the corresponding cyanogenic glucoside *in planta*.

1.1.8.   Approaches to UGT identification and functional analysis

Although the annotation of an encoded enzyme e.g. as a UGT most probably denotes its activity as a transferase of an activated sugar to small-molecule acceptors, this knowledge does not provide a clue towards its native substrate(s), not to mention its in vivo function. Considerable advances in plant biology already led to the elucidation of several UGT functions (1.1.6), but the vast majority of UGT isoforms still remain 'orphan' enzymes.

The first plant UGT-encoding gene was unexpectedly identified by Nobel laureate Barbara McClintock who discovered the genetic instability of transposons in maize. She studied the dark pigmentation of maize grains conferred by the mutation of Bronze1, which later turned out to encode a flavonoid UGT (Dooner and Nelson, 1977). The corresponding gene was cloned through the transposon tag from maize (Fedoroff et al., 1984).

As a more systematic approach, the direct purification and characterization of proteins was the only method available in the ´premolecular´ age to characterize and differentiate individual GTs. Purification has been achieved by a combination of anion exchange, hydrophobic interaction, and dye ligand chromatography (Vogt and Jones, 2000). Once the proteins are purified, their enzyme activities toward glycosylation of specific substrates can be investigated and the corresponding genes can be cloned by the derived nucleotide sequences from the amino acids. An example of a successful isolation and partial protein sequencing using the classical biochemical methods is the 1,2 rhamnosyltransferase, a key enzyme in the biosynthesis of the bitter flavonoids of citrus (Frydman et al., 2004).

But the purification and characterization of proteins directly from plants is a difficult task and the progress on their identification and characterization is relatively slow. Often the proteins are of low abundance, and purification to homogeneity is difficult to achieve. Accordingly, much data was obtained with partially purified enzymes which could lead to erroneous assumptions on substrate specificities due to contamination with other enzymes. Additionally, UGTs are generally labile, which further renders their purification difficult (Chapple, 1998).

The development of genomics and bioinformatics greatly facilitated the identification of plant GTs. The PSPG-box consensus sequence provided a good starting point for searching new putative glycosyltransferases from databases and characterizing the new enzymes through expression in heterologous systems. Furthermore, based on the conserved amino acid sequence of GTs, degenerate primers could be designed in order to clone new putative enzyme candidates. This technique led to the identification of several GTs from different plant sources (Ford et al., 1998; Moraga et al., 2004; Masada et al., 2009). Whole genome sequencing of the model plant *Arabidopsis thaliana* (The-*Arabidopsis*-Genome-Initiative, 2000) finally identified a very large UGT superfamily and opened new opportunities for phylogenetic analysis of higher plant UGTs (Li et al., 2001), as well as a basis for a further better understanding of structure-function relationships. Additionally, the huge abundance of publicly available microarray expression data provides a vast amount of information that has been exploited only sparsely to date. Extensive analysis of gene (co-) expression and stress inducibility might lead towards novel hypotheses regarding biochemical and biological functions of UGTs, as already shown in other cases (Ehlting et al., 2008). New assumptions on potential functions can then be addressed by experimental approaches.

The identification of *in vitro* substrate specificity of an enzyme alone does not give a clear conclusion about the true biological function of this particular enzyme. Several aspects have to be considered which could influence substrate specificity in the *in vivo* system and broad substrate specificity *in vitro* does not necessarily mean the enzyme accepts the same range of substrates *in planta*. Regulation of gene expression, substrate availability and possible involvement in multienzymatic complexes may have a drastic influence on enzyme activity *in vivo* (Winkel-Shirley, 1999; Jones and Vogt, 2001; Ross et al., 2001). Competition between different enzymes for the same substrate may also play an important role *in planta* (Bowles et al., 2005). Therefore, the use of loss-of-function mutants and overexpression lines is a common and important tool for functional gene analysis. Phenotypic analyses of metabolite pool perturbation can be analyzed by up- and downregulation of gene expression in transgenic plants. Approaches are also necessary which integrate available *in vitro* data with the corresponding metabolite and transcript profiles (Achnine et al., 2005; Tohge et al., 2005). Integration of metabolite profiling with independent evidence, in particular of transcriptional co-expression and comparative genomics, has strongly facilitated the elucidation of metabolic pathways and assignment of enzymatic activities (Hirai et al., 2005; Yonekura-Sakakibara et al., 2008; Matsuda et al., 2009; Ohta et al., 2010). The fast development of improved techniques for high-throughput metabolomic analysis greatly increases the potential for rapid

and large scale non-targeted screening of similarities and dissimilarities in plant mutant populations and will hopefully help us to gain new insights into the precise biological roles of plant secondary product glycosyltransferases.

1.2.   AIM OF THIS WORK

The goal of this work was to further our understanding of the role of plant secondary metabolism glycosyltransferases in plant responses to environmental stresses.

As a starting point, a study of publicly available microarray-based expression data of *UGT* stress responses should reveal the distribution of stress inducibility throughout the whole *UGT* family of *Arabidopsis thaliana* and point out highly stress responsive genes as a criterion to select them as candidate genes for further functional analysis.

Molecular genetic approaches (loss-of function mutants, ectopic overexpression, and expression patterns) and phenotypic characterization (including abiotic and biotic challenges) were combined with non-targeted metabolome analyses employing ultra-high resolution FT-ICR mass spectrometry. This strategy aimed at obtaining information on the affected pathway and physiological function and at possibly identifying *in vivo* substrate(s) without any other prior knowledge apart from the broad stress inducibility of the candidate *UGT* genes.

2. *UGT* STRESS INDUCTION ANALYSIS AND SELECTION OF CANDIDATE GENES

In order to analyze the distribution of transcriptional responses to exogenous stresses within the *Arabidopsis thaliana UGT* genes and to select highly responsive candidate genes for further functional analysis, public expression data of plants exposed to several abiotic and biotic stress cues were examined. 120 *UGT* genes with corresponding AGI locus identifiers were extracted from the CAZy database. 119 of them were found to be represented on the ATH1 microarray represented by a total of 112 different probe sets. 105 *UGT* genes are represented by gene-specific probes, while seven hybridize to two highly related genes each. Normalized expression data from Columbia wild-type leaves or seedlings were retrieved from the BAR database (bbc.botany.utoronto.ca; Toufighi et al. 2005).

A large group of *UGT* genes was induced in one or several experiments, but stress responsiveness was not equally distributed across the genes analyzed. In both abiotic and biotic stress experiments a clear clustering of stress-dependent induction was observed (Figure 4A; Methods). Forty percent of all analyzed *UGT* representing probe sets accounted for 75% of the significant stress dependent upregulations. Individual members of almost all phylogenetic groups (Ross et al., 2001) evolved towards stress inducibility (Figure 4B). Some clustering of stress responsiveness could be observed for Group D which is thought to be involved in stress responses caused by exposure to pathogens, hydrogen peroxide and salicylic acid (Langlois-Meurinne et al., 2005).

Most of the top-ranking genes induced by abiotic stress cues also appear among the top pathogen induced candidates. It is known that abiotic and biotic stresses regulate different but overlapping sets of genes. Reactive oxygen species for example play an important role at the point of convergence between abiotic and biotic stress response pathways (Fujita et al., 2006). A further example is a cis element involved in rapid wound response which was also found in several genes as well by both abiotic and biotic stress cues (Walley et al., 2007), indicating a general overlap between genes induced by biotic as well as abiotic stress cues. Consistently, most of the *UGTs* highly responsive to oxidative stress and wounding are also found among the top pathogen-responsive genes.

Some of the *UGTs* which turned out to be broadly stress-responsive were already known to be functionally related to plant stress responses. UGT76E12 and UGT71B8 for example are both able to glycosylate quercetin, an important antioxidative compound in plants, *in vitro* (Lim et

al., 2004). *UGT73B3* and *UGT73B5* seem to be important for plant defense response as shown by the decreased resistance to *Pseudomonas* infection in the corresponding knockout mutants (Langlois-Meurinne et al., 2005). UGT74F2 glycosylates salicylic acid, one of the most important defense related hormones *in planta* (Dean and Delaney, 2008; Song et al., 2008). UGT84B1 showed high activity towards the auxin indole-3-acetic acid *in vitro* (Jackson et al., 2001) and when constitutively overexpressed *in planta*, UGT84B1 was shown to be able to disturb IAA homeostasis (Jackson et al., 2002). Other UGTs, listed among the top 20 stress-induced candidates were shown to glycosylate other plant hormones *in vitro* (UGT73C1/2 and UGT85A1: cytokinins (Hou et al., 2004); UGT71B6: ABA (Lim et al., 2005)). It is not surprising that genes related to hormone metabolism show strong responses to both biotic and abiotic challenge, as plant hormones are known to play important roles in responses towards both pathogen challenge as well as resistance to environmental stresses.

Several genes show neither strong biotic nor abiotic induction (Figure 4A). Genes belonging to this group might have housekeeping functions or might be developmentally regulated rather than stress-dependent. In this cluster, for example, members of the subgroups *UGT80* and *UGT81* can be found which show higher sequence similarity to non plant *UGTs* and code for housekeeping genes involved in plant lipid biosynthesis (Paquette et al., 2003). Another example is *UGT74C1* which is proposed to be involved in developmentally regulated rather than stress-induced glucosinolate biosynthesis (Petersen et al., 2002; Gachon et al., 2005).

The functions of most *UGTs* which are highly responsive to abiotic and biotic stress cues still remain unknown.

As shown in Figure 4, *UGT76B1* and *UGT87A2* are the two top stress-induced candidates. Both genes are broadly responsive to biotrophic and necrotrophic pathogens as well as to several abiotic stress cues such as UV-B, wounding, oxidative and osmotic stress. However, nothing was known about their function or any involvement in plant stress response. A functional characterization of these interesting candidates using a genetic approach will be described in this work.

18

A
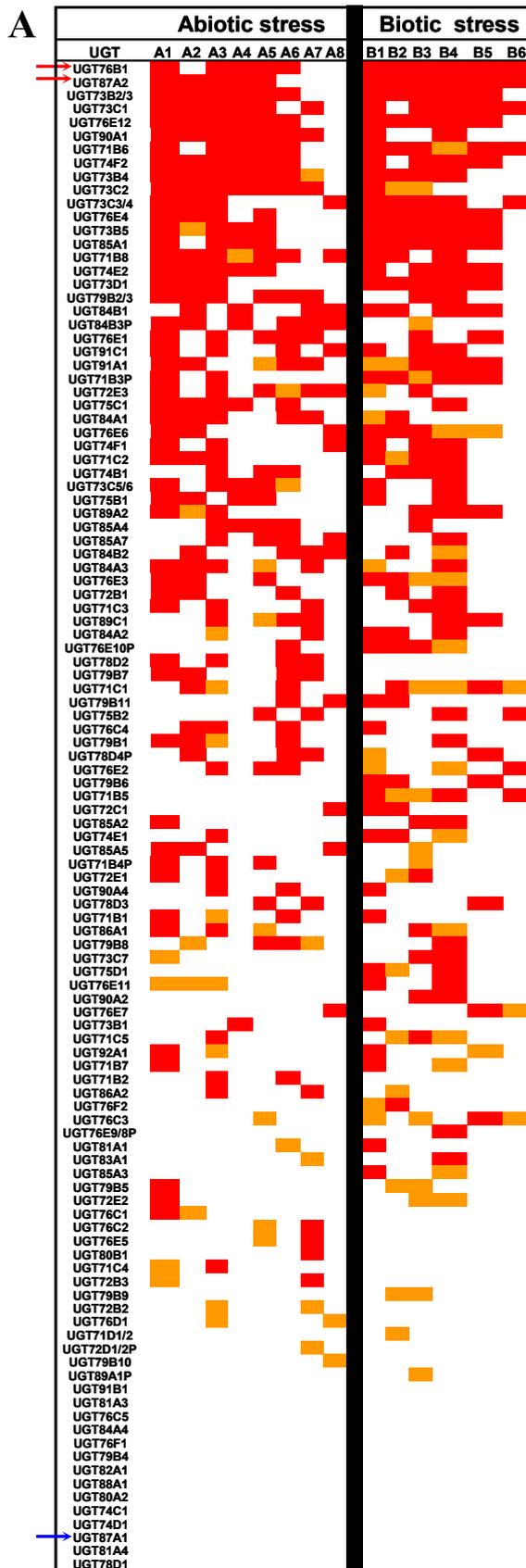
Figure 4. Stress responsive expression of *UGTs* in *A. thaliana* leaves and seedlings based on Affymetrix ATH1 microarray data.

A) The distribution of maximal inductions to abiotic and biotic stress factors among all *UGT* members is shown. More than twofold inductions are indicated in red. Genes are sorted from highest to lowest abiotic and biotic stress inducibility using mutual ranking. Candidate genes selected for further analysis (*UGT76B1* and *UGT87A2*), are highlighted by a red arrow. *UGT87A1*, a close homolog of *UGT87A2* (see section 4.1.8) is marked with a blue arrow. A1: Osmotic; A2: Salt; A3: UV-B; A4: Oxidative; A5: Wounding; A6: Drought; A7: Cold; A8: Heat; B1: *P. syringae* pv. tomato DC3000 (vir); B2: *P. syringae* pv. phaseolicula (avir); B3: *Phytophtora infestans*; B4: *Botrytis cinerea*; B5: *P. syringae* pv. maculicola ES4326 (vir); B6: *Erysiphe orontii*. **B)** Relative number of inductions (≥ 2-fold), per member of the different phylogenetic *UGT* groups (Ross et al., 2001).

B

19
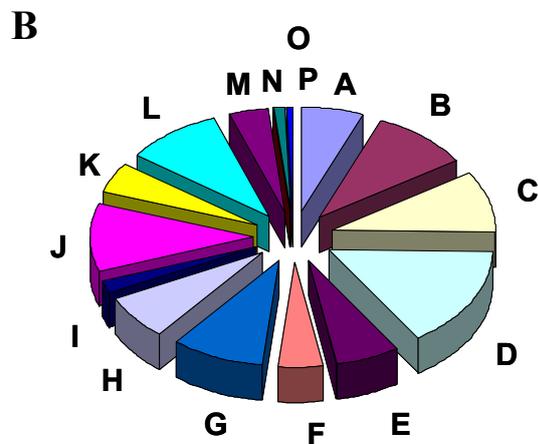
3. UGT76B1 CONJUGATES ISOLEUCIC ACID AND SUPPRESSES PLANT DEFENSE AND SENESCENCE

Plants, as sessile organisms, had to evolve elaborate mechanisms to cope with environmental stresses and to organize defense or tolerance. These measures involve a complex reprogramming of plant cells, which relies on major changes in gene expression, protein modification and a range of different compounds active in defense and signaling. Several small-molecule hormones such as salicylic acid (SA), jasmonic acid (JA), ethylene, and abscisic acid play crucial roles in regulating responses of plants to both biotic and abiotic stresses. Their signaling pathways interact with each other in synergistic as well as antagonistic manners enabling the plant to fine-tune its response to the stressor(s) encountered (Jones and Dangl, 2006; Spoel et al., 2007; Koornneef and Pieterse, 2008). Mostly, SA- and JA-mediated signaling pathways are triggered when plants have to defend themselves against pathogens. Whereas biotrophic pathogens (bacteria, fungi, viruses) are mostly combated by the SA pathway and might be hampered by the activation of the JA response, the opposite prioritization of defense signaling is mobilized to battle necrotrophic pathogens (bacteria, fungi) and herbivores.

Constitutive production of signaling molecules and the concomitant expression of defense genes is energetically costly and reallocation of resources towards defense seems to decrease plant overall fitness (Heil and Baldwin, 2002; Lorrain et al., 2003). Therefore, plants need a tight control of the defense response and its suppression in the absence of pathogen attack or other stresses (Heidel et al., 2004; Bolton, 2009).

Arabidopsis genetics has defined a plethora of genes involved in both SA and JA signaling and their interplay. A number of mutants resulted in enhanced susceptibility to biotrophic pathogens and suppression of SA responses thereby defining crucial steps in SA signaling. These include components of the MAP kinase signaling pathway like *ERD1*, *MPK3* and *MPK6*, genes related to SA biosynthesis (*ICS1/SID2*, *PAD4*, and *EDS1*), central downstream regulators of SA signaling like *NPR1*, as well as *WRKY* and *TGA* transcription factors. Induction of these transcription factors eventually leads to the activation of SA-responsive genes, including *PR* genes, which are involved in defense responses. Similarly, mutations in e.g. *JAR1*, *COI1*, and *JIN1* defining different steps in JA signaling negatively affect the JA pathway (Kazan and Manners, 2008). Resistance towards necrotrophic pathogens is reduced in the corresponding mutants concomitant with the abolished induction of marker genes like

the defensin *PDF1.2*. In contrast, several gain-of-resistance *Arabidopsis* mutants show constitutive defense responses in the absence of (biotrophic) pathogen attack, such as *mlo*, *mpk4*, *wrky*, *acd*, *lsd*, *hrl1*, *hlm1*, or *dnd* affecting pathogen perception and response or leading to primed defense (Greenberg et al., 1994; Petersen et al., 2000; Devadas et al., 2002; Balague et al., 2003; Lorrain et al., 2003; Consonni et al., 2006; Journot-Catalino et al., 2006; Genger et al., 2008). Other interesting classes of mutants with enhanced resistance affecting various steps in signal transduction are *cpr* mutants, named after the *CONSTITUTIVE ACTIVATION OF PR* genes and several suppressors of *npr1* mutants, such as *ssi* and *sni*. These mutants are usually characterized by transcriptional activation of *PR* genes and constitutive accumulation of SA (Bowling et al., 1994; Li et al., 1999; Shah et al., 1999; Gou et al., 2009). In addition, several of the mutants resistant to biotrophic pathogens exhibit retarded growth and/or accelerated senescence. Notably, developmental senescence is at least in part controlled by an SA-dependent pathway (Buchanan-Wollaston et al., 2005).

It has been shown that some of the genes mentioned above exert opposite effects on the SA and JA pathways. These genes include *MPK4*, *WRKY* transcription factors, and *NPR1*, which activate SA, but suppress JA responses. Thus, they are integral to the SA-JA cross talk (Koornneef and Pieterse, 2008; Vlot et al., 2009).

The previously uncharacterized glucosyltransferase *UGT76B1* was selected in the first part of this work as the top stress-induced isoform of the 122-member *UGT* gene family (Figure 4). It was broadly up-regulated by both abiotic and biotic cues such as UV-B irradiation, osmotic, oxidative, drought or wounding stresses as well as in response to both biotrophic and necrotrophic pathogens. Furthermore, it was one of only three *UGT* genes (with *UGT72B1*, *UGT75B1*) that were induced by both SA and JA (methyl jasmonate) application. Since the *UGT76B* subfamily only contains this unique member, *UGT76B1* may have an important and specific role in plant stress responses. In the following study, a genetic approach combined with non-targeted metabolome analysis was used to study whether *UGT76B1* had any function in plant stress responses.

The results presented show that *UGT76B1* is a novel player in the SA-JA signaling pathways and their crosstalk. Independent *ugt76b1* knockout lines exhibited enhanced resistance towards *Pseudomonas syringae* infections, yet progressed earlier into senescence. In contrast, UGT76B1 overexpression resulted in the opposite phenotypes. Using a non-targeted metabolomic approach based on ultra-high resolution Fourier-transform ion cyclotron resonance mass spectrometry (FT-ICR MS) and by combining information from knockout

and overexpression lines, we could pinpoint isoleucic acid as an endogenous substrate of UGT76B1. Collectively, these findings and additional expression studies indicate that UGT76B1 is a novel player in SA- and JA-mediated responses. It acts as a negative regulator of SA-dependent plant defense in the absence of pathogens, promotes the JA response, and negatively influences the onset of senescence. Potential roles of the *UGT76B1* substrate and amino acid derivative isoleucic acid in relation to models of the SA and JA signaling pathways are discussed.

3.1.   RESULTS

3.1.1.   Isolation and characterization of *ugt76b1* single knockout mutants

The availability of several independent loss-of-function mutants is an important experimental tool to explore new gene related processes. Publicly accessible seed collections (NASC, INRA and GABI) were screened for available T-DNA insertion lines. Two independent loss of function mutants SAIL_1171A11 and GT_5_11976 in two different genetic backgrounds (Col-0, L*er*) were obtained from the NASC stock center (Scholl et al., 2000). Both lines were verified by PCR genotyping and sequencing further confirmed the position of the insertion. Also, a 3:1 segregation, using the respective resistance markers, was verified after backcrossing indicating that the mutation was inherited as a single locus in both cases. RT-PCR analysis using gene specific primers confirmed the lack of *UGT76B1* transcripts in both lines (Figure 5B). Homozygous, single insertion lines from SAIL_1171A11 and GT_5_11976 were named as *ugt76b1-1* and *ugt76b1-2* knockout mutants respectively.

A   *UGT76B1* (AT3G11340)
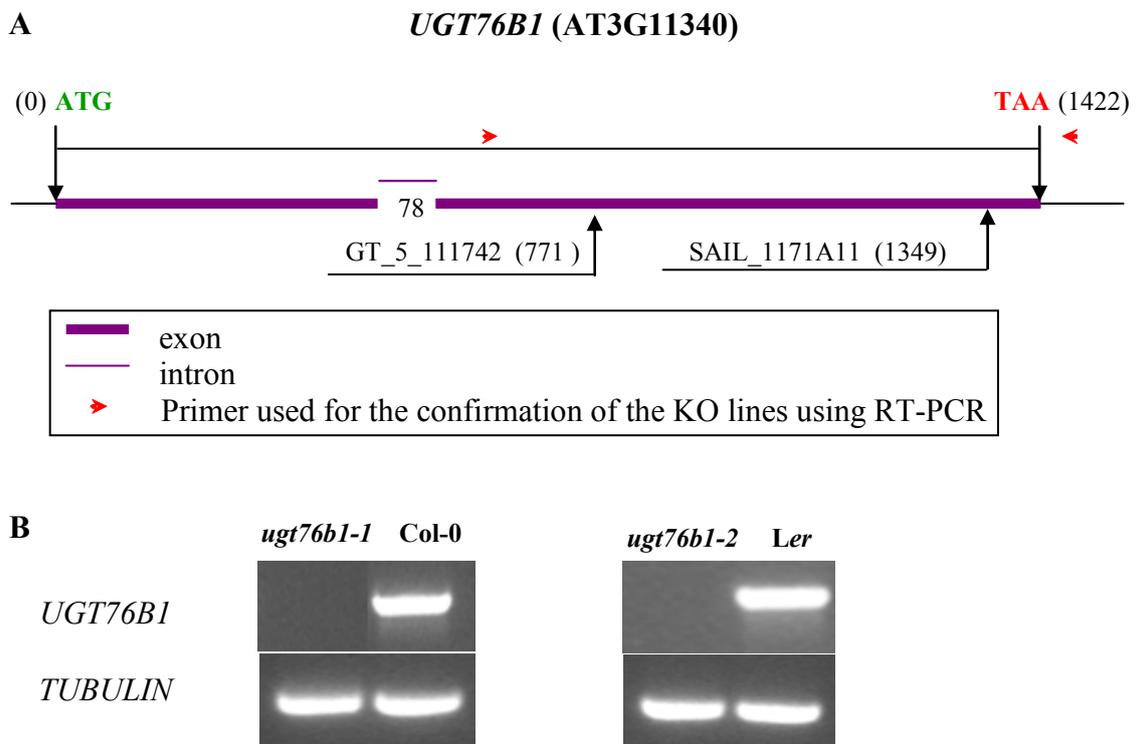
Figure 5. Molecular characterization of *ugt76b1* knockout lines.

(A) Position of the insertions within *UGT76B1* (At3g11340). **(B)** RT-PCR analysis of *UGT76B1* transcript levels in *ugt76b1-2* (GT_5_111742) and *ugt76b1-1* (SAIL_1171A11) compared to their corresponding wild-type lines. *TUBULIN9* (At4g20890) transcript levels were assessed as a control.

24

3.1.2. Production and characterization of *UGT76B1* overexpression lines

Arabidopsis lines overexpressing *UGT76B1* under the control of CaMV 35S-derived constitutive promoters were generated and characterized as described in 5.2.1.6. For seven independent and homozygous single insertion lines per each vector (pB2GW7 and pAlligator2) a RT-qPCR was used on leaf material to identify lines showing a successful overexpression in the T2 generation. From three lines each, which showed a significantly higher transcript amount compared to the wild type, only two maintained the overexpression in the next generation (T3), see Figure 6. From these, one single insertion line from each construct was selected for further experiments, named *UGT76B1-OE-7* (pB2GW7) and *UGT76B1-A-5* (pAlligator2).

UGT76B1 Overexpression lines
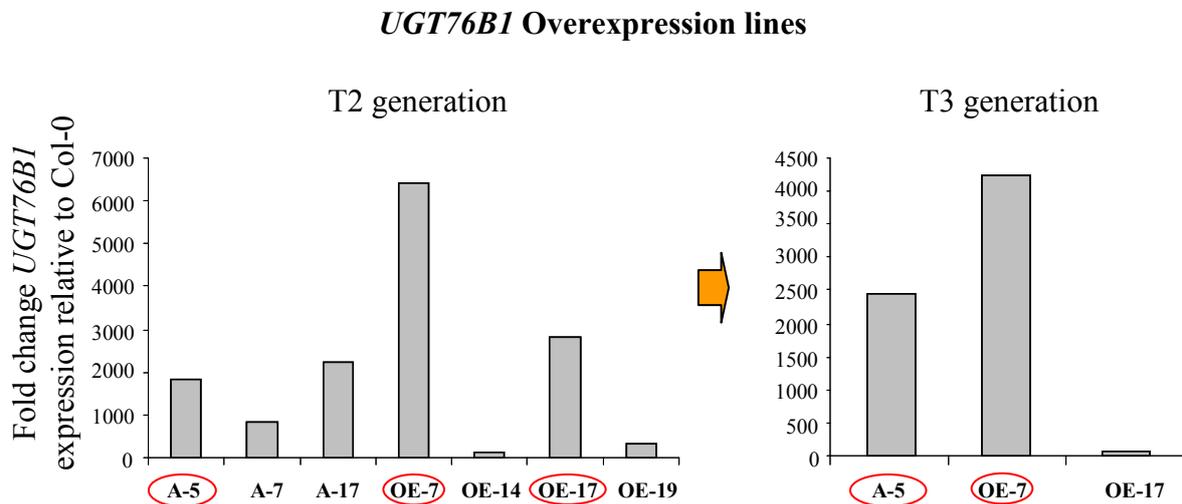
Figure 6. Molecular characterization of *UGT76B1* overexpression lines.

RT-qPCR of *UGT76B1* overexpression lines in two subsequent generations (T2 and T3). Lines *UGT76B1-OE-7, -14, -17,* and *-19* are based on the binary vector pB2GW7, whereas pAlligator2 was used for generating *UGT76B1-A-5, -7,* and *-17* (5.2.1.6). Plant material of the T3 generation was used for subsequent experimental analyses.

3.1.3. *UGT76B1* expression affects onset of senescence

UGT76B1 overexpression and *ugt76b1* knockout lines were examined for morphological or developmental phenotypes associated with a change in *UGT76B1* expression. All genotypes germinated at the same time. No obvious morphological differences were found in lines with altered *UGT76B1* expression compared to the wild type except for a tendency for smaller rosettes of the *ugt76b1* knockout lines and for enlarged rosettes in the case of the *UGT76B1* overexpression lines (Figure 7).
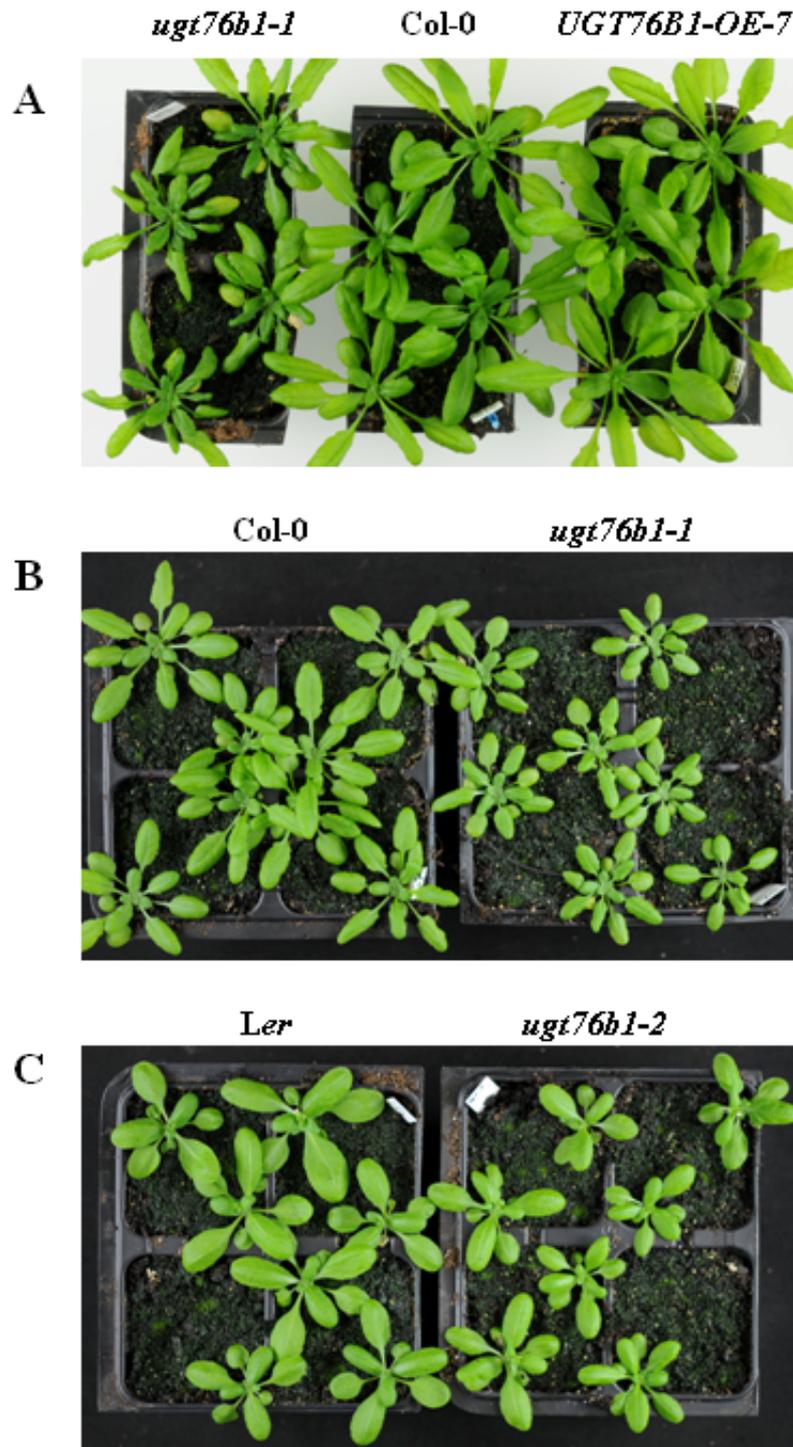
Figure 7. Growth phenotype of *ugt76b1* knockout mutants and *UGT76B1-OE-7* overexpression line.

(A) Phenotype of 5-week-old *ugt76b1-1* and *UGT76B1-OE-7* plants compared to Col-0. **(B)** and **(C)** growth phenotypes of four-week-old *ugt76b1-1* and *ugt76b1-2* compared to their wild-type background (Col-0 and L*er*, respectively).

In addition, mutant and overexpression lines showed a clearly altered, opposite onset of developmental and dark-induced senescence. The knockout plants developed yellowing of leaves six weeks after germination, while the wild type did not yet show any signs of senescence (Figure 8). After nine weeks the loss-of-function mutant was completely senescent. At this stage, the wild type only started to show first signs of yellowing in most leaves and displayed increased anthocyanin accumulation, both hallmarks of early leaf senescence. In contrast, the overexpression line still showed mostly dark green leaves and nearly no signs of yellowing, although anthocyanins started to accumulate (Figure 8). No difference in the onset of flowering could be observed between wild-type and mutant lines (data not shown). This indicated that the earlier (knockout) or later (overexpression) appearance of leaf yellowing might be caused by an altered onset of the developmentally induced senescence program rather than by a generally accelerated or decelerated developmental program, respectively.

The same visible differences were found analyzing dark-induced senescence in detached leaves (see Methods 5.2.1.8). After five days *ugt76b1-1* showed clear yellowing, the wild type also seemed to start yellowing but much less pronounced, whereas the leaves of the overexpression line were still fully green (Figure 8). The second knockout line *ugt76b1-2* showed the same senescence-related phenotypes (Figure 9).
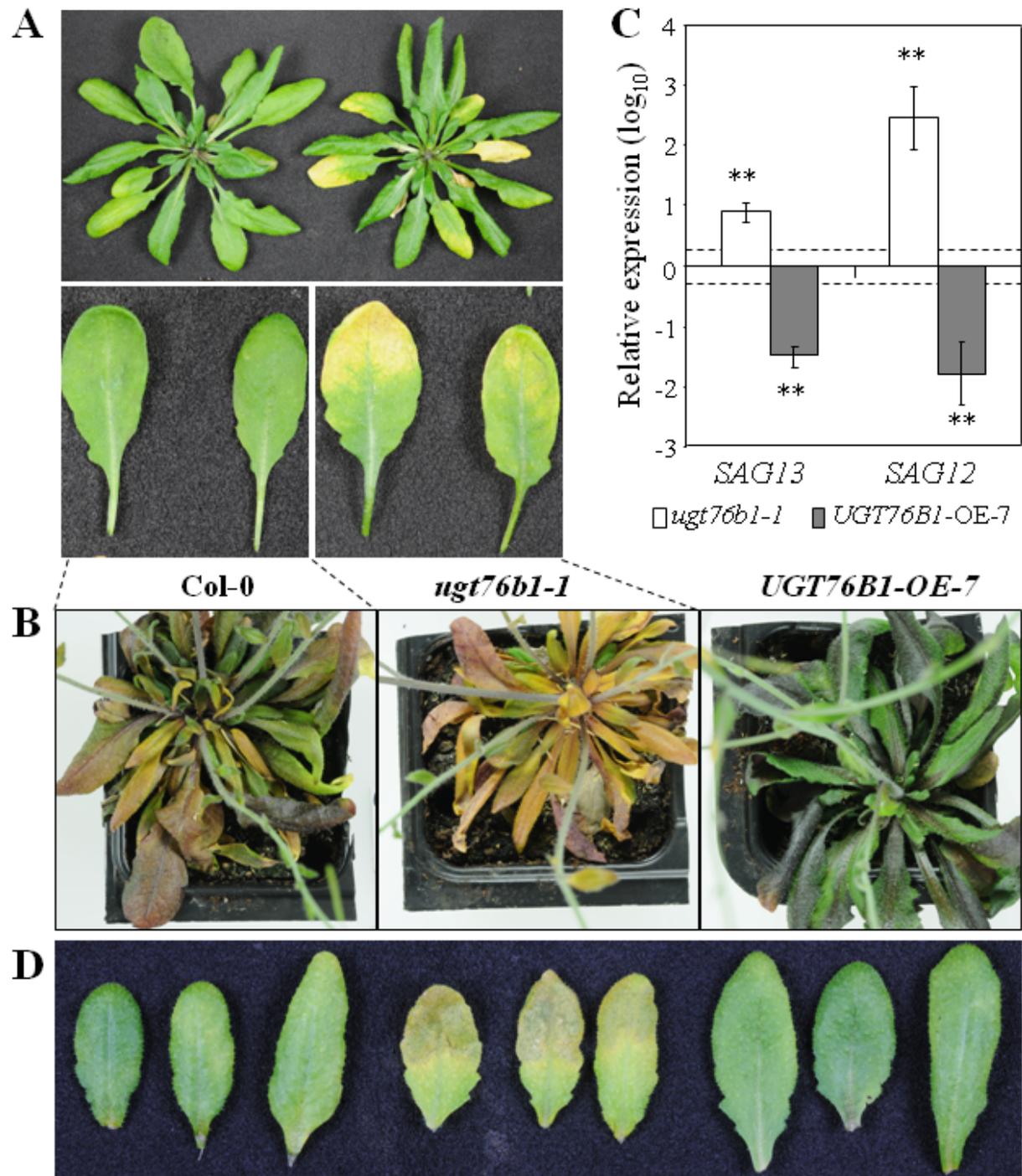
Figure 8. Senescence phenotypes of *UGT76B1* knockout and overexpression lines.

(A) Natural senescence in 6 ½-week-old Col-0 and *ugt76b1-1* mutant plants.

(B) Natural senescence in 9-week-old Col-0, *ugt76b1-1* and *UGT76B1-OE-7* plants.

(C) Relative quantification of senescence associated marker genes *SAG13* and *SAG12* in wild-type and *ugt76b1-1* and *UGT76B1-OE-7* plants. Transcript levels were normalized by the endogenous content of *Ubiquitin 5* and *S16* transcript and expressed relative to the levels quantified for Col plants. Arithmetic means and standard errors of the probes from two individual experiments each including three independent replicates were calculated after $\log_{10}$-

transformation of normalized data. Stars indicate significance of the difference to the wild-type line: ** p-value < 0.01.

(D) Dark induced senescence in Col-0, *ugt76b1-1* and *UGT76B1-OE-7* plants. Excised leaves from 5-week-old-plants were kept in water and dark for 5 days.

In order to confirm that the leaf yellowing of *ugt76b1-1* was due to an accelerated onset of developmentally induced senescence two markers genes were monitored. *SAG13* (encoding a short-chain alcohol dehydrogenase) was induced during early during senescence whereas *SAG12* (encoding a cysteine protease) was specifically activated during the later stages of developmentally controlled senescence, when the leaves started to show clearly visible yellowing (Weaver et al., 1998). RNA from seven-week-old plants (leaves 7-9) was used to monitor marker-gene expression by RT-qPCR. Both senescence marker genes *SAG12* and *SAG13* showed a clear induction in *ugt76b1-1* knockout plants compared to the wild type, whereas expression was much lower or nearly undetectable (for *SAG12*) in *UGT76B1-OE-7* (Figure 8C).
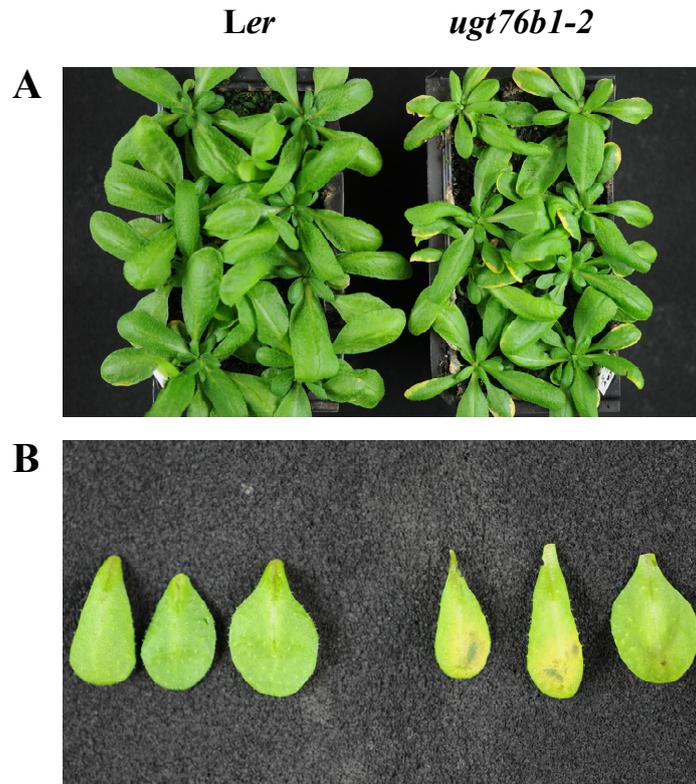
Figure 9. Early senescence of the second knockout line *ugt76b1-2* compared to L*er* (wild-type background).

(A) Natural senescence in 5-week-old plants.
(B) Dark induced senescence in 3-week-old plants.

3.1.4. **_UGT76B1_ overexpression and loss-of-function alter pathogen susceptibility in an opposite manner**

To analyze the influence of changing _UGT76B1_ expression on plant defense towards biotic stressors, plants with altered _UGT76B1_ expression were analyzed for their susceptibility to biotrophic pathogens. To this end five-week-old plants were inoculated with different concentrations of avirulent _Pseudomonas syringae_. 30 h after inoculating leaves with 10^7 cfu ml^{-1} Col-0 wild-type leaves showed a strong hypersensitive response while the knockout plant did not show any visible symptoms (Figure 10 right). Using a lower inoculum (5 10^6 cfu ml^{-1}), inoculated Col-0 wild-type leaves did not show visible symptoms after 30 h whereas _UGT76B1_ overexpression lines showed strong hypersensitive response (Figure 10 left).

Inoculum 5 10^6 cfu ml^{-1}   **Inoculum 10^7 cfu ml^{-1}**

Col-0   **_UGT76B1-OE-7_**   **Col-0**   **_ugt76b1-1_**

Figure 10. Pathogen susceptibility of _UGT76B1_ knockout and overexpression lines. Inoculated leaves 30 h after inoculation with _Ps-avir_. Plants 5-week-old.

To check whether the observed phenotypes of _UGT76B1_ knockout and overexpression lines after infection were due to decreased/increased bacterial growth and consequent hypersensitive response, the bacterial growth was measured in mutant and wild-type plants at different time points after bacterial inoculation. Whole leaves of _ugt76b1-1_, _UGT76B1-OE-7_ and Col-0 were inoculated with 5 10^5 cfu ml^{-1} _Pseudomonas syringae_ D3000 AvrRpt2 (_Ps-avir_). The bacteria showed the typical proliferation of _Ps-avir_ in Col-0 30 h and 78 h after inoculation. In the knockout plant, nearly no bacterial growth was observed pointing to a significantly reduced susceptibility, whereas in the overexpression line the bacterial population strongly increased indicating a reduced resistance (Figure 11). Similar results were obtained with the virulent _Pseudomonas syringae_ DC3000 (_Ps-vir_). The _ugt76b1_ knockout mutant showed a strongly reduced bacterial growth, whereas bacterial susceptibility was increased in the overexpression line (Figure 11). In both cases, after infection with virulent

and avirulent *Pseudomonas* strains, *UGT76B1* expression negatively correlated with plant resistance.
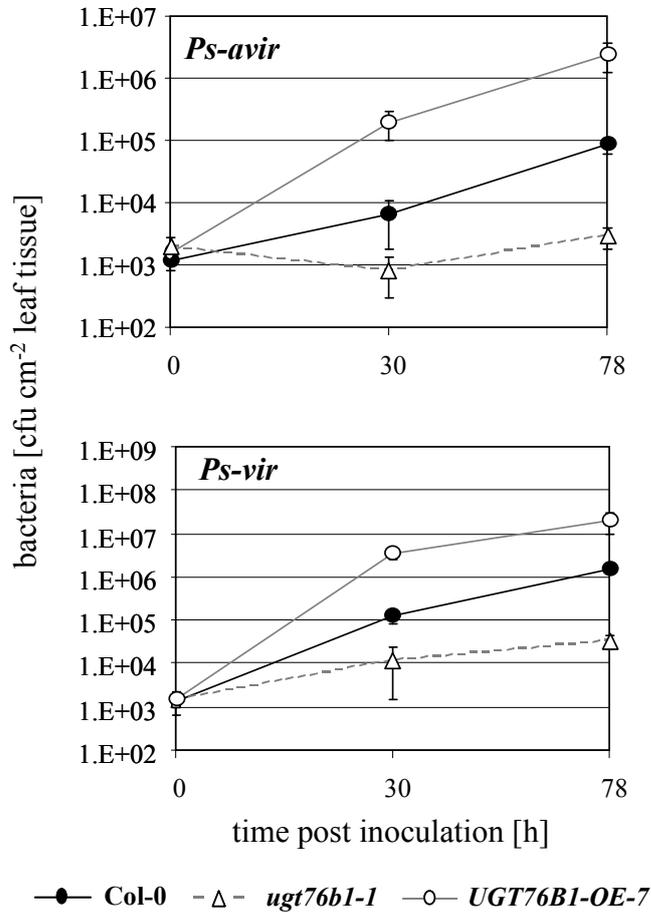
Figure 11. Bacterial growth of avirulent and virulent *Pseudomonas syringae* in *Arabidopsis* leaves of wild-type, *ugt76b1-1* and *UGT76B1-OE-7* plants.

Leaves were infiltrated with an inoculum of $5 \cdot 10^5$ cfu ml^{-1} of *Ps-avir* (upper graph) and *Ps-vir* (lower graph). Bacteria (cfu cm^{-2}) were quantified 30 h and 78 h after inoculation. The graph represents the mean and SD of three replicates. The experiment was repeated with similar result.

Pathogen resistance due to loss of *UGT76B1* could be confirmed by visual analysis of the second knockout line *ugt76b1-2* 30 h after inoculation with *Ps-avir* (Figure 12).

Figure 12. Pathogen resistance of *ugt76b1-2* compared to L*er* (wild-type background).

Pictures were taken 30 h after infiltration with $5 \cdot 10^6$ cfu ml^{-1} *Ps-avir*.

3.1.5. Defense marker gene expression is constitutively altered in *UGT76B1-OE-7* and *ugt76b1-1* lines

As gain-of-resistance mutants may show constitutively enhanced transcript levels of defense-response genes, the expression of several defense marker genes was analyzed in *UGT76B1-OE-7* and *ugt76b1-1* lines using relative quantification by RT-qPCR. *PAD4* and *EDS1* act upstream from SA biosynthesis, but are also induced by SA (Rusterucci et al., 2001). *PR1* is a pathogen and SA responsive gene, which is a well established marker gene for the defense responses of *Arabidopsis* against *Pseudomonas* (Uknes et al., 1992). *SAG13* is an early senescence marker, which is also induced by several stress factors and SA (Weaver et al., 1998). *WRKY70* encodes a transcription factor and is an important regulator in the interplay of SA- and JA-related plant defense responses (Li et al., 2004). *PDF1.2* and *VSP2* are marker genes frequently used to monitor JA and ethylene responses (Pieterse et al., 2009), whereas *LOX2* involved in JA biosynthesis is activated by a positive feedback loop (Bell et al., 1995; Sasaki et al., 2001).

Changing *UGT76B1* expression had a strong effect on the transcript level of these defense-related genes (Figure 13). *PR1*, *PAD4*, *EDS1*, *WRKY70* and *SAG13* were induced in leaves of five-week-old untreated *ugt76b1-1* knockout plants compared to the wild type. In contrast, JA-responsive genes *PDF1.2* and *VSP2* as well as *LOX2* were down-regulated. *UGT76B1-OE-7* showed the opposite regulation for all measured genes. *PR1*, *PAD4*, *EDS1*, *WRKY70* and *SAG13* were downregulated, whereas *VSP2* and *LOX2* were upregulated. The upregulation of *PDF1.2* in *UGT76B1-OE-7* was more variable in different experiments.
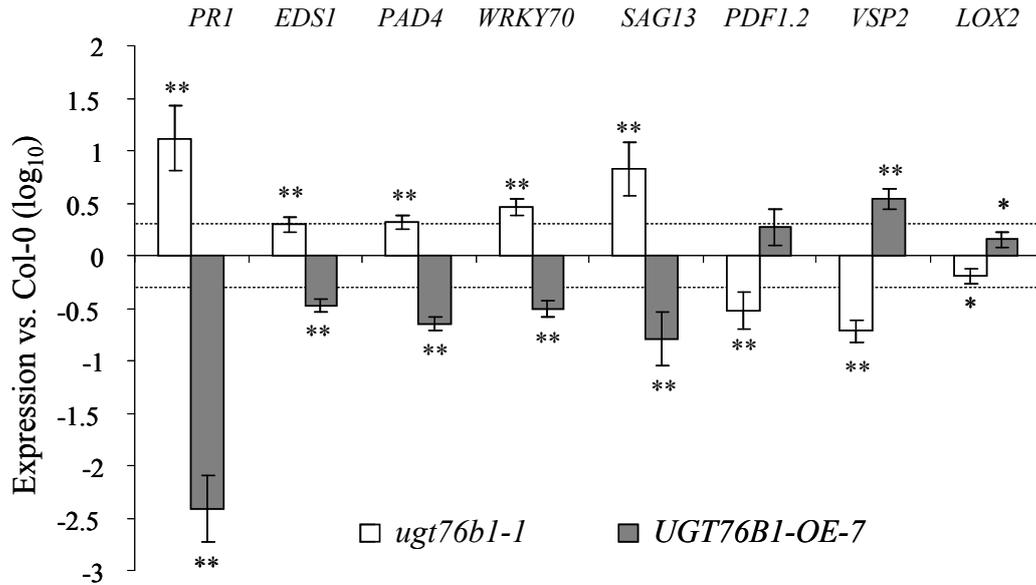
Figure 13. Defense marker gene expression in *ugt76b1-1* and *UGT76B1-OE-7* plants (before pathogen infection).

Gene expression of *PR1*, *EDS1*, *PAD4*, *WRKY70*, *SAG13*, *PDF1.2*, *VSP2* and *LOX2* in 5-week-old *ugt76b1-1* and *UGT76B1-OE-7* measured by RT-qPCR. Expression levels were normalized to *UBIQUITIN5* and *S16* genes. Values are relative to Col-0 wild type expression. Arithmetic mean and standard error for $\log_{10}$-transformed data of two individual experiments each consisting of three independent replicates were calculated using ANOVA. Stars indicate significance of the difference to the wild-type line: ** p-value < 0.01, * p-value < 0.05. The dashed, horizontal lines indicate twofold change.

To exclude an age-dependent effect on defense gene expression (Kus et al., 2002), *PR1* and *SAG13* were also analyzed in younger, three-week-old plants. Both genes showed a similar, opposite regulation in young knockout and overexpression lines (Figure 14).
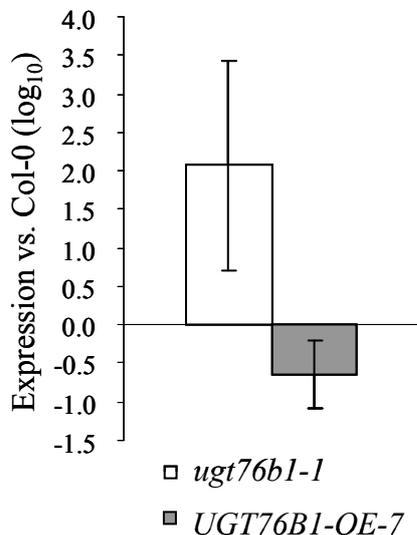
Figure 14. Relative quantification of *PR1* expression at early time point.

Graph shows of relative *PR1* expression in three-week-old *ugt76b1-1* and *UGT76B1-OE-7* plants. Transcript levels were normalized by the endogenous content of *UBQ5* and *S16* transcript and expressed relative to the levels quantified for Col-0 plants (see 5.2.4.7).

In order to test whether the overexpression line was able to induce defense genes after pathogen challenge, thereby indicating that it has the potential to perform a functional signal transduction pathway, transcription of *PR1* and *SAG13* was analyzed in wild-type, mutant and transgenic plants after bacterial inoculation (Figure 15). In wild-type plants *PR1* and *SAG13* were induced 24 h after infection with *Ps-avir* to similar levels as those constitutively expressed in the *ugt76b1* loss-of function mutant. In the overexpression line, expression of both *PR1* and *SAG13* reached similar levels as in wild-type plants 24 h after pathogen challenge. Thus, the general ability to perceive and respond to the pathogen was not altered in *UGT76B1-OE-7*.
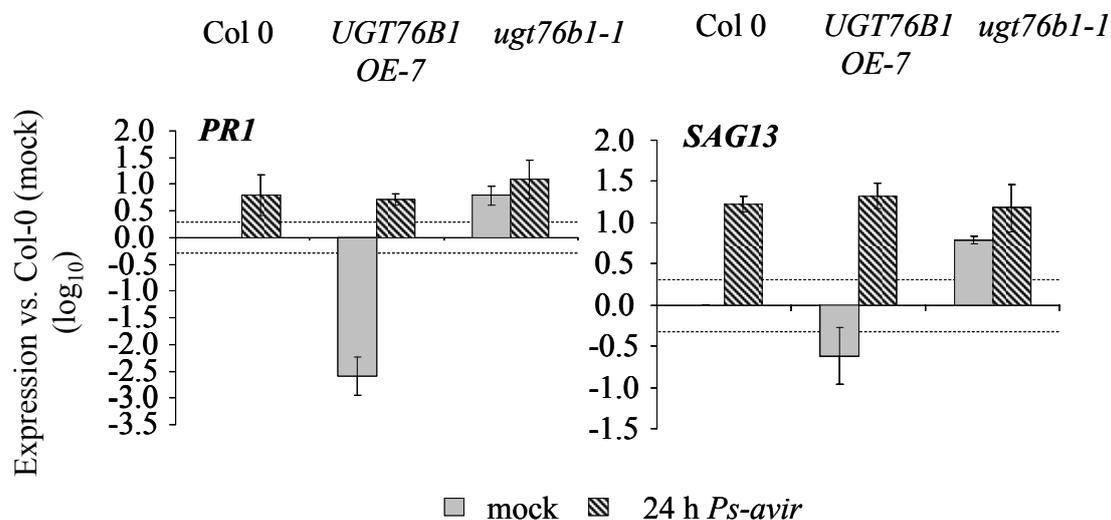
Figure 15. Defense marker gene expression in *ugt76b1-1* and *UGT76B1-OE-7* plants after pathogen infection.

Transcript levels of *PR1* and *SAG13* in five-week-old wild-type plants 24 h after infection (5 10^5 cfu ml^{-1} *Ps-avir*) measured by RT-qPCR. Values are relative to expression 24 h after mock treatment and log$_{10}$ transformed. Graph represents the mean and SD of three replicates. The dashed, horizontal lines indicate twofold change.

3.1.6. Endogenous levels of free SA and SAG are elevated in *ugt76b1*

EDS1 and *PAD4* are essential regulators of basal resistance and are known to control the accumulation of the signaling molecule salicylic acid (Zhou et al., 1998; Rusterucci et al., 2001). In addition, several gain-of-resistance mutants with transcriptional activation of *PR* genes are known to have increased levels of SA and SAG (Silva et al., 1999; Balague et al., 2003; Gou et al., 2009). It was therefore assessed whether the high level of defense gene expression in *ugt76b1-1* plants correlated with higher endogenous SA levels (Figure 16). Indeed, *ugt76b1-1* showed a considerably higher basal level of SA and also a higher level of

SAG than detected in wild-type plants in the absence of any inducer. In contrast, the overexpression line contained an amount of free SA that was similar to that in wild-type plants showing even a tendency for repression, but curiously also higher levels of the SA conjugate. The SA ester level did not significantly change in overexpression lines, but was slightly increased in the knockout mutant (Figure 16).
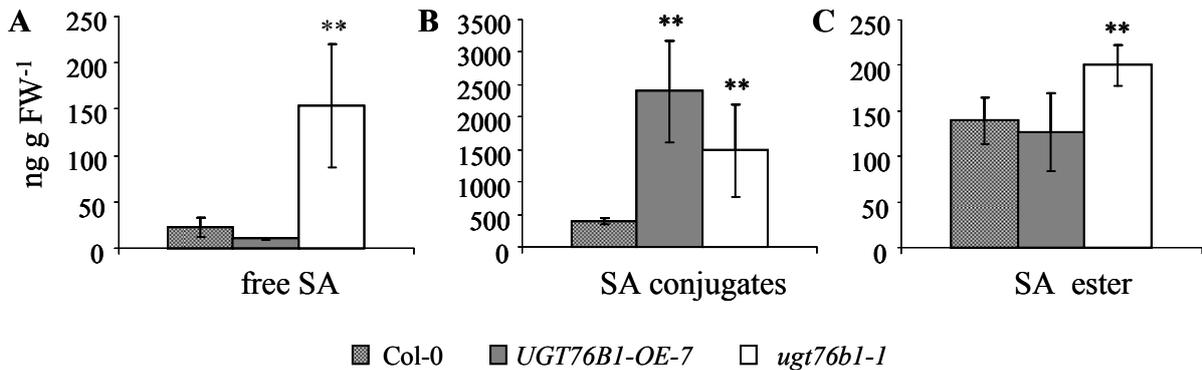
Figure 16. Salicylic acid (SA) and conjugated SA levels in five-week-old seedlings of the wild type, *ugt76b1-1* and *UGT76B1-OE-7*.

Values represent the means and standard deviations obtained from five replicates. Stars indicate significance of the difference to the wild-type line: ** p-value < 0.01. The experiment was repeated with similar results.

3.1.7. *UGT76B1* is induced early after pathogen infection

In order to determine at which time point after pathogen infection *UGT76B1* transcription was activated, the time course of *UGT76B1* expression after pathogen infection compared to other defense marker genes known to be induced at early or late phases during the defense response was analyzed. Figure 17 shows the time course of *UGT76B1*, *SAG13*, *WRKY70*, *EDS1*, *PAD4* and *PR1* expression during the incompatible interaction of wild-type plants with *Ps-avir*. *PR1* as well as *SAG13* were highly induced 24 h after pathogen inoculation. *UGT76B1* as well as *WRKY70*, *EDS1* and *PAD4* clearly preceded the upregulation of *PR1* and *SAG13*.
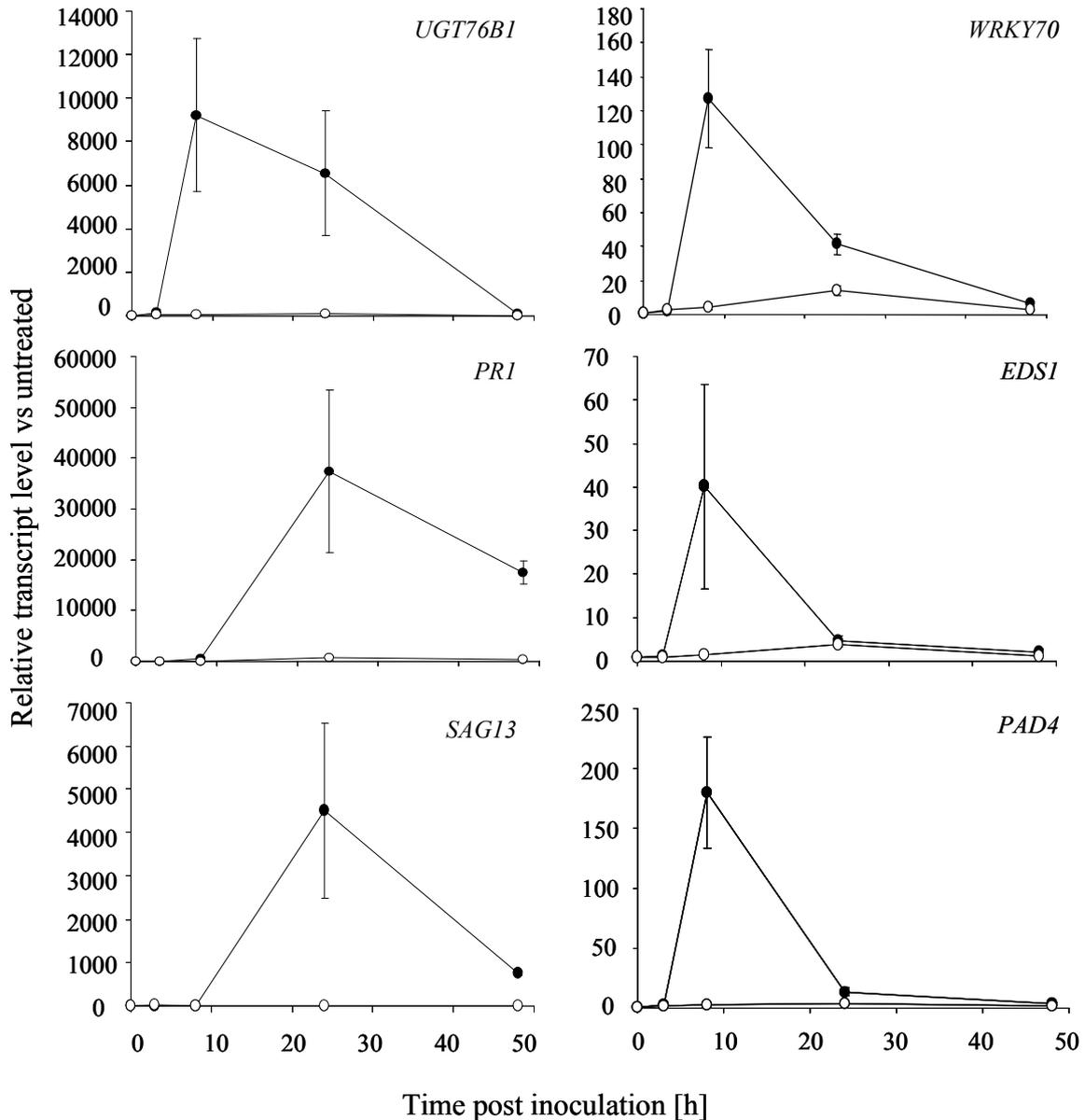
Figure 17. RT-qPCR expression profiles of *UGT76B1*, *WRKY70*, *EDS1* and *PAD4* after infection with avirulent *Pseudomonas syringae*.

Transcript levels were quantified at the indicated time points after inoculation with *Ps-avir* (closed circles) and mock (10 mM MgCl$_2$; open circles) treatment. The transcript level (relative expression) was normalized to the transcript abundance of *UBIQUITIN5* and *S16* genes (see Methods 5.2.4.7). Values correspond to the mean and SD of triplicates. The experiment was repeated with similar results.

3.1.8.   *UGT76B1* expression does not alter jasmonic acid perception

Marker gene expression analysis showed that *UGT76B1* had a positive effect on the expression of JA responsive genes. Several mutants affected in JA signaling such as *jar1* (Staswick et al., 1992), *jin1* (Berger et al., 1996), and *coi1* (Feys et al., 1994) showed reduced sensitivity to JA, tested by MeJA inhibition of primary root elongation. It was therefore

interesting to test whether *ugt76b1* mutants and *UGT76B1* overexpression lines also showed an altered sensitivity to JA. As shown in Figure 18 this was not the case. *UGT76B1-OE-7* and *ugt76b1-1* showed the same inhibition of primary root growth on plates containing 50 μM MeJA (the JA methyl ester), indicating a functional JA signaling pathway.
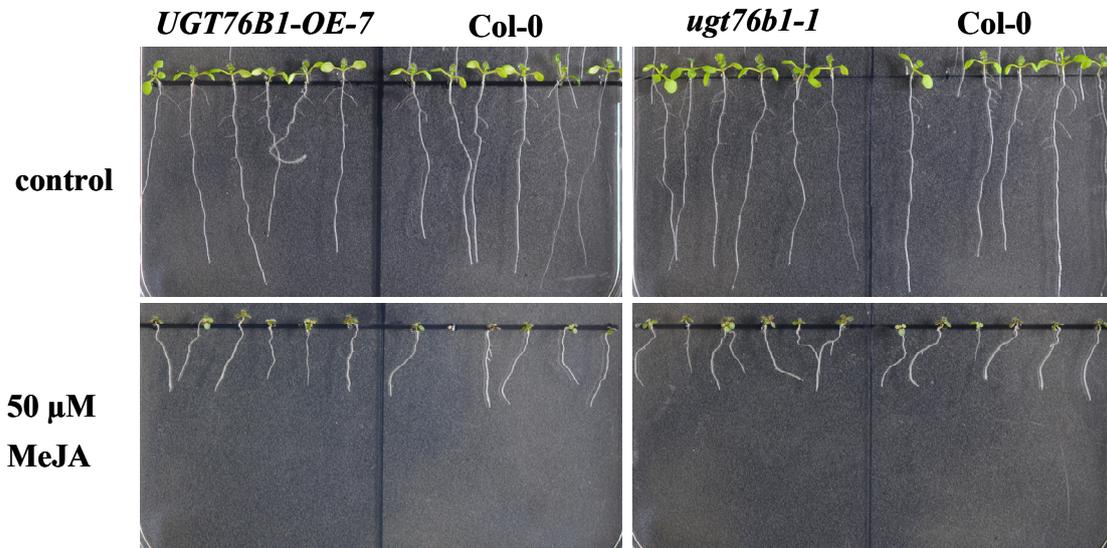
Figure 18. *ugt76b1-1* knockout and *UGT76B1-OE-7* plants showed inhibition of root growth on MeJA-containing medium similar to wild-type plants.

Pictures were taken after 10 days growth on plates containing 50 μM MeJA.

3.1.9. Spatial expression pattern of *UGT76B1*

To analyze the expression of *UGT76B1* in different plant organs and at different developmental stages, transgenic lines carrying a *UGT76B1$_{pro}$*:GUS-GFP transgene were produced by *Agrobacterium*-mediated transformation. Two segregating, independent single insertion lines, *UGT76B1$_{pro}$*:GUS-GFP-2 and *UGT76B1$_{pro}$*:GUS-GFP-12 were selected for further analysis. Plants of different developmental stages (8 d, 17 d, 28 d and 36 d) showed consistent GUS activity among two independent transgenic lines (see 5.2.6 for details). *UGT76B1* was expressed all over the roots except in root tips (Figure 19D). Stronger expression was found in young roots and in lateral roots (Figure 19A). Optical cross sections of a lateral root by confocal laser scanning microscopy recording GFP fluorescence of the same promoter:GUS-GFP lines mainly revealed *UGT76B1* expression in the root cortex and endodermis (Figure 19E). GUS staining of aerial plant parts showed *UGT76B1* expression in very young leaves (Figure 19B), hydathodes (Figure 19C and F), sepals and style (Figure 19H). Expression in mature leaves of young plants (17 d) was patchy (Figure 19F). In older four-week-old plants, expression in leaves was reduced (Figure 19G). GUS staining also

showed induction of *UGT76B1* expression after *Pseudomonas* inoculation and wounding (Figure 19I and J).
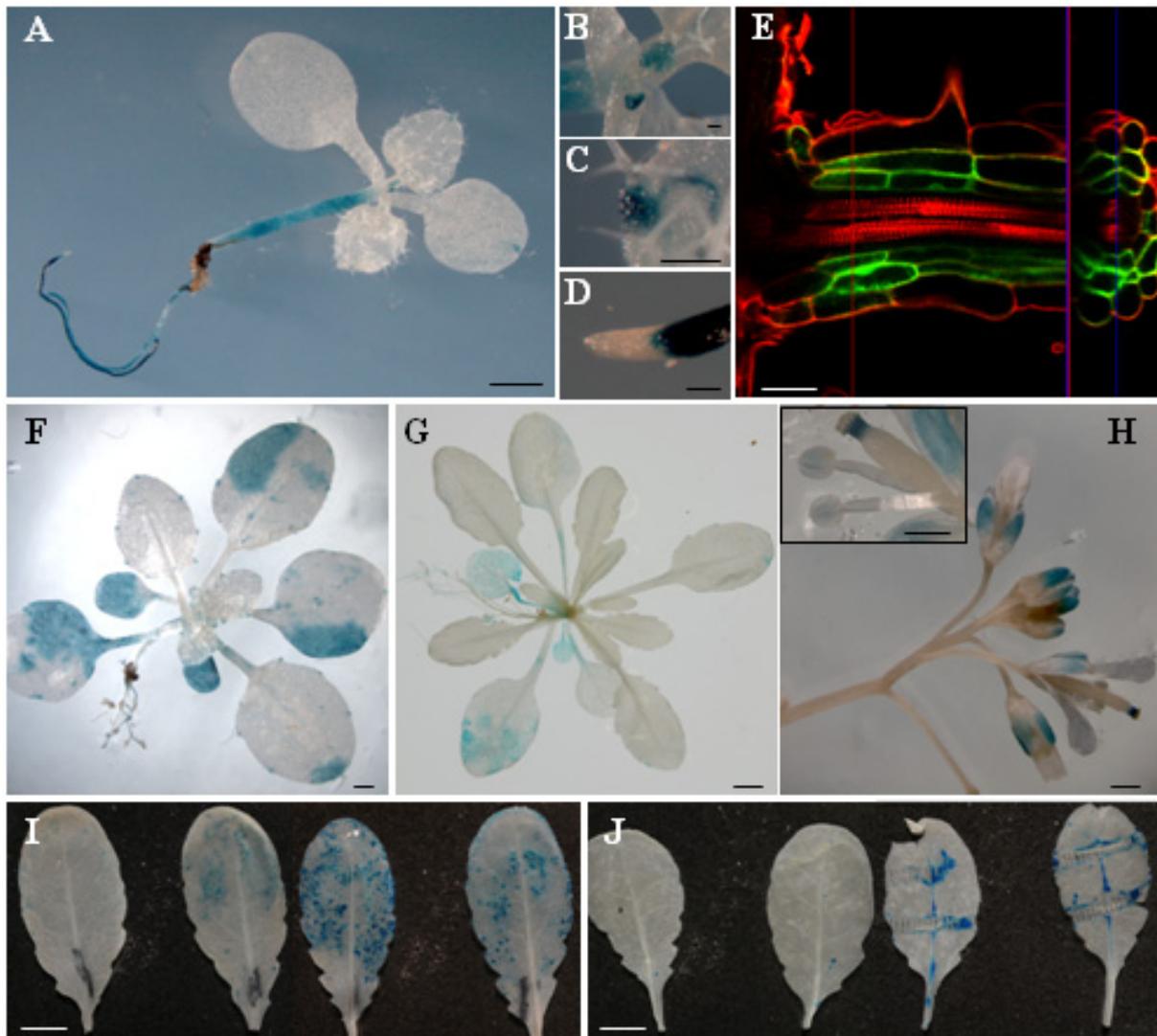
Figure 19. Localization of *UGT76B1* expression using *UGT76B1*pro:GUS-GFP lines.

Transgenic plants harboring *UGT76B1*pro:GUS-GFP constructs were stained for GUS activity in different developmental stages **(A-D, F-J)** or examined for GFP fluorescence by confocal microscopy **(E)** (see 5.2.6). Results were consistent among at least two independent transgenic lines. Bars = 1 mm (A, F), 0.1mm (B-D), 30 μm (E), 0.5 cm (G, I, J), and 0.5 mm (H).
(A-D) 8-day-old seedling with leaf primordia **(B)**, leaf hydathodes **(C)**, and root tip **(D)**.
(E) Roots from one-week-old seedlings grown on agar plates. Cell walls were counterstained with propidium iodide. **(F)** 17-day-old plant. **(G)** 28-day-old plant. **(H)** Inflorescence of 36-day-old plant. **(A,B,F,G)** *UGT76B1*pro:GUS-GFP-12.**(C,D,E,H)** *UGT76B1*pro:GUS-GFP-2.
(I) Two leaves of five-week-old plants 8 h after mock treatment (left) and after inoculation with *Ps-avir* (right).
(J) Two leaves before (left) and 6 h after (right) mechanical wounding using a forceps.

3.1.10. Non-targeted metabolome analysis reveals correlation between isoleucic acid glucoside formation and *UGT76B1* expression

Since there was neither an indication of the *UGT76B1* substrate nor the affected metabolic pathway, a completely non-targeted strategy was embarked to obtain such information. An ultrahigh-resolution 12 Tesla FT-ICR mass spectrometer run in the negative ionizing mode was employed to compare the metabolic profile of *UGT76B1* overexpression lines and *ugt76b1* mutants with their respective wild type. Root material from plants grown in hydroponic culture (see Figure 20) was used as a starting material for metabolite extraction, because *UGT76B1* was mainly expressed in roots and showed only lower expression in leaves under unstressed conditions.

Figure 20. Expression of *UGT76B1* in roots of seedlings grown in hydroponic culture.

Seedlings from *UGT76B1~pro~:GFP-GUS* fusion lines were stained for GUS activity after 2 weeks growth in hydroponic cultures (see 5.2.1.5).

A stringent, combinatorial screening for metabolite changes was performed across the two independent knockout lines in two different wild-type backgrounds (Col-0 and L*er*) and both independent overexpression lines. By setting a stringent p-value (< 0.01) and by filtering for metabolites, which showed consistent and opposite regulation in knockout and overexpression plants, two metabolites were found, the accumulation of which was significantly and positively correlated with *UGT76B1* expression. Both m/z peaks were repressed in the knockout and induced in the overexpression lines (Figure 21A; Methods). In addition, both peaks were significantly enhanced as compared to the wild type in leaf material of the *UGT76B1* overexpression lines, although with an overall lower intensity than in roots (Figure 22). Due to the high accuracy in m/z determination, an exact molecular formula could be assigned for both (Figure 21A).
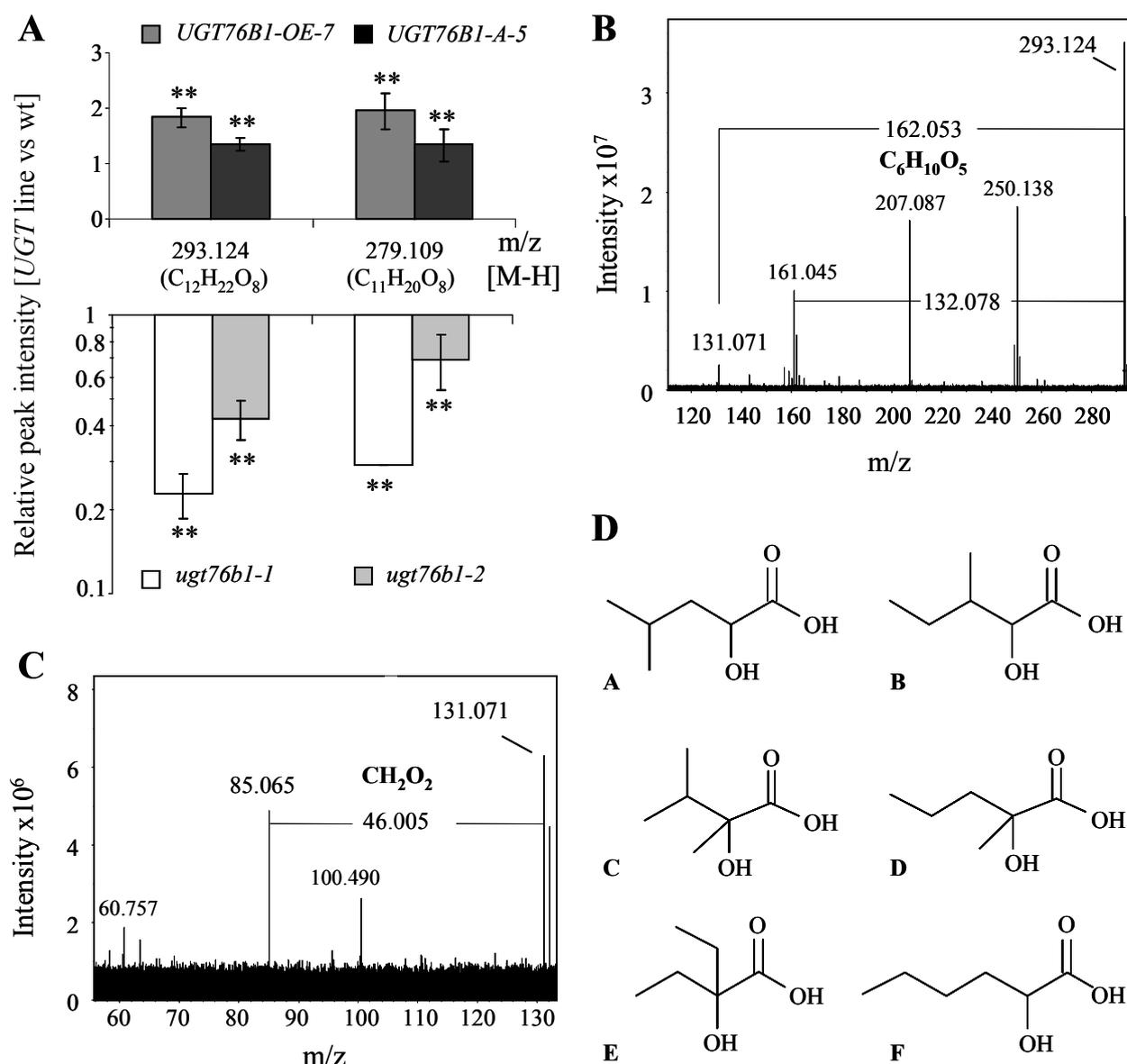
Figure 21. Non-targeted metabolome analysis of *UGT76B1* overexpression and *ugt76b1* knockout lines.

(A) Metabolic changes found in roots of two independent knockout lines and two independent overexpression lines compared to the respective wild type. Means and standard deviation of three independent biological replicates with two technical replicates each are displayed. m/z 279 was nearly undetectable and undetectable in *ugt76b1-2* and *ugt76b1-1*, respectively. Therefore, a default value for the *ugt76b1-1* peak was used for calculating the relative intensity (Methods). Stars indicate significance of the difference to the wild type: ** p-value < 0.01. The predicted molecular formulae are indicated. The experiment was independently repeated with similar results.

(B) Fragmentation pattern of m/z 293. The loss of m/z 162 confirmed the presence of a glucosidic moiety. Other major peaks at m/z 207 and 250 could be unequivocally excluded as m/z 293-derived fragments; they were originating from electrical noise and from an N-containing contaminant, respectively. In contrast, m/z 161 was in agreement with a radical anion of deprotonated glucose, which was directly produced from m/z 293.

40

(C) Further in-cell fragmentation led to the elimination of CH_2O_2 (formic acid), which restricted the nature of the aglycon to α-hydroxy carboxylic acid isomers.

(D) Six possible isomeric molecular structures of the aglycon $C_6H_{12}O_3$.

Using a Strata NH2 column a partial concentration and cleaning of the extracts was achieved enabling fragmentation studies. Loss of a fragment with m/z 162 confirmed that the molecule with m/z 293 was a glucoside (Figure 21B). No glucoside loss could be observed upon fragmentation of the second peak (m/z 279). Loss of the glucosidic moiety from m/z 293 led to a smaller compound with m/z 131. The molecular formula of this residual aglycon was $C_6H_{12}O_3$. Further in-cell fragmentation led to the loss of a formic acid (m/z 46) moiety and the formation of a second fragment m/z 85. According to a previous study this behavior confirmed that the aglycon of m/z 293 was an α-hydroxy carboxylic acid with a free β-hydrogen (Bandu et al., 2006). Thus, six possible structures could be suggested for the aglycon m/z 131 (Figure 21C). Structures A, C, D, and F could be excluded, because the fragmentation of the corresponding standard compounds gave rise to further fragments, which had not been detected after fragmentation of the unknown aglycon from the plant extract (m/z 131) (Figure 23). Both compounds B and E gave the same fragmentation pattern as the unknown plant peak and therefore constituted possible candidate structures of the aglycon.
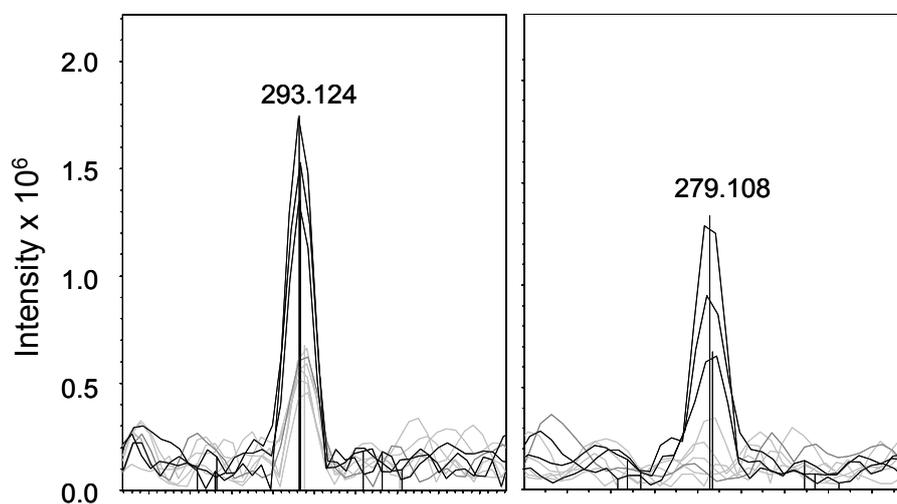
Figure 22. Detection of m/z 293.124 and m/z 279.108 in leaves of Col-0 and *UGT76B1-OE-7* plants.

Both peaks were also significantly increased in leaf material of 4-week-old *UGT76B1-OE-7* plants. Col-0: (grey line); *UGT76B1-OE-7* (black line).
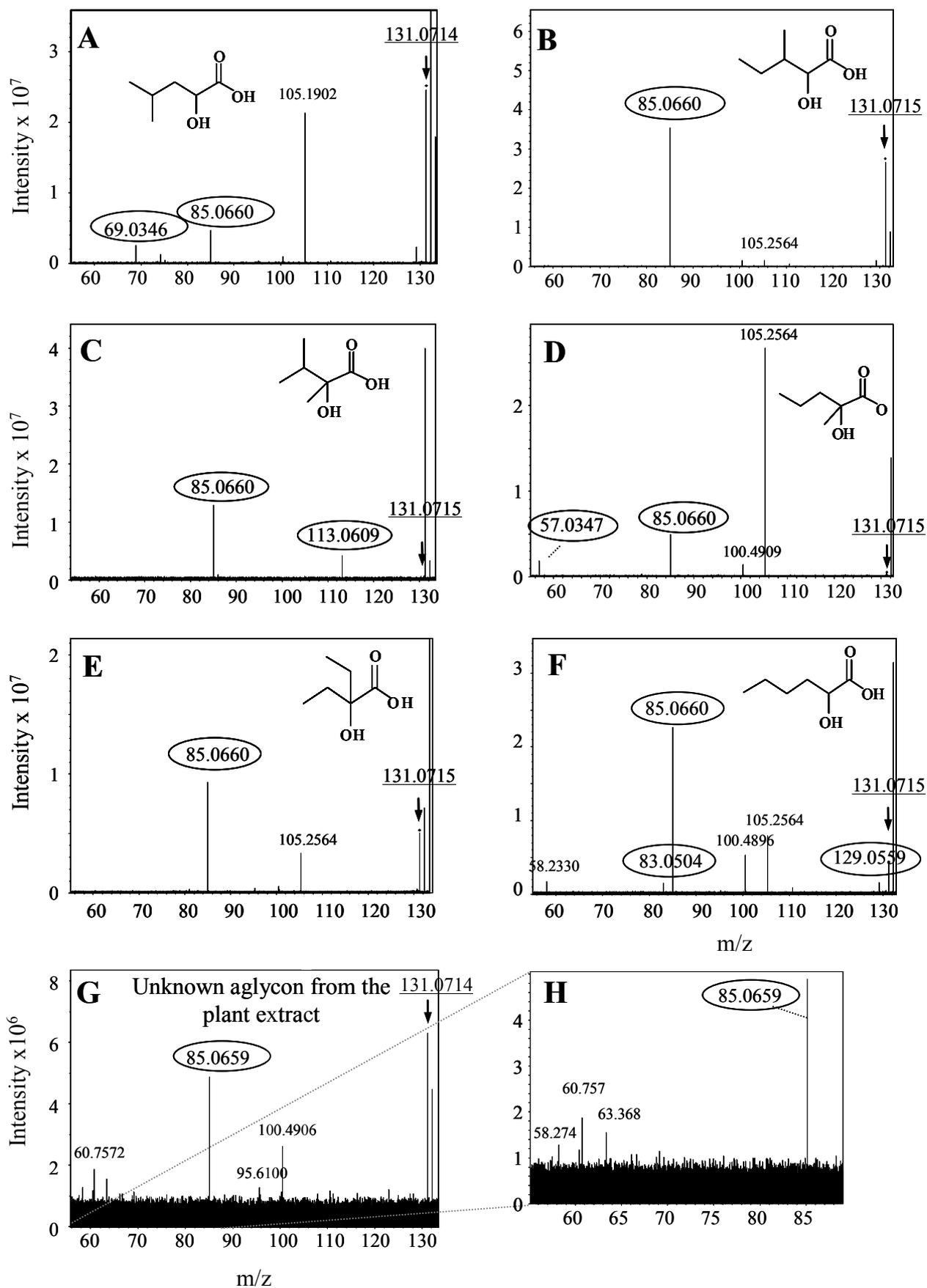
Figure 23. Fragmentation patterns of the unknown aglycon (derived from m/z 293) from the plant extract and of putative $C_6H_{12}O_3$ isomers.

The precursor ion is underlined and its position indicated by an arrow. Generated fragments are encircled to distinguish them from noise peaks. The obtained fragmentation patterns of compound A and F corresponded to published data (http://www.massbank.jp/). Only structures B and E showed the same fragmentation pattern as the unknown aglycon from the plant extract **(G)** and were therefore selected for *in vitro* glucosylation studies.

(A-F) Fragmentation of six $C_6H_{12}O_3$ isomeric reference compounds as indicated.

(G, H) Fragmentation of the plant extract-derived aglycon. The region below m/z = 85 is enlarged in **(H)** to visualize the absence of fragments observed in experiments with some of the isomeric reference compounds.

3.1.11.   *In vitro* activity of recombinant UGT76B1 towards isoleucic acid

In order to further elucidate the structure of the UGT76B1 substrate, compounds B and E were tested as potential substrates of recombinant UGT76B1 *in vitro*. As shown in Figure 24C, UGT76B1 glucosylated isoleucic acid (compound B, 2-hydroxy-3-methylpentanoic acid), whereas it showed no activity towards 2-ethyl-2-hydroxybutyric acid (compound E, see Figure 25). Thus, isoleucic acid turned out to be a substrate of UGT76B1, which was in accordance with the observation of plant extracts derived from *ugt76b1* knockout and *UGT76B1-OE* lines. As high levels of SA conjugates were found in the *UGT76B1* overexpression line, the activity of the recombinant protein was also tested towards SA. Formation of SAG could indeed be observed, although only a minor peak compared to the substrate SA was detected (Figure 24F). However, this SA-glucosylating ability of UGT76B1 may only relate to the enhanced SA glucosides found in the ectopic overexpression line, but it does not reflect the endogenous role of UGT76B1, since the *ugt76b1-1* knockout showed even enhanced SA glucoside levels (Figure 16).
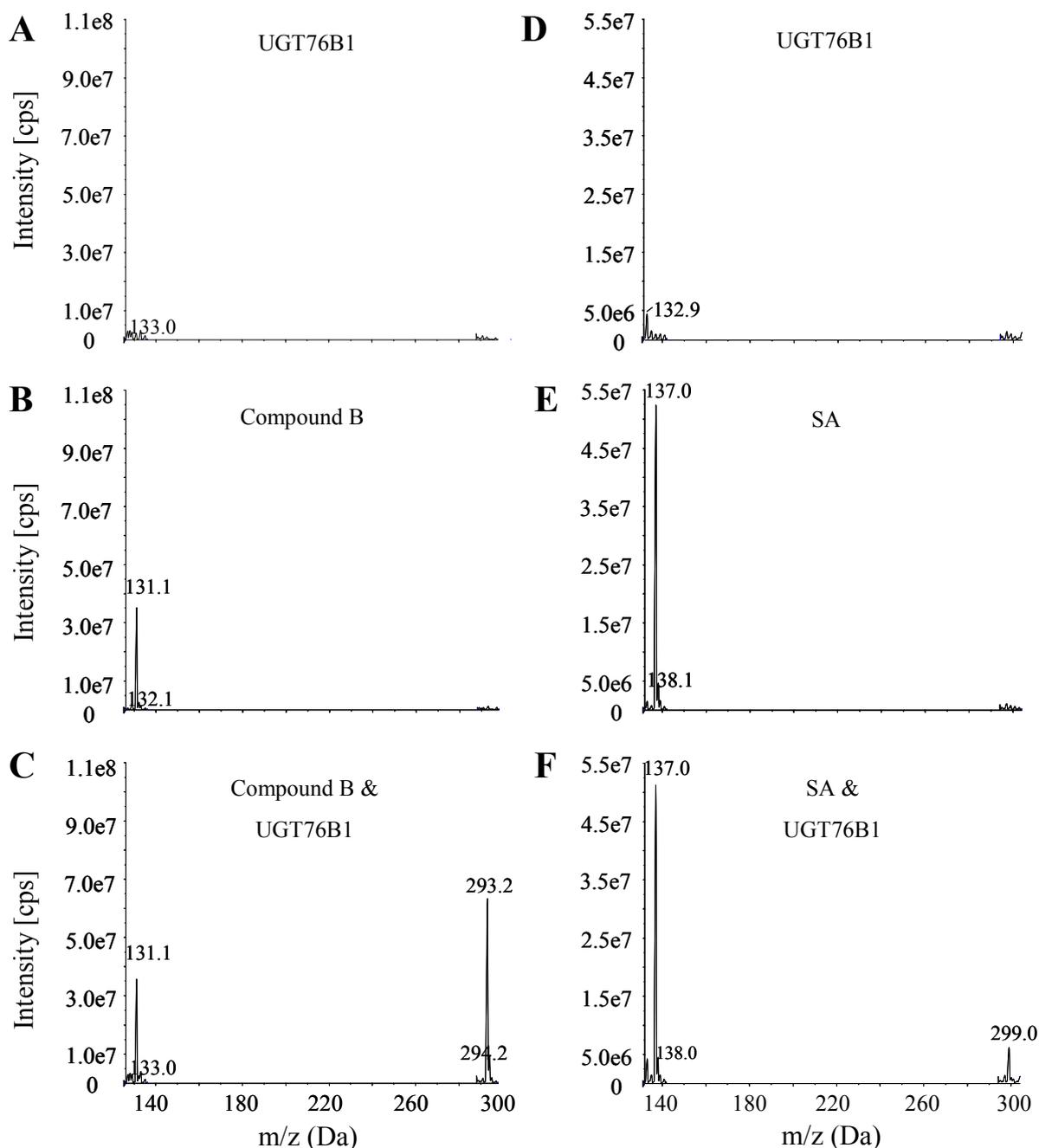
Figure 24. *In vitro* activity assay of UGT76B1.

Activity of recombinant UGT76B1 was tested towards (A-C) isoleucic acid (2-hydroxy-3-methylpentanoic acid, compound B) and (D-F) salicylic acid. The reactions were analyzed by mass spectrometry (Methods). The m/z values of the corresponding substrates and products are indicated. The experiment was independently repeated with similar results.

(**A, D**) Mass spectra of enzyme reactions without substrate.

(**B, E**) Mass spectra of enzyme reactions without enzyme.

(**C, F**) Mass spectra of complete reactions.
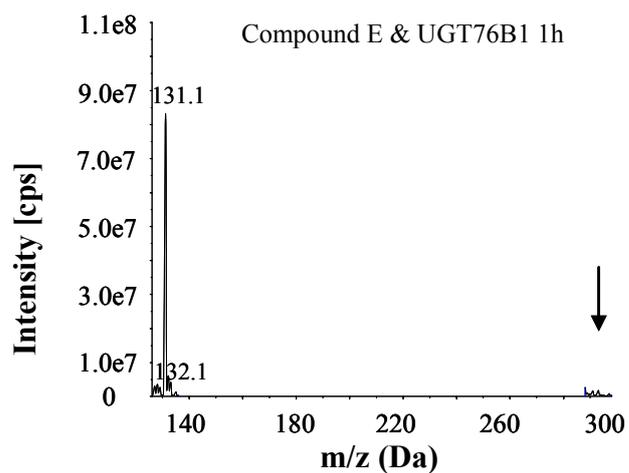
Figure 25. *In vitro* **activity assay of UGT76B1 towards 2-ethyl-2-hydroxybutyric acid.**

Activity of recombinant UGT76B1 was tested towards 2-ethyl-2-hydroxybutyric acid (compound E) (Methods). The arrow indicates the expected mass for a potential product, which was not found here in contrast to Figure 24C.

3.2. DISCUSSION

Plant secondary metabolite glycosyltransferases constitute a large enzyme family. They are presumed to be involved in the biosynthesis, homeostasis and regulation of the activity of numerous small molecular compounds in plants. However, enzyme-substrate relations and physiological roles of individual isoforms remain mostly obscure. In order to extend the knowledge on UGTs, publicly available databases were used to identify top-ranking stress induced UGT candidates, which might have important and yet unknown functions in plant responses to biotic and abiotic stresses. *UGT76B1*, the top-ranking isoform among stress-responsive UGTs, is present as a single isoform in its subclass [Figure 4; (Ross et al., 2001)]. Analysis of related Brassicaceae genomes revealed a highly conserved, single copy homolog (M. Das and G. Haberer, personal communication). These features suggested a unique and important function in plant stress responses.

3.2.1. Non-targeted metabolomics approach leads to identification of the UGT76B1 substrate

Despite major advances in plant biology due to genome annotations and omics approaches, a majority of gene products are still orphan enzymes without specific substrates and physiological roles (Fridman and Pichersky, 2005; Saito et al., 2008; Hanson et al., 2010). Although the annotation of an encoded enzyme e.g. as a UGT most probably denotes its activity as a transferase of an activated sugar to small-molecule acceptors, this knowledge does not provide a clue towards its native substrate(s), not to mention its *in vivo* function. In the case of UGTs, even sequence homology to already known isoforms does not allow to deduce substrate classes (Vogt and Jones, 2000; Bowles et al., 2006). Nevertheless, integration of metabolite profiling with independent evidence, in particular of transcriptional co-expression and comparative genomics, has strongly facilitated the elucidation of metabolic pathways and assignment of enzymatic activities (Hirai et al., 2005; Yonekura-Sakakibara et al., 2008; Matsuda et al., 2009; Ohta et al., 2010). In the case of the broadly stress-inducible *UGT76B1* gene co-expression analyses did not indicate an assignment which could hint towards a class of potential substrates. Thus, the use of a non-targeted approach employing ultra-high resolution FT-ICR mass spectrometry was aimed to obtain information on the affected pathway or substrate without any other prior knowledge. Non-targeted FT-ICR MS data are well suited to identify and differentiate metabolic patterns from distinct situations based on multivariate analyses (Ohta et al., 2010). In contrast to this approach, here a pairwise

comparison of m/z values from crude extracts of *UGT76B1* overexpression, *ugt76b1* loss-of-function, and wild-type lines was performed. Only two peaks fulfilled the criteria being both underrepresented in two independent knockout lines (in different accessions as background) and upregulated in two overexpression lines (Figure 21). Thus, this combinatorial approach allowed to pinpoint informative molecules from the non-targeted metabolome analyses. Since further fragmentation of these m/z peaks indicated that one of them was a glucoside, it was highly suggestive that it indicated the *in planta* product of UGT76B1. Eventually, enzymatic tests using the recombinant enzyme proved its ability to glucosylate the predicted aglycon *in vitro* and thereby established isoleucic acid as the UGT76B1 substrate.

3.2.2. *UGT76B1* affects SA-JA crosstalk and is affected by perturbations of the SA and JA pathways

SA and JA defense signaling pathways are known to interact in a partially antagonistic manner (Kloek et al., 2001; Spoel et al., 2003; Koornneef and Pieterse, 2008). Both *UGT76B1* overexpression and loss-of-function led to a disturbed equilibrium between these two pathways suggesting a role in SA-JA crosstalk. The complete loss of *UGT76B1* function led to constitutive enhancement of the SA-dependent defense and repression of the JA pathway, whereas *UGT76B1* overexpression led to the opposite effects (Figure 13 and Figure 26). Accordingly, knockout plants were more resistant to *Pseudomonas* infection, whereas *UGT76B1* overexpression rendered plants highly susceptible. On the other hand, *UGT76B1* expression was induced after *Pseudomonas* infection in the same time frame as the SA-dependent marker genes *PAD4*, *EDS1* and *WRKY70* and prior to *SAG13* and *PR1* (Figure 17 and Figure 26). These apparently contradicting findings indicated that *UGT76B1* might play an important role in suppressing the SA response in unchallenged conditions, while being required to attenuate it after pathogen attack. Controlled suppression of defense responses is important to avoid deleterious consequences and significant costs for the plant (for details see page 21). Consistent with its role in promoting the JA pathway *UGT76B1* was induced after wounding (Figure 19). The constitutive expression of *UGT76B1* found in hydathodes and young tissues could be involved in local enhancement of the JA pathway providing protection against herbivores or necrotrophs at these more vulnerable sites (Hugouvieux et al., 1998; Sprague et al., 2007).
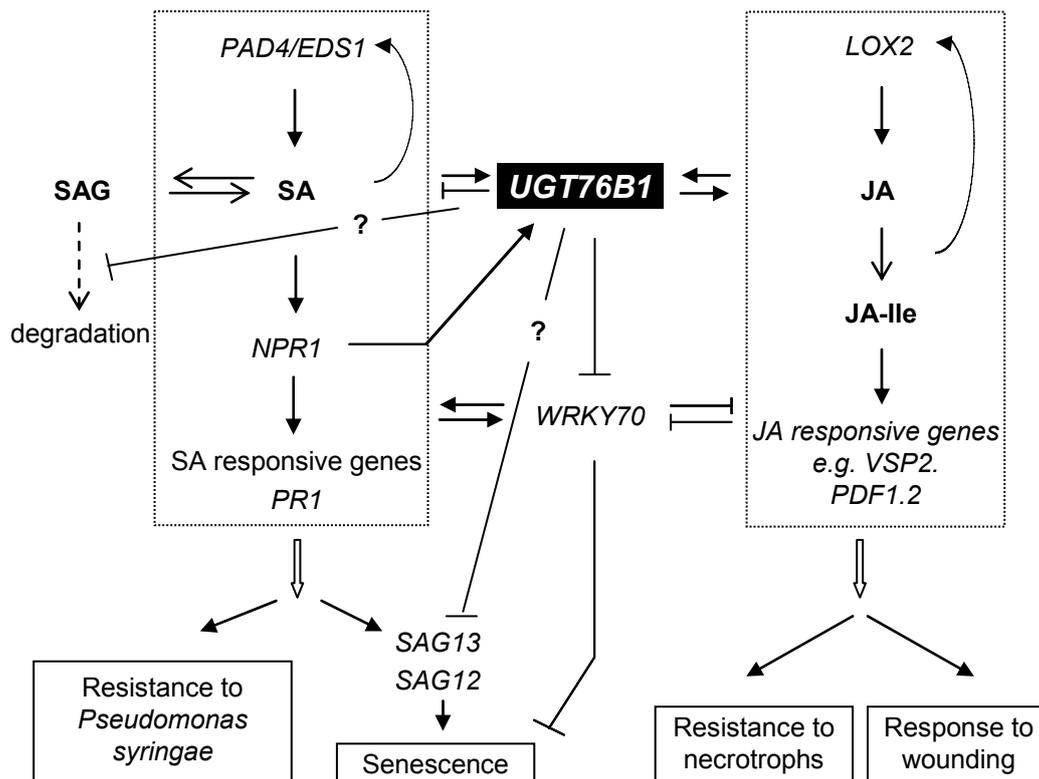
Figure 26. Proposed model of the involvement of *UGT76B1* as a novel mediator in SA-and JA-dependent regulation of defense responses and senescence.

The scheme shows two pathways regulating defense against (hemi-) biotrophic and necrotrophic pathogens and senescence. *UGT76B1* induces the JA response and represses the SA dependent pathway having a negative influence on the resistance to *P. syringae* and the onset of senescence. Only those signal transduction components, which are relevant to the discussed role of *UGT76B1*, are shown. Signaling molecules (bold), important transformations (open arrowhead), positive effect (closed arrowhead), negative effects ($\perp$) and important genes are indicated.

The induction or repression of *UGT76B1* expression of several mutants, which affect the SA pathway in unstressed conditions, provided additional evidence to correlate the glucosyltransferase with defense pathways in agreement with its SA-suppressive function (Figure 27). Profiling of *UGT76B1* expression in *Arabidopsis* mutants *cpr5*, *mkk1 mkk2* and *mpk4* revealed that the gene was highly induced in these plants, which displayed constitutively enhanced SA-dependent defenses (Bowling et al., 1997; Brodersen et al., 2006; Pitzschke et al., 2009). In contrast, *UGT76B1* expression was suppressed in mutants such as *eds1*, *sid2* (*eds16*) and *pad4* (Glazebrook et al., 1996; Feys et al., 2001; Wildermuth et al., 2001), which were impaired in SA-dependent responses (Zimmermann et al., 2005).

Arabidopsis thaliana (experimental)	<-3	-2	- 1	0	1	2	3 >	*Arabidopsis thaliana* (control)
cpr5							●	Col-0
mkk1 mkk2							●	Col-0
npr1						●		Col-0
mpk4					●			L*er*-0
pad4			●					Ws-0
sid2		●						Col-0
eds1		●						Ws-0
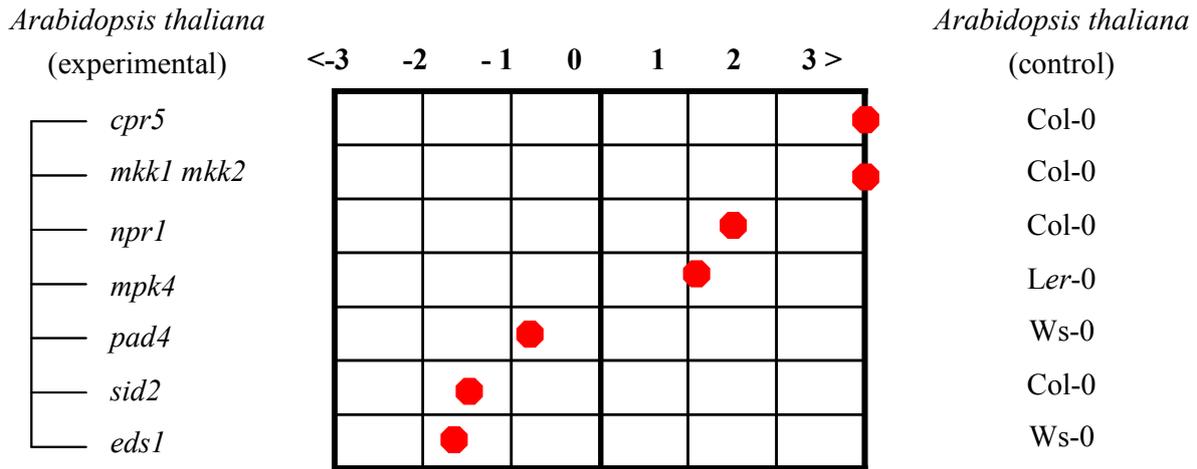
Figure 27. *UGT76B1* expression in several mutant backgrounds.

Picture was adapted from Genevestigator (Zimmermann et al., 2005). Relative expression is indicated in $\log_2$-scale. Experiment IDs of the related experiments are available at https://www.genevestigator.com.

Collectively, the observations and these data propose *UGT76B1* as a novel player in the SA-JA crosstalk acting as a negative modulator and attenuator of the SA response, while it positively affects the JA-dependent pathway. However, the general stress perception and SA/JA signal transduction pathways seemed to be functional independent of *UGT76B1* expression. This was demonstrated by the full inducibility of *PR1* after pathogen infection in *UGT76B1-OE-7* or by the root growth inhibition upon methyl jasmonate treatment in *ugt76b1-1* (Figure 15 and Figure 18).

3.2.3.   Integration of *UGT76B1* in SA-JA crosstalk

The integral role of *UGT76B1* in SA-JA crosstalk is further emphasized by the fact that it is the only *UGT* gene, except for *UGT72B1* and *UGT75B1*, which is induced by both methyl jasmonate and SA application. Therefore, links with two important players in the SA- and JA-response were examined.

NPR1 is an important central player mediating the SA response and suppressing JA-dependent reactions (Cao et al., 1997; Glazebrook, 2005; Koornneef and Pieterse, 2008; Vlot et al., 2009). Upon an SA stimulus oligomeric NPR1 is reduced in the cytosol and the released monomers are targeted to the nucleus, where they invoke SA-dependent downstream transcription in concert with TGA transcription factors. Spoel et al. (2003) provided evidence for a separate cytosolic function of NPR1 in repressing JA signaling. Transcriptional analyses

in *npr1-3*, in which nuclear targeting of NPR1 is abolished, while its cytosolic function to repress the JA response is retained, showed that *UGT76B1* induction is – at least in part – dependent on the nuclear function of NPR1 (Wang et al., 2006). In addition, Blanco et al. (2009) demonstrated that *UGT76B1* could be at least partially induced by SA in an NPR1-independent manner in the *npr1-1* mutant, in which both NPR1 functions were abolished. On the other hand, *npr1-1* vs. wild type expression analyses indicated an activation of *UGT76B1* in the *npr1* loss-of-function mutant (Figure 27). This finding would corroborate an NPR1-independent and even SA-independent upregulation of *UGT76B1*. Furthermore, since *npr1-1* is hampered in its ability to suppress the JA pathway in an SA-dependent manner, UGT76B1 might be linked to the cytosolic function of NPR1 in SA-JA crosstalk (Figure 26).

The transcription factor WRKY70 has important functions in integrating signals from the antagonistic JA and SA pathways. It acts as a negative regulator of JA-responsive genes and as a positive regulator of SA-induced genes and resistance to *Pseudomonas* (Li et al., 2004; Glazebrook, 2005; Ülker et al., 2007). *UGT76B1* deregulation in this work correlated with *WRKY70* transcription in accordance with WRKY70´s role in SA-JA crosstalk. Therefore, UGT76B1 could affect SA-JA crosstalk through WRKY70. The early and parallel upregulation of both *UGT76B1* and *WRKY70* after *Pseudomonas* infection would then relate to an attenuating function of UGT76B1 on *WRKY70* expression (Figure 17 and Figure 26). In this respect it should be noted that the role of WRKY70 in modulating SA-JA responses is not absolutely certain. Antisense suppression gave inconsistent results regarding changes in JA-responsive gene expression (Li et al., 2004; Ren et al., 2008). It was also unclear, whether *WRKY70* expression led to changes in free SA (Wang et al., 2006). Wang et al. (2006) suggested that WRKY70 acts both as a negative regulator of SA biosynthesis and as a positive stimulus of SA signaling. In this work, the *ugt76b1* knockout showed enhanced *WRKY70* expression, which was positively correlated with both SA biosynthesis and SA signaling. Therefore, UGT76B1 might overrule the effects of WRKY70 or it might act independently of WRKY70 (Figure 26).

At the metabolic level *UGT76B1-OE* lines exhibited enhanced SA glucose conjugate levels (Figure 16). This finding clearly demonstrated that an enhanced amount of SA conjugates did not relate to pathogen resistance. With respect to the role of UGT76B1 in the SA pathway, the increase in SA glucosides might be only a side-effect of the ectopic overexpression and the ability of UGT76B1 to conjugate SA. Alternatively, UGT76B1 could repress the hydrolysis or degradation of SA glucosides and thereby lead to its accumulation (Figure 26).

3.2.4. *UGT76B1* impacts on plant senescence

The onset of leaf senescence is influenced by various internal and environmental signals, such as stress and nutrient supply that are integrated with plant age. Unfavorable environmental factors can prematurely induce the senescence program (Lim et al., 2007). In addition to external stimuli, internal factors influence plant aging, as mutants with constitutive expression of defense responses frequently also show an accelerated onset of senescence (Yoshida et al., 2002; Barth et al., 2004; Consonni et al., 2006). Conversely, older plants showed enhanced pathogen resistance (Kus et al., 2002). These observations can be related to a considerable overlap between genes involved in defense and senescence signaling (Weaver et al., 1998; Quirino et al., 1999; Miao and Zentgraf, 2007). Some genes involved in the senescence process even seem to be directly regulated by SA (Quirino et al., 1999). Induction of *SAG12* during leaf senescence for example depends on the presence of SA (Morris et al., 2000). Similarly *WRKY53*, an important positive regulator at the early stage of leaf senescence, is induced by SA (Miao and Zentgraf, 2007). Furthermore, the early onset of senescence observed in the *mlo* mutant was shown to be due to increased SA levels (Consonni et al., 2006), whereas an SA-deficient *nahG* line showed delayed developmental senescence (Buchanan-Wollaston et al., 2005).

In line with the above, constitutive expression of defense related genes and increased SA accumulation could lead to the early onset of senescence in *ugt76b1* mutants. This conclusion is corroborated by the opposite findings in *UGT76B1-OE-7*. Supposedly, the SA pathway is involved mainly in developmentally triggered, but not in dark-induced senescence (Buchanan-Wollaston et al., 2005; van der Graaff et al., 2006). Since alteration in *UGT76B1* expression affected both types of senescence in this study, the discussed impact of *UGT76B1* on the equilibrium between the SA and JA signaling pathways seems to play a role not only in developmental but also in dark-induced senescence. A possible link between these two types of senescence is that H_2O_2 and SA have been shown to induce each other forming a feed-forward loop (Shirasu et al., 1997; Mateo et al., 2006; Vlot et al., 2009). H_2O_2 is an important reactive oxygen species (ROS) in plants and ROS-associated genes seem to play important roles in both developmental and dark-induced senescence (Navabpour et al., 2003; Guo and Crawford, 2005; Zimmermann and Zentgraf, 2005).

WRK70 is known as a negative regulator of senescence (Ülker et al., 2007), which contradicts our observation in *ugt76b1* knockout and *UGT76B1* overexpression lines where induced or repressed *WRKY70* expression correlated with an early or delayed onset of senescence, respectively. Therefore the observed senescence phenotype in *ugt76b1* mutants appears to

overrule the negative regulation by *WRKY70* (Figure 26). Alternatively, upregulation of *WRKY70* in *ugt76b1* could be a downstream countermeasure to the early onset of senescence observed in this mutant with the opposite effect in the *UGT76B1* overexpression line.

3.2.5.   Potential implications of isoleucic acid glucosylation in defense responses

The UGT76B1-dependent formation of isoleucic acid (ILA) glucoside negatively correlated with pathogen resistance and onset of senescence. Neither ILA nor its glucoside had been described before in *Arabidopsis*. However, ILA has been characterized in humans as the reduced form of 2-keto-3-methylvaleric acid, a degradation product of the branched-chain amino acid isoleucine (Mamer and Reimer, 1992; Podebrad et al., 1997). A genetic defect in the further oxidation of this product led to its accumulation along with other degradation products and the amino acids themselves in the maple sirup urine disease (Mamer and Reimer, 1992).

A correlation analysis based on microarray data at ATTED-II (Obayashi et al., 2009) provided additional evidence for a relationship of the *Arabidopsis*-derived ILA to amino acid metabolism. *UGT76B1* expression was linked to *LIPOAMIDE DEHYDROGENASE 2* (see Figure 28), a gene encoding a component of the branched-chain keto acid dehydrogenase complex, which catalyzes the oxidative decarboxylation of α-keto acid derivatives of Val, Leu or Ile (Binder et al., 2007). In addition, amino acid measurements of *ugt76b1-1* and *UGT76B1-OE-7* showed a significant disturbance of amino acid concentrations. Branched chain amino acids were increased in *ugt76b1-1*. One hour after wounding (induction of Ja-Ile conjugation) Ile, Val and Leu were increased in the knockout and reduced in the overexpression lines (Supplemental Figure 1). These results could be in accordance with reduced/increased glycosylation of a branched chain amino acid precursor. However, one should be aware that changes in amino acid levels could also be due to the differential onset of senescence in these lines. Concentrations of Ile, Leu, GABA, Tyr and Arg for example are known to increase during onset of leaf senescence (Diaz et al., 2005).
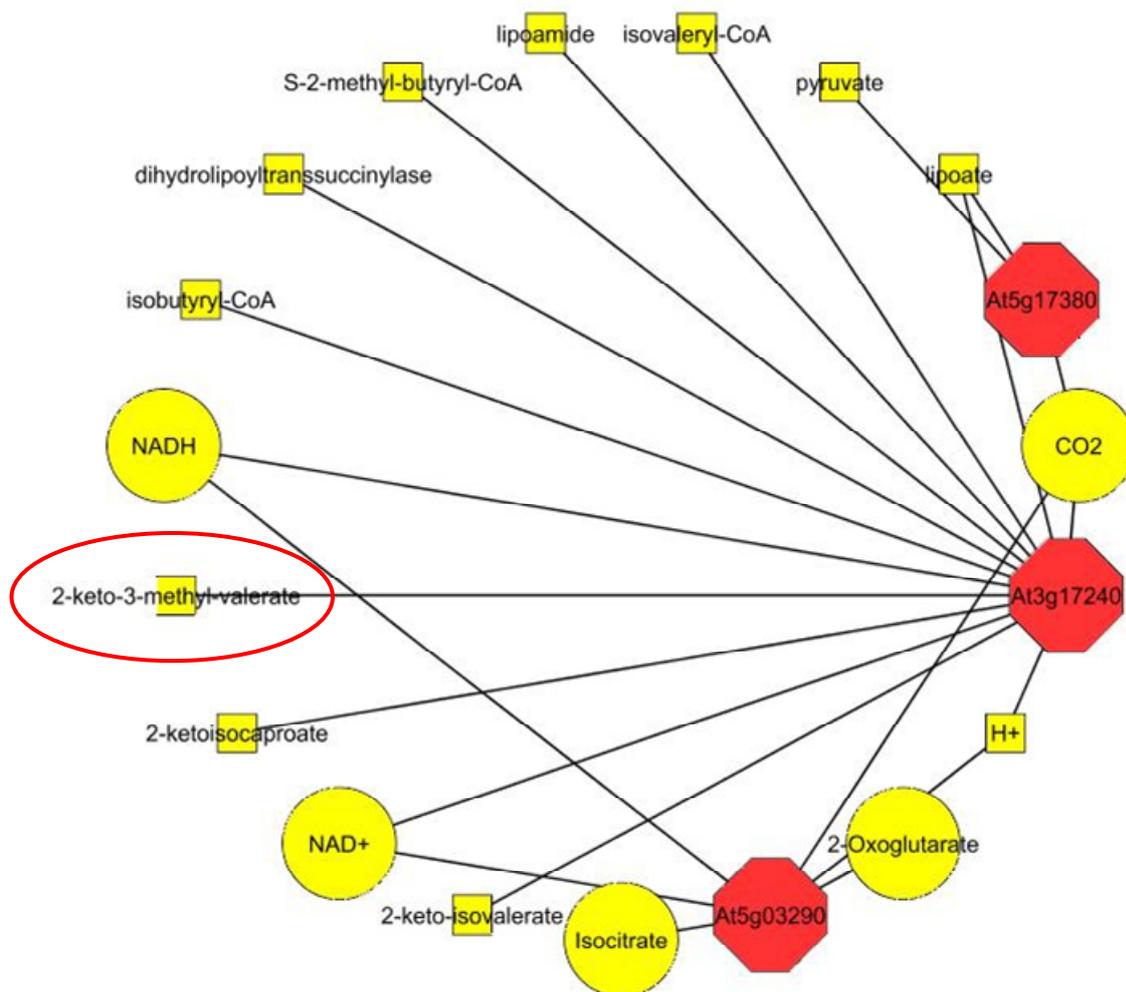
Figure 28. Network between genes correlated with *UGT76B1* hint to a relation of *UGT76B1* with branched chain amino acid degradation pathways.

The top ten genes coregulated with *UGT76B1* (http://atted.jp/) were analyzed by the Gene Networks tool at www.virtualplant.org (Obayashi et al., 2009). *At3g17240* (*LIPOAMIDE DEHYDROGENASE 2, LPD2*) is a gene encoding a component of the multienzyme α-keto acid dehydrogenase complex, which catalyzes the oxidative decarboxylation of the branched-chain α-keto acids derived from Val, Leu, and Ile.

The second compound with m/z 279 ($C_{11}H_{20}O_8$) found to be correlated with *UGT76B1* expression in our non-targeted metabolomics approach differed from the ILA-glucoside peak (m/z 293, $C_{12}H_{22}O_8$) by one CH_2 moiety. Therefore, it could represent the corresponding glucosylated compound derived from Val metabolism, although fragmentation did not yield cleavage of a glucose residue. Amino acid-derived molecules have also been related to *Arabidopsis* defense reactions by the involvement of two aminotransferases ALD1 and AGD2, which supposedly catalyze an amino transfer in opposite directions acting on an unknown α-keto acid/ α-amino acid couple (Song et al., 2004). The authors found that *agd2*

mutants were more resistant to *Pseudomonas syringae* infection, while *ald1* plant showed increased susceptibility.

Plant hormones are known to be regulated by conjugation with amino acids. In particular, Ile is known to be conjugated to JA forming JA-Ile, the main bioactive form of the hormone (Staswick and Tiryaki, 2004; Fonseca et al., 2009). SA can be also conjugated to amino acids (reviewed in Vlot et al., 2009) and overexpression of GH3.5, an enzyme potentially involved in this conjugation led to enhanced pathogen resistance and SA accumulation (Park et al., 2007).

Although the existence of several SA and JA amino acid conjugates is known, the direct involvement of amino acids in defense has been shown only in case of JA-isoleucine, which is the major bioactive form of jasmonate (Staswick and Tiryaki, 2004; Fonseca et al., 2009).

In the case of UGT76B1 it can be speculated that glucosylation of a degradation product or biosynthetic precursor of Ile could impact on the amino acid-hormone conjugation via a yet unknown mechanism and thereby influence defense responses.

Additionally, UGT76B1 could be involved in the synthesis of protective plant compounds. The biosynthesis of branched chain amino acids, for example, is known to be connected to the biosynthesis of aliphatic glucosinolates (Binder et al., 2007; Knill et al., 2008). If UGT76B1 was involved in wounding response (see induction after wounding Figure 19J) and defense towards chewing insects (JA defense response), glucosylation of the proposed amino acid precursors could also be a point of regulation for glucosinolate biosynthesis. Glucosinolate biosynthesis is known to be induced by wounding and insect attack.

Alternatively, ILA, its glucoside or its glucoside formation could be involved in another indirect way influencing SA and/or JA signaling. Thus, future research has to shed new light on the relationship between plant defense pathways, amino acid-derived metabolites and small-molecule glucosylation.

4. TOWARDS A FUNCTION OF STRESS INDUCIBLE *UGT87A2*

UGT87A2 was selected for further characterization because of its strong responsiveness to several biotic and abiotic cues, which suggested an important stress related role (Figure 4). The transcript was induced at least twofold in nearly all infection experiments, but also by several abiotic cues, i.e. as osmotic stress, UV-B irradiation, salt, oxidative stress and wounding. However, no involvement in any metabolic pathway or stress-related function was known.

The *UGT87* family comprises only two members, *UGT87A1* and *UGT87A2*. Only *UGT87A2* was highly stress responsive whereas *UGT87A1* did not respond to any treatment (Figure 4).

A genetic approach and non-targeted metabolome analysis should give hints about putative roles of *UGT87A2* in plant defense reactions. Analysis of transgenic plants harboring promoter-reporter gene fusions revealed specific expression of *UGT87A2* in hydathodes and root tips of young seedlings. Older plants also showed strong expression in anthers and filaments, older sepals, stigmata, tips of the siliques and silique internodes. Further, *UGT87A2* was strongly induced in all senescent organs and after treatment with an SA analog.

Non-targeted metabolome analysis of plants having altered glycosyltransferase expression did not reveal significant metabolic changes in two independent loss-of-function mutants, whereas independent overexpression lines showed several m/z peaks indicating up-regulated metabolites. Further characterization of these compounds led to the identification of a new metabolite, ascorbic acid 2-O-ß-glucoside, in *Arabidopsis*. Together with the upregulation of other putative compounds, the results suggest potential roles for *UGT87A2* in ascorbic acid homeostasis or cell wall biosynthesis.

4.1. RESULTS

4.1.1. Isolation and characterization of *ugt87a2* single knockout mutants

Two independent loss of function mutants GABI_686D07 and SALK_124038 were obtained as important experimental tool for *UGT87A2*. Insertion lines were verified by PCR genotyping and sequencing further confirmed the position of the insertion (Figure 29). Loss of the corresponding transcript was verified by RT-PCR. Lines from GABI_686D07 and SALK_124038 were named as *ugt87a2-1* and *ugt87a2-2* knockout mutants respectively.

A   ***UGT87A2* (At2g30140)**
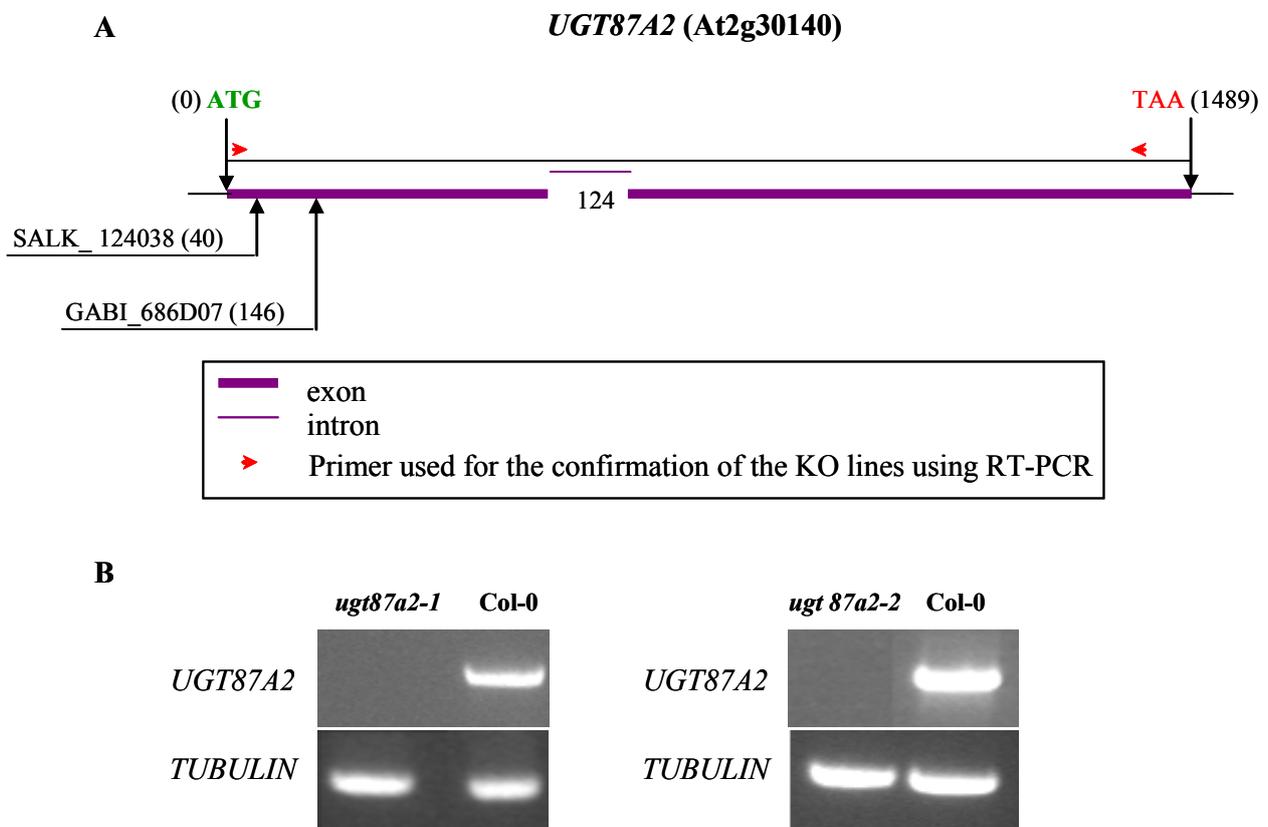
Figure 29. Molecular characterization of *ugt87a2* knockout lines.

(A) Position of the insertions within *UGT87A2* (At2g30140). **(B)** RT-PCR analysis of *UGT87A2* transcript levels in *ugt87a2-1* (GABI_686D07) and *ugt87a2-2* (SALK_124038) compared to their corresponding wild-type lines. *TUBULIN9* (At4g20890) transcript levels were assessed as a control.

4.1.2. Production and characterization of *UGT87A2* overexpression lines

In addition to the loss-of-function mutants, *Arabidopsis* lines expressing *UGT87A2* under the control of CAMV 35S-derived constitutive promoter were generated and characterized as described in 5.2.1.6. For seven independent and homozygous single insertion lines per each

vector (pB2GW7 and pAlligator2) a RT-qPCR was used on leaf material to identify lines showing a successful overexpression in the T2 generation. From three lines each, which showed a significantly higher transcript amount compared to the wild type, only two maintained the overexpression in the next generation (T3, see Figure 30). These were selected for further experiments, named *UGT87A2-OE-19* and *UGT87A2-OE-6*.

UGT87A2 Overexpression lines
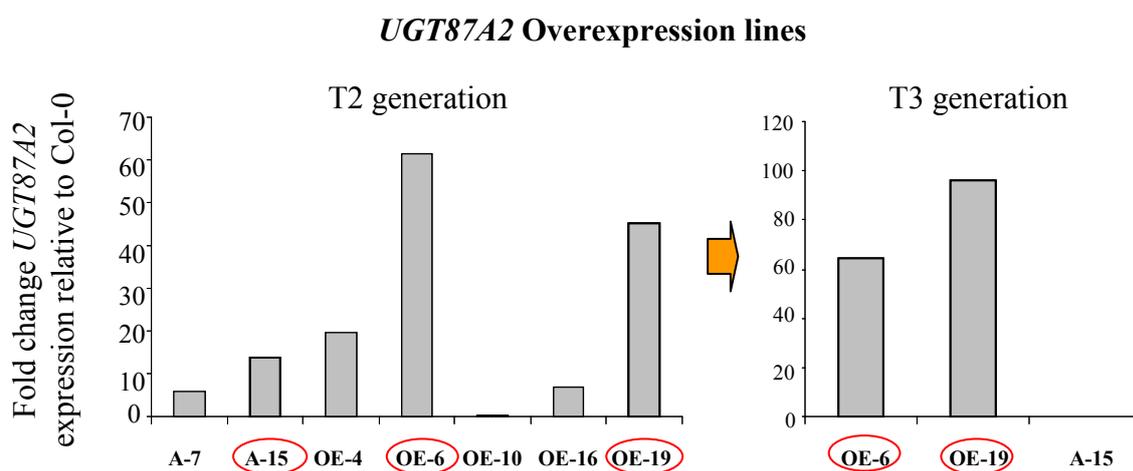
Figure 30. Molecular characterization of *UGT87A2* overexpression lines.

RT-qPCR of *UGT87A2* overexpression lines in two subsequent generations (T2 and T3). Plant material of the T3 generation was used for subsequent experimental analyses. Lines *UGT87A2-OE-6/10/16/19* are based on the binary vector pB2GW7, whereas pAlligator2 was used for generating *UGT87A2-A-7/15* (5.2.1.6).

4.1.3.   Cellular localization of *UGT87A2* expression and induction

To analyze the expression of *UGT87A2* in different plant organs and at different developmental stages, transgenic lines carrying an *UGT87A2*pro:GUS-GFP transgene were produced by *Agrobacterium*-mediated transformation. Two segregating, independent single insertion lines, *UGT87A2*pro:GUS-GFP-18 and *UGT87A2*pro:GUS-GFP-4 were selected for further analysis. Plants of different developmental stages (8d, 17d, and 36d) were analyzed, showing consistent GUS activity among two independent transgenic lines.

Specific expression of *UGT87A2* was found in hydathodes (Figure 31A, B) and root tips (A$_1$). In older plants, a strong expression was found in anthers and filament, older petals and sepals, stigmata, tips of the siliques and silique internodes (Figure 31C). Expression was also found in stomata and surrounding cells in the upper part of the hypocotyl (A$_2$). Further, *UGT87A2* seems to be strongly induced in senescent organs such as cotyledons of older plants (Figure 31B) and older petals (Figure 31C) and also senescent leaves as shown in the BAR database

(bbc.botany.utoronto.ca). A strong induction was observed in leaves 24 h after benzothiadiazole (BTH) treatment (Figure 31D, E).
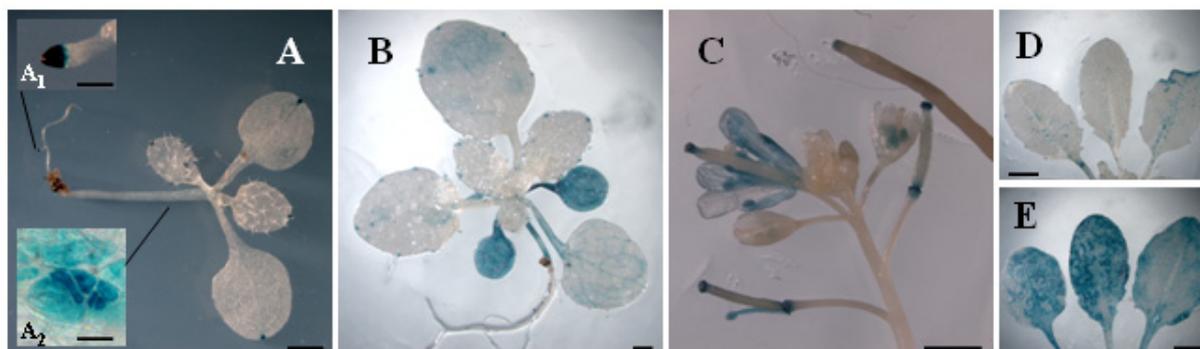
Figure 31. Cellular localization of *UGT87A2* expression using *UGT87A2*pro:GUS-GFP lines.

Transgenic *UGT87A2*pro:GUS-GFP-18 lines were stained for GUS activity in different developmental stages.
(**A**) 7-day-old seedling; (**B**) 17-day-old plant; (**C**) 28-day-old inflorescence and flowers; (**D**) before and (**E**) 24 h after BTH treatment.
Bars = 1 mm (A-C), 0.5 cm (D,E), 0.5 mm (A$_1$), 20 µm (A$_2$).

A strong induction of *UGT87A2* expression was also found in roots of plants grown on plates containing half Murashige and Skoog (MS) medium compared to growth on soil (Figure 32 vs. Figure 31A and B, 5.2.1.4). In order to get more detail about *UGT87A2* expression in roots, one-week-old seedlings of transgenic lines carrying the *UGT87A2*$_{pro}$:GUS-GFP fusion were analyzed with a confocal laser scanning microscope. Seedlings were grown on agar plates and stained with propidiumiodide to label the cell walls.

Figure 32. Seedling of *UGT87A2*pro:GUS-GFP lines grown on MS plates.

10-day old seedling grown on MS plates, stained according to 5.2.6. Picture shows strong induction of *UGT87A2* expression in roots of *UGT87A2*$_{pro}$:GUS-GFP-18 compared to Figure 31A, B.

Optical root cross sections showed expression of *UGT87A2* mainly in the root cortex and pericycle (Figure 33A). Expression in the root tip seemed to be localized mainly in the root cap (Figure 33B) and lateral root primordia (Figure 33C, D).
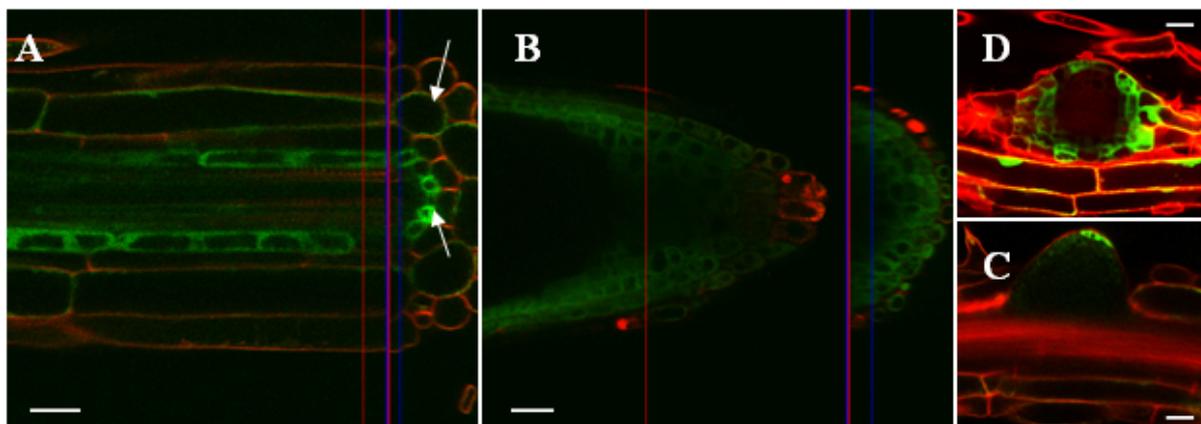
Figure 33. CLSM using *UGT87A2*pro:GUS-GFP lines.

Figure shows root sections from one-week-old seedlings grown on agar plates. Cell walls were counterstained with propidium iodide. (**A**) root cross section, arrows indicate pericycle (lower) and cortex (upper); (**B**) cross section of a main root tip; (**C**) forming lateral root; (**D**) cross section of (**C**). (A, B) *UGT87A2*pro:GUS-GFP-18, (C, D) *UGT87A2*pro:GUS-GFP-4. Bars = 25μm.

4.1.4. Towards putative substrates of UGT87A2 using non-targeted mass spectrometry

No obvious morphological differences were found in lines with altered *UGT87A2* expression compared to the wild type. Several stress conditions were applied to search for an influence of *UGT87A2* expression with regard to stress tolerance. The selection of the stressors was based on induction analysis using the BAR database (bbc.botany.utoronto.ca). No difference could be found in susceptibility towards biotic stressors such as *Ps-vir* (Supplemental Figure 2), nor towards abiotic stress cues such as UV-B treatment, osmotic and salt stress (Supplemental Figure 3). Since there was also neither an indication of the *UGT87A2* substrate nor the affected metabolic pathway, plants having altered *UGT87A2* expression were subjected to a non-targeted metabolomics approach to get more information about the impact of a loss or gain of *UGT87A2* function on plant metabolism. A 12 Tesla FT-ICR mass spectrometer run in the negative ionization mode was employed to compare the metabolic profile of *UGT87A2-OE* and *ugt87a2* mutant lines with their genetic background Col-0.

Leaf material of four-week-old plants was used as starting material. As *UGT87A2* was strongly inducible by BTH treatment (Figure 32 D, E), *ugt87a2* plants and Col-0 were treated with BTH (BION[TM], 0.254 mg/ml) 48 h before harvesting. For analysis of the overexpression lines vs. wild type, plants without prior treatment were used as starting material for metabolite extraction. Several metabolites were found to be upregulated in both overexpression lines

UGT87A2-OE-6 and *UGT87A2-OE-19* (Figure 34), whereas no significant metabolic changes could be found consistently in the two independent knockout lines (Supplemental Table 4).
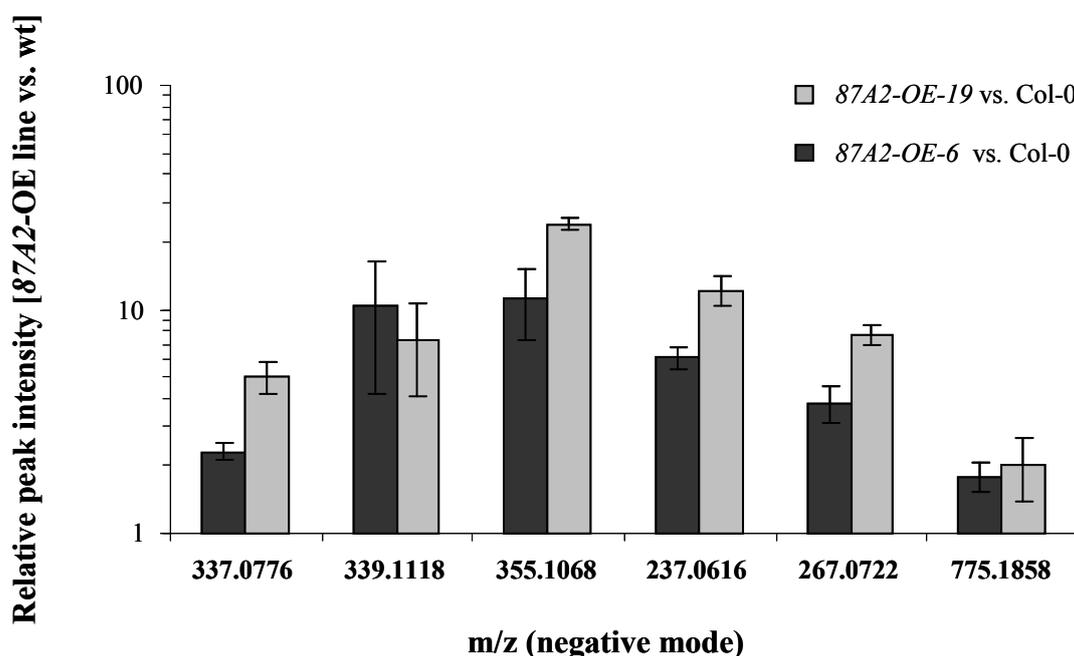
Figure 34. Metabolic changes found in *UGT87A2* overexpression lines (p-value < 0.01).

Means and standard deviation of three independent biological replicates, two technical replicates each are displayed. Peaks with m/z 339 and m/z 355 were not detectable in Col-0 (see Supplemental Table 3).

Due to the high accuracy in m/z determination, an exact molecular formula could be assigned to most peaks (Table 1). No distinct molecular formula could be assigned to m/z 775. Due to its high molecular mass several possible elemental compositions fitting the measured m/z ratio existed. Searching for possible molecular structures based on the identified formulas, half of the peaks could be attributed to putative compounds (Table 1).

No possible compound could be found for the two sulfur containing peaks m/z 339 and m/z 355. The ion m/z 237 ($C_8H_{14}O_8$) might be 2-keto-3-deoxy-D-manno-octulosonic acid (KDO), a glycosyl residue of the pectic polysaccharide rhamnogalacturonan II (RG-II) present in plant cell walls and undoubtedly also in *Arabidopsis* (Zablackis et al., 1995; Seveno et al., 2010). Anion m/z 267 ($C_9H_{16}O_9$) fits several possible molecular structures, but none of them has been described in *Arabidopsis* yet. KDN (2-keto-3-deoxy-D-glycero-D-galactononononic acid), for example, is a sialic acid that occurs widely among vertebrates and bacteria, but is thought to be absent in plants (Zeleny et al., 2006). Although mannosylglycerate (a thermoprotectant found in thermophilic bacteria), another putative candidate with m/z 267, exists in *A. thaliana*

according to Masstrix (5.2.7.1.4), this could not be confirmed by any other database or publication.

Table 1. Molecular formulas and putative compounds induced in *UGT87A2* overexpression lines.

The last column shows the molecular formula of the resulting fragment after glucoside fragmentation if observed (n.a.: not analyzed; n.d.: not detected). The ion m/z 337 was selected for further identification.

m/z [M-H]	Predicted molecular formula [M]	Putative compound	Glucose fragmentation ($-C_6H_{10}O_5$)
337.0776	$C_{12}H_{18}O_{11}$	ascorbic acid-glucoside?	$C_6H_8O_6$
339.1119	$C_{13}H_{24}O_8S$	?	$C_7H_{14}O_3S$
355.1069	$C_{13}H_{24}O_9S$	?	n.a.
237.0616	$C_8H_{14}O_8$	KDO (polysaccharide; biosynthesis cell wall)	n.d.
267.0722	$C_9H_{16}O_9$	mannosylglycerate, KDN?	n.d.
775.1857	n.i.	-	n.a.

4.1.5. Unknown compound with m/z 337 is identified as an ascorbic acid glucoside

As the main focus was to get hints on diagnostic metabolic changes or even on putative *UGT87A2* substrates, *UGT87A2*-induced peaks were analyzed primarily for glucosides. Fragmentation of glucosidic structures can lead to both, heterolytic or homolytic cleavage yielding the aglycon fragment ion $[Y_0]^-$ and the radical aglycon ion $[Y_0\text{-H}]^-$, respectively. The expected mass losses are 162 and 163 for a heterolytic and homolytic glucoside cleavage, respectively. Fragmentation studies revealed that two of the *UGT87A2*-induced peaks (m/z 337 and m/z 339) were glucosides and therefore putative substrates of *UGT87A2*. The ion m/z 337 showed mainly heterolytic, but also homolytic cleavage of a glucose moiety (Figure 35a), whereas for m/z 339 only glucoside elimination (heterolytic cleavage) could be observed (Supplemental Figure 4).

Whereas no compound could be found with the molecular formula $C_{13}H_{24}O_8S$ (m/z 339), $C_{12}H_{18}O_{11}$ (m/z 337) was identified as putative ascorbic acid glucoside. As m/z 339.111 was also undetectable in the wild-type line, the peak with m/z 337.077 was selected for further identification.

Ascorbic acid-2-O-α-glucoside (AA-2G[TM]) is the only stereoisomer which is commercially available, widely used in cosmetics, by the pharmaceutical industry and as a food additive

(Yamamoto et al., 1990a; Yamamoto et al., 1990b; Mandai et al., 1992). Naturally occurring stereoisomers of AA-2G, 2-O-β-D-glucopyranosyl-L-ascorbic acid (AA-2βG) and 6-O-β-D-glucopyranosyl-L-ascorbic acid have been identified in *Lycium barbarum* fruit and Cucurbitaceae, respectively (Toyoda-Ono et al., 2004; Hancock et al., 2008). No ascorbic acid glucoside has been described in *Arabidopsis thaliana* yet. Fragmentation analysis of the peak originating from the plant extract compared to the commercial standard AA-2G[TM] (Hayashibara Biochemical Laboratories, Japan) should give hints on the structure of the unknown compound. As shown in Figure 35, the m/z 337 ion from the *UGT87A2-OE-19* plant extract showed similar fragmentation pattern as AA-2G[TM]. Further, fragmentation of the ascorbic acid aglycon verified the loss of the first fragment ($C_2H_4O_2$) from the ascorbic acid part of the molecule (Figure 35c, Figure 36).

The results presented confirmed that m/z 337 was an ascorbic glucoside, but at this point the stereochemistry of the molecule remained unknown. Ascorbic acid-2-O-α-glucoside (AA-2G[TM]) is only a commercial conjugate, which has not been described from natural sources yet. Additionally, both heterolytic and homolytic glucoside cleavage could be observed for the unknown m/z 337, whereas AA-2G only showed homolytic cleavage. Both strongly suggest that the plant compound with m/z 337 was not the α-glucoside. Instead, 2-O-β-D-glucopyranosyl-L-ascorbic acid (AA-2βG) is a naturally occurring stereoisomer and putatively also identical with the unknown compound found in *Arabidopsis* plants.
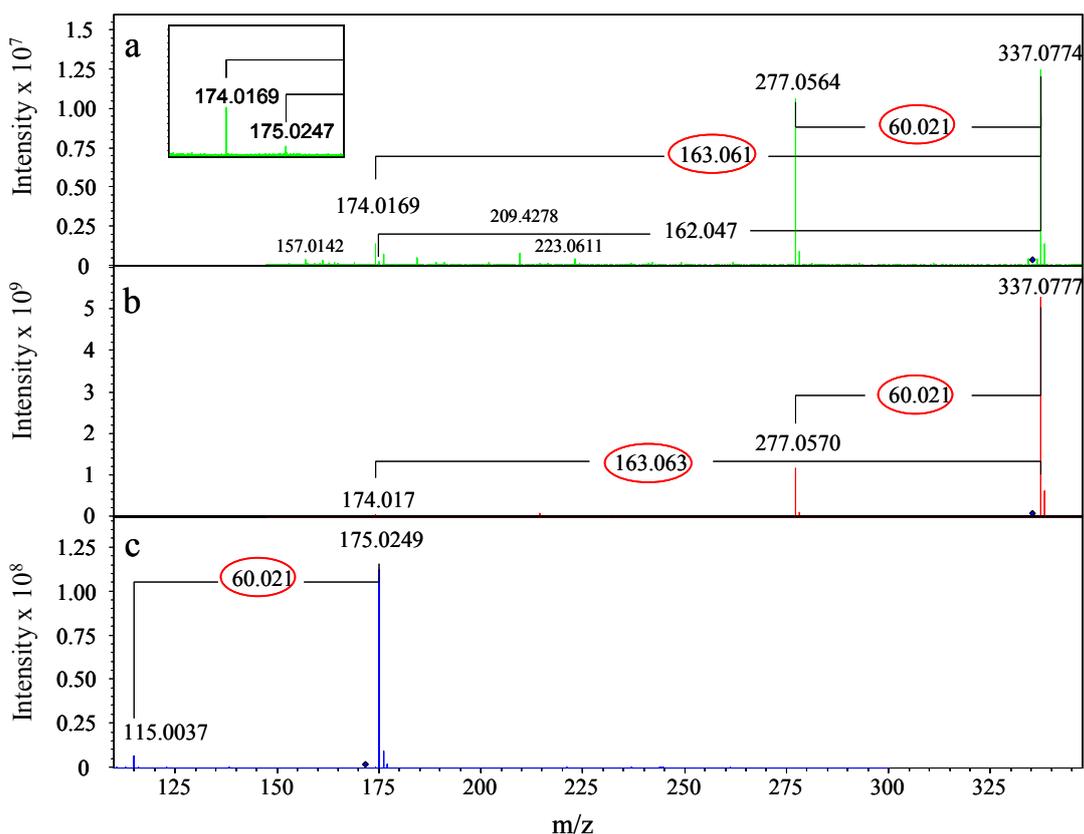
Figure 35. Identification of m/z 377 as an ascorbic acid glucoside.

Fragmentation patterns of (a) m/z 337 from the plant extract (*UGT87A2-OE-19*), (b) AA-2G[TM] and (c) ascorbic acid. Collision energy: 15eV. Loss of 163 Da confirms homolytic glucoside cleavage, whereas loss of 60 Da ($C_2H_4O_2$) originates from the ascorbic acid part of the molecule.
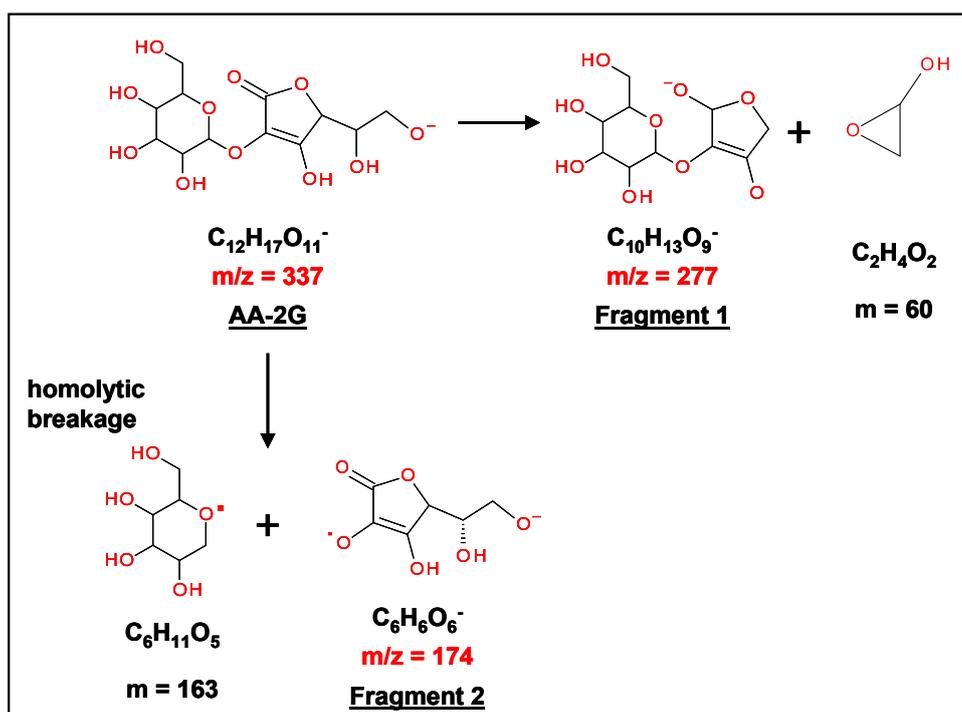
Figure 36. Fragmentation pathway of ascorbic acid 2-O-α-glucoside (AA-2G[TM]).

4.1.6. **Confirmation of induction of ascorbic acid-2-O-β-glucoside in**
UGT87A2-OE-19 using HPLC analysis

To get further information on the stereochemistry of the unknown plant compound with m/z 337, a new approach using HPLC analysis was used. Tai and Gohda (2007) established a convenient method to separate the α-glucoside and β-glucoside conjugates of ascorbic acid using hydrophilic interaction chromatography. As AA-2βG is not commercially available, _Lycium barbarum_ fruit extract, known to contain huge amounts of AA-2βG (Tai and Gohda, 2007), was used as a natural standard for HPLC analysis.

As shown in Figure 37 (A-C), the 2-O-β-D-glucopyranosyl-L-ascorbic acid peak from _Lycium_ was comigrating with a minor HPLC peak, which was enhanced in the _UGT87A2_ overexpression line (see also Supplemental Figure 7). Exact comigration of the unknown peak with AA-2βG was confirmed by a _UGT87A2-OE-19_ plant extract spiked with _Lycium_ fruit extract (Figure 37D). The corresponding peak from _UGT87A2-OE-19_ was collected and the corresponding m/z 337 confirmed via FT-ICR-MS (Figure 37E).
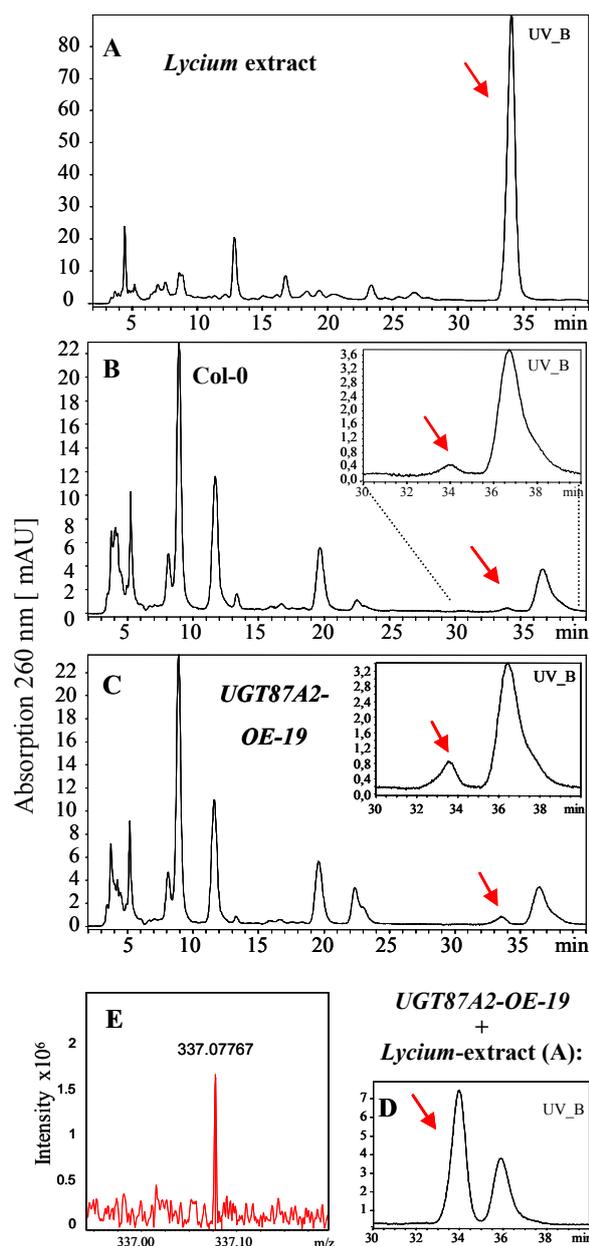
Figure 37. HPLC chromatograms indicating the presence and induction of AA-2ßG (red arrow).

(A) *Lycium barbarum* plant extract.
(B) wild-type plant extract (Col-0).
(C) *UGT87A2-OE-19* plant extract.
(D) (C) spiked with a small amount of (A) to confirm coelution of both peaks.
(E) FT-ICR-MS signal m/z 337, detected in the collected peak.

4.1.7.   Analysis of the *in vitro* activity of recombinant UGT87A2 towards ascorbic acid

To test whether UGT87A2 was able to glycosylate ascorbic acid *in vitro*, the activity of the recombinant enzyme was tested towards this putative substrate. As shown in Figure 38, no glucoside formation could be observed after incubating the enzyme for one hour in the presence of ascorbic acid (5.2.5.2). Even after 3 hours of incubation no product formation could be observed (results not shown). Nothing is known about substrate specificity of UGT87A2, therefore no positive control reaction could be performed to check, if the recombinant protein showed any activity. Although glycosylation of ascorbic acid could not

be confirmed, due to the lack of a positive control, it can not be excluded as a putative substrate.
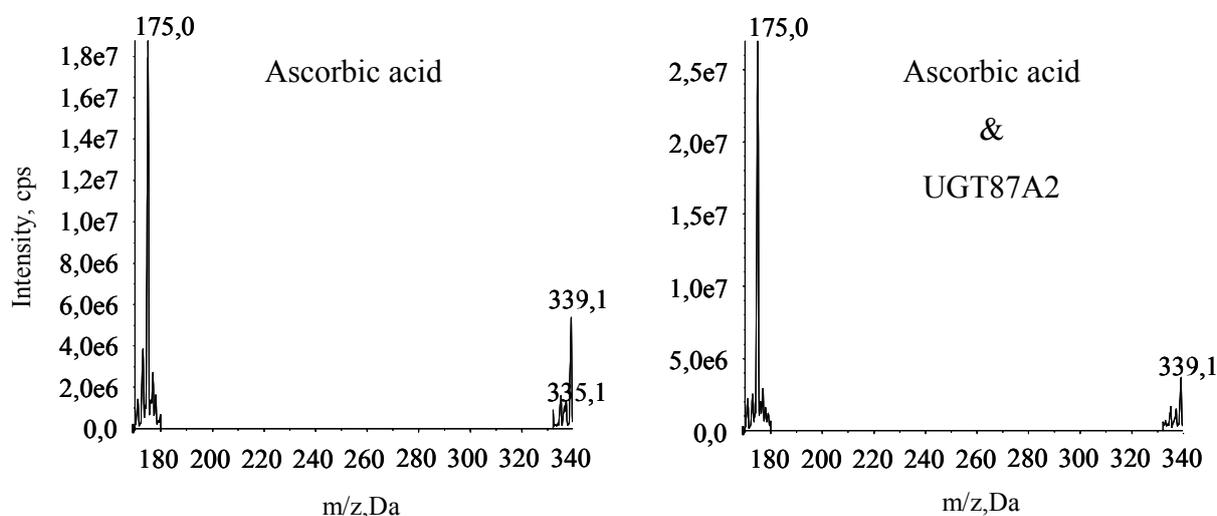
Figure 38. *In vitro* **activity assay of UGT87A2 towards ascorbic acid.**

Reactions were analyzed by mass spectrometry (5.2.5.2). The m/z values of the corresponding substrate and product are m/z 175 and m/z 337 respectively. The experiment was independently repeated with similar results.

4.1.8. *UGT87A1* is a close homolog of *UGT87A2*

Although several metabolites were found to be induced in *UGT87A2-OE* lines, no significant metabolic changes could be found in the *ugt87a2* knockout lines. A possible explanation for that could be the existence of a redundant gene with a similar function which would compensate the loss of *UGT87A2* in the knockout lines. *UGT87A2* indeed has a close homolog, namely *UGT87A1* (Ross et al., 2001), which shows 76% protein identity (see Supplemental Figure 5).

Co-expression analysis of *UGT87A1* using ATTED (http://atted.jp/) shows the highest mutual rank co-expression score with a putative ascorbate oxidase (Supplemental Figure 6).

UGT87A1 shows only low expression, but is expressed in similar tissues compared to its homolog *UGT87A2* (Figure 39). As shown in Figure 4, *UGT87A1* was also not inducible by any biotic or abiotic stress factor which could point out a fundamental physiological function, whereas the highly responsive *UGT87A2* seemed to function specifically during stress response.
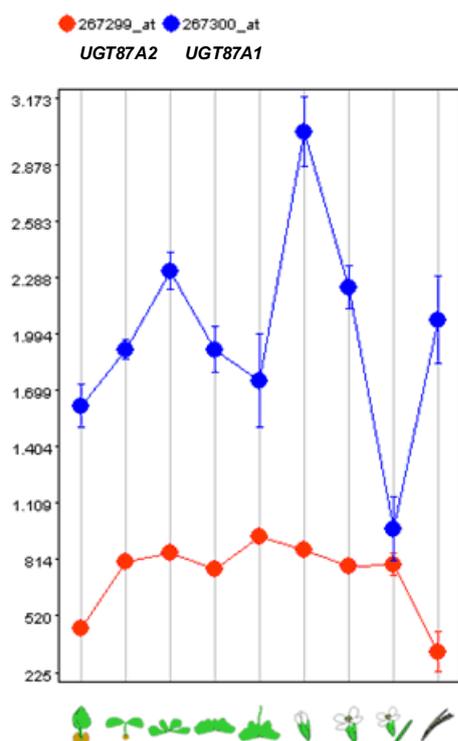
Figure 39. Expression profiles of *UGT87A2* and *UGT87A1*.

(https://www.genevestigator.com)

4.1.9.   Generation of *ugt87a2* amiR*UGT87A1* by amiRNA technology

To test our hypothesis that *UGT87A1* and *UGT87A2* have redundant functions, a further approach generating a double knockout-knockdown was started. The fact that both genes are linked close to each other on chromosome 2 did not allow to generate a double mutant by crossing two single knockouts. The amiRNA technology is an effective tool for specific gene silencing especially when two closely linked genes or several related target genes need to be silenced. It exploits endogenous miRNA precursors to generate small RNAs that direct gene silencing in plants (Schwab et al., 2006). Here the amiRNA technology was used to downregulate *UGT87A1* in *ugt87a2* mutant background. *ugt87a2-1* lines were transformed with an amiR-*UGT87A1* construct to generate *ugt87A2-1* amiR*UGT87A1* lines (see 5.2.4.8.2). The artificial microRNA designer WMD2 was used for selection of an appropriate target site. It delivers several amiRNA candidates based on different criteria such as sequence specificity, complementarity and other principles for amiRNA (Schwab et al., 2006). Two different amiR constructs (amiR-1 and amiR-13), targeting different regions in *UGT87A1* mRNA, were used for plant transformation. Both showed no off-targets and are located in mRNA regions with a somewhat open conformation as predicted by the RNAfold web server (Figure 40). amiR-1 was located closer to the 5´ end, whereas amiR-13 targeted a region closer to the 3´ end of the mRNA.

67

A

	sequence	perfect match hybridization energy (kcal/mole)	hybridization energy (kcal/mole)	target sequence
amiR-1	TTGACACAAAACACGTAGCCG	-43.29	-37.66	CAGCUACGUGUUUUGUGUCAU
amiR-13	TATGATGTAAGTATGGGCGGT	-43.89	-34.45	AUCGCCGAUACUUACAUCAUU

B

>gi|18402275 (**At2g30150** mRNA)
AUGCCUUGGCCAGGAAGAGGCCACAUCAACCCAAUGUUAAACCUCUGCAAAAGCCUCGUCCGGCGAGACCCAAACCU
CACCGUCACAUUCGUCGUCACCGAAGAAUGGCUCGGGUUCAUCGGGUCCGACCCGAAACCUAACCGGAUCCAUUUCG
CCACUCUCCCCAACAUCAUUCCCUCCGAGCUCGUCCGAGCCAACGACUUCAUCGCCUUCAUCGACGCCGUCCUCACC
AGAUUAGAAGAGCCGUUCGAACAGCUACUUGACCGUCUAAACUCUCCUCCCCACCGCAAUCAUCGCCGAUACUUACAUC
AUUUGGGCAGUACGUGUAGGCACAAAAAGGAAUAUUCCGGUGGCUUCUUUCUGGACUACGUCAGCCACGAUUCUCUC
CCUCUUCAUUAACUCCGAUCUUCUCGCAAGUCACGGCCAUUUUCCGAUCGAAUCAAAACUAGACGAGAU
UGUUGAUUACAUCCCCGGUUUAUCUCCGACAAGACUCAGUGACUUACAGAUCUUACACGGCUAUAGUCAUCAAGUCUU
CAAUAUAUUCAAAAAGUCUUUCGGUGAGCUUUAUAAAGCUAAGUAUCUUCUCUUCCCUUCUGCUUAUGAGCUCGAACC
AAAAGCCAUUGACUUUUUCACUUCCAAGUUUGAUUUCCCGGUUUACUCCACUGGUCCGUUAAUACCCUUGGAAGAACU
AUCCGUUGGAAAUGAGAAUAGAGAACUUGAUUACUUUAAGUGGCUUGAUGAGCAACCUGAAAGCUCUGUUCUUUACA
UAUCUCAAGGGAGUUUUCUUUCAGUCUCCGAAGCUCAGAUGGAGGAGAUUGUUGUAGGAGUUAGAGAGGCUGGAGU
UAAGUUCUUUUGGGUGGCUCGUGGGGGGUGAGUUAAAGCUUAAGGAGGCUCUUGAAGGUAGCUUGGGGUGUUGUGGU
GAGCUGGUGUGAUCAGCUACGUGUUUUGUGUCAUGCGGCUAUAGGCGGGUUUUGGACGCAUUGCGGGUAUAACUCG
ACAUUGGAAGGGAUAUGUUCGGGAGUACCGUUGCUUACAUUUCCUGUUUUUUGGGAUCAGUUUCUGAAUGCUAAGAU
GAUUGUUGAGGAGUGGAGUGGAAUGGGGAUCGAGAGGAAGAAGCAGAUGGAGUUGUUGAUAGUGAGUGAUGAGAG
AUCAAGGAAUUGGUAAAAAGGUUUAUGGAUGGAGAGAGUGAAGAAGGGAAAGAGAUGAGAAGAAGGACUUGUGAUCU
CAGUGAGAUAUGUCGUGGAGCGGUUGCGAAAGGUGGUUCUUCUGAUGCUAACAUCGAUGCUUUCAUUAAAGAUAUUA
CUAAGAUCGUGUGA
.....(((((..(((((((..((((..((((..........((((((......(((((((((.(((........))).))((.((((((.(((....))).)))))..((.((((..(((((.....))))))....)))).))((.(((((.(((((((.(((.(((((((((.((..
..(((..))))((((((((((((..((((..((.....)))((((..(((((.(((((((.(.(((((........)))))).))..))...........((((((.......(((.(((((-(((.((-(((...))-..))))-))))).)))........(((.....))))))))))))))).))
)))..............(((((((((((((((((((..(((((((((-(((.(((((.(((-...(((((((((.((-.(((-..(((......((((...))(((((...(((((((((-...((((((((((.-.(((((((((.-((((((.((-((.-((.......))))-..))))))..-)))
)))......(((((((.....((((((((.(((((((...(((((-.((....(((.((((((.......(((((((....((((((((...(((((((((((-.(((((((((.(((((((..(((((...(((((.......)))))...)))))....))))))))..(((((((.((((((.((((((((
(((.(((((((.....))))))).((((((...))))..-........)))))))))...-))).)).))).))).-((((((.(((((((((....((......))-.))))))))....))))).))))-)))..)))))))...))))))-.))))))))))))))-)))).))-)))))...))))
))))))))))))....-))))))))))).-))))))))))))))))))))))((((((.-((((((.-(((.((......))).-..))-...))))))..))).-))).-))--))).......)).)).----)).-)))))).-.)))).-))))-.....-((((((.....))))(((((...)))))..)).-.)
)).)))))..))).-)))))))))..-)))..-)))))))).-)))))-.)))).-.)))))))))))))..))-)))))))).-(((((.....))))..............))).-)))))))..))))))))..))))))))))......-(((-.....(((((...)))))...)))))))).-.)
))))......)))))))))))...))))(((((((((.(((-.................)))))).))).
(-415.14)

Figure 40. Selection of amiRNAs targeting *UGT87A1*.

(A) Selected amiRNAs.
(B) Position of the selected amiRNA candidates in *UGT87A1* mRNA sequence. The dot
bracked notation shows the conformation of the estimated secondary structure with amiRNA
location. Unpaired bases are represented by dots, a base pair between base x and y is
represented by a '(' at position x and a ')' at position y. The RNAfold server
(http://rna.tbi.univie.ac.at/cgi-bin/RNAfold.cgi) from the Vienna RNA Websuite (Gruber et al.,
2008) was used for secondary structure prediction.

Cloning of the amiRNAs and plant transformation were performed as described in 5.2.4.8.1.
Molecular analysis of amiRNA plants was performed by RT-qPCR in primary transformants
(T1 generation). Selected transformants which showed successful *UGT87A1* downregulation
were selected for further characterization in the T2 generation. As shown in Figure 41A, both
amiRNA constructs led to downregulation of *UGT87A1*, although amiR-1 showed a much
stronger effect. *ugt87a2 amiR-87A1-1* lines showed 73-92% reduction of *UGT87A1*
expression compared to the wild-type plant, except one line (amiR-1-5), which surprisingly
showed a high induction of *UGT87A1*. In contrast, only 24-66% reduction could be observed

in the *ugt87a2 amiR-87A1-13* lines (Figure 41A). Seven lines were selected for a second molecular analysis in the T2 generation, all of them showed successful inheritance of the amiRNA functionality (Figure 41B).

Figure 41. Molecular characterization of *ugt87a2-1* amiR-*UGT87A1* lines.

RT-qPCR of *ugt87a2* amiR-*UGT87A1* lines was performed in two subsequent generations (T1 and T2) after transformation. Lines selected for further analysis are marked with a red box. Plant material of the T2 generation was used for subsequent experimental analyses.

Two lines, *ugt87a2* amiR-*UGT87A1-1-6* and *ugt87a2* amiR-*UGT87A1-1-9* were selected for further analysis. A metabolome analysis (as described in 5.2.7.1, one experiment) of these lines [harvested 48 h after BTH treatment (BION^{TM}, 0.254 mg/ml)] revealed no significant changes compared to the wild-type in any of the masses that were induced by *UGT87A2* overexpression (see Supplemental Table 5). Data from one single experiment indeed showed

several m/z peaks with significant difference compared to the wild type. These could give hints at additional pathways affected by *UGT87A2* and *UGT87A1* expression, although measurements have to be confirmed by an independent experiment.

4.2.   DISCUSSION

4.2.1.   Ascorbic acid 2-O-ß-glucoside is a new compound identified in *A. thaliana* which is induced in *UGT87A2* overexpression lines

L-ascorbic acid (vitamin C) is a primary antioxidant in both animals and plants and serves as an important reactant in hydroxylation and other redox reactions. Mammals have to ingest L-ascorbic acid (AA) with their diet as they lost the capability of its synthesis. AA deficiency causes the common scurvy disease. Plants provide the major source of dietary vitamin C. In plants ascorbate plays an important role in developmental processes such as flowering, senescence and morphogenesis (Barth et al., 2006; Olmos et al., 2006) and in the regulation of cell signaling (Pignocchi and Foyer, 2003) as well as in transcription and/or stabilization of specific mRNAs (Arrigoni and De Tullio, 2002). It is also involved in defense reactions against biotic (Barth et al., 2004; Pavet et al., 2005; Goggin et al., 2010) and abiotic stresses such as high temperature (Larkindale et al., 2005), ozone (Conklin and Barth, 2004), high light (Müller-Moulé, 2008) and serves as a cofactor in the synthesis of plant hormones (Arrigoni and De Tullio, 2002). No viable mutant has been found so far that is totally devoid of ascorbate (Smirnoff et al., 2001), which further underlines the importance of this small molecule. Therefore, research towards a better understanding of its biosynthesis and metabolism is of huge interest and may have potential applications in enhancing environmental stress tolerance in plants as well as in elevating the nutritional value of food (Hemavathi et al., 2010; Wang et al., 2010).

Due to its protective and antioxidant capacity, ascorbate is widely used as an additive in the pharmaceutical, cosmetic, and food industry. However, AA is intrinsically unstable and several attempts have been made modifying its structure in order to increase stability. Glycosylation is known to change the stability and solubility of molecules and plays an important role in the compartmentation of small molecules. Among several AA conjugates, ascorbic acid-2-O-α-glucoside (AA-2G) is the most widely used in industry (Yamamoto et al., 1990a; Yamamoto et al., 1990b; Mandai et al., 1992). AA-2G is synthesized from AA and α-glucans by regioselective transglycosylation with cyclodextrin glucanotransferase from *Bacillus stearothermophillus* (Aga et al., 1991). It is highly stable, but after oral administration it is rapidly hydrolyzed to generate the active AA (Nakamura and Oku, 2009). Naturally occurring stereoisomers of AA-2G, 2-O-β-D-glucopyranosyl-L-ascorbic acid (AA-2βG) and 6-O-β-D-glucopyranosyl-L-ascorbic acid (AA-6βG) have been identified in *Lycium* fruit and Cucurbitaceae, respectively (Toyoda-Ono et al., 2004; Hancock et al., 2008). The

latter authors showed that only AA-6βG had a strong reducing activity towards dichlorophenolindophenol (DCPIP). DCPIP reduction by AA requires both the C2 and C3 hydroxyl groups (Rao et al., 1987). In contrast to AA-6βG, AA-2G^{TM} was also completely resistant to oxidation by either H_2O_2 or ascorbate oxidase. Oxidation by both, H_2O_2 or ascorbate oxidase, needs a free hydroxyl group at the C2 position of the ascorbic acid molecule (Isbell and Frush, 1979; Casella et al., 1999).

By performing a non-targeted metabolome analysis a compound in *Arabidopsis thaliana* leaf extract was identified the molecular formula of which was identical to an ascorbic acid glucoside. Mass spectrometric fragmentation studies and HPLC analyses revealed it to be AA-2βG. Overexpression of *UGT87A2*, a highly stress inducible glycosyltransferase, led to up-regulation of this compound among few other metabolites. The induction of ascorbic acid 2-O-β-glucoside *in planta* through overexpression of a *UGT*-gene highly suggests that AA-2βG is an endogenous compound of *Arabidopsis thaliana* and does not stem from exogenous contamination. No ascorbic acid glucoside conjugate had been identified so far in *Arabidopsis* and results indicate a new step of ascorbic acid metabolism and regulation in this model plant species.

Concentration and redox status of the AA pool in plants is tightly controlled, but despite huge research efforts progress towards understanding the underlying mechanisms, the responsible control mechanisms for AA biosynthesis and degradation remain still largely unknown (Wolucka and Van Montagu, 2007; Linster and Clarke, 2008). Considerable uncertainties remain concerning the genetic and biochemical controls of pathway flux (Hancock and Viola, 2005) as well as the control of AA distribution at the whole plant level. AA-2βG could serve as stable storage and even transport form of AA, without an antioxidant capacity, which could easily be activated after β-glucosidase treatment. AA conjugation could be part of the still unknown mechanisms controlling the AA pool and its redox status.

In *Lycium* plants AA-2ßG was only found in fruits and detected in neither leaf nor root. The content in fresh fruit was about 0.2-0.3%, which is comparable to the ascorbic acid content of fresh lemons (Toyoda-Ono et al., 2004). Nothing was known about a possible role of ascorbic acid glycosylation in *Lycium* species. In Cucurbitaceae, AA-2ßG was found mainly in the phloem. Hancock et al. (2008) postulated that AA conjugates may play a role in phloem loading of AA in members of this family and other symplastic loaders.

4.2.2. **UGT87A2 has putative functions in ascorbic acid homeostasis or in cell wall biosynthesis**

Overexpression of *UGT87A2* led to induction of several m/z peaks in the non-targeted metabolome analysis. Two of the *UGT87A2*-induced mass peaks could be identified as glucosides in leaves, which indicated putative *in planta* substrates of UGT87A2. One of them (m/z 339) could not be detected in the wild-type line. The CAMV 35S promoter used for construction of the overexpression lines leads to ubiquitous expression in all tissues. The overexpressed protein therefore comes in contact with new compounds in tissues where it is not expressed under natural conditions and hence can lead to unspecific glucosylation events. Glucosides which appear in overexpression lines but cannot be detected in the wild type are putatively produced through unspecific glucosylation events, although one has to keep in mind that the compound could also be below the detection limit of the MS instrument.

The second peak, induced in *UGT87A2* overexpression lines, but also detectable in the wild type, was identified as ascorbic acid 2-O-β-glucoside. Although glucosylation of ascorbic acid (AA) could not be confirmed with recombinant UGT87A2, due to the lack of a positive control to check the activity of the recombinant protein, AA cannot be excluded as a putative substrate. No obvious phenotype could be detected in plants with increased ascorbic acid conjugates. A tight regulation of AA levels exists in plants (Smirnoff et al., 2001). Thus, although conjugation of AA is enhanced in *UGT87A2* overexpression lines, no substantial changes in free AA levels could be detected in these lines as shown by HPLC analysis (Supplemental Figure 7). This might also be the reason why *UGT87A2* overexpressors did not show obvious phenotypes.

According to several studies, low AA causes premature senescence (Barth et al., 2004; Conklin and Barth, 2004). Induction of *UGT87A2* in senescing leaves [4.1.3 and BAR (bbc.botany.utoronto.ca)] would increase AA glucosylation and could lead to the export of conjugated AA from senescing into younger tissues.

UGT87A2 is constitutively expressed in root tips (Figure 31 and Figure 33). The same was observed for VTC2 (Müller-Moulé, 2008), an enzyme catalyzing the first step in AA biosynthesis. It could be assumed that part of the ascorbic acid synthesized was converted directly into a stable storage or transport form through glucosylation. Further, cell proliferation in the quiescent center is also thought to be linked to AA levels and the redox status (Jiang and Feldman, 2005). At this point it would be interesting to have a deeper look at the root morphology to find putative different root phenotypes.

Concentration and redox status of the AA pool is tightly controlled and variable across different tissues. As an example, the AA pool in root tissue, with 30% dehydroascorbic acid (DHA) is more oxidized (Cordoba-Pedregosa et al., 2003) than in most aerial parts which contain about 10% DHA (Noctor, 2006). It would be worthwhile to analyze the amount of AA-2βG in root tissue - increased levels of conjugated AA would hint to a new mechanism controlling free AA levels and the cell redox status. The use of leaf tissue homogenates for the analysis could be the reason for the low amount of AA-2βG detected (Figure 37). AA conjugates found in Cucurbitaceae for example could only be detected in exudates of aerial parts, but were undetectable in whole tissue homogenates.

Among the other compounds induced through *UGT87A2*, m/z 237, most probably represents KDO, a glycosyl residue of the pectic polysaccharide rhamnogalacturonan II (RG-II) present in primary cell walls of several plants including *Arabidopsis* (Zablackis et al., 1995; Seveno et al., 2010). This is supported by the fact that no glucoside loss could be observed for m/z 237 (Table 1).

Plant cell walls are an extracellular matrix surrounding the cell protoplast, composed of a highly integrated and structurally complex network of polysaccharides, including cellulose, hemicelluloses and pectin (Cosgrove, 2005). In addition to their functions in plant growth and development, plant cell walls also play an important role in plant response to environmental cues and are a storage site of many biologically active signaling molecules. Cell walls are the first plant barriers against pathogen invasion and sensing their integrity is one mechanism by which plants may detect pathogen attack. Breakdown products of plant cell walls for example function as potent elicitors of plant-defense responses. Accordingly, several plant cell wall mutants show altered pathogen resistance [reviewed in Hématy (2009)].

Although KDO is not a direct product of *UGT87A2*, its induction in *UGT87A2* overexpression lines could hint to a putative role of *UGT87A2* in cell wall biosynthesis and/or further support its role in ascorbic acid homeostasis. AA and RG-II both share a common biosynthetic precursor, GDP-D-mannose (Wheeler et al., 1998; Smirnoff et al., 2001). The connection between ascorbic acid and cell wall biosynthesis due to their common precursor has been shown in several cases (see Figure 42). E.g. the depletion of GDP-mannose through a mutation in CYTOKINESIS DEFECTIVE 1, an enzyme catalyzing the production of GDP-mannose, led to changes in cell wall composition (Lukowitz et al., 2001). Additionally, a weak mutation in the same gene (GDP-mannose pyrophosphorylase) led to deficiency in ascorbic acid production in the *vtc1* mutant (Conklin et al., 1999). Gilbert et al. (2009) made similar observations in tomato plants that were RNAi-silenced for GDP-D-mannose 3,5-

epimerase (GME), an enzyme that produces GDP-L-galactose from GDP-D-mannose. Its downregulation in tomato led to loss of fruit firmness and increase of rhamnogalacturonan labeling in addition to reduced AA biosynthesis, further underlining the intersection between L-ascorbate and cell wall polysaccharide biosynthesis.

Finally, although it is not clear in which of both processes *UGT87A2* is directly involved, induction of ascorbic acid 2-O-β-glucoside and a cell wall component in the overexpression lines hint to a putative role of *UGT87A2* in ascorbic acid homeostasis or in cell wall biosynthesis due to their common biosynthetic precursor GDP-D-mannose.
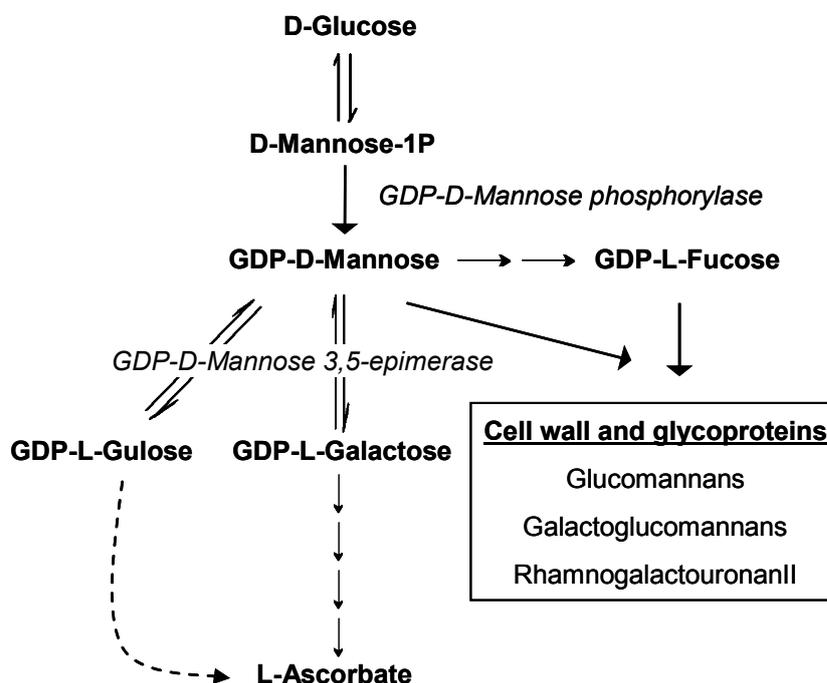
Figure 42. L-ascorbic acid biosynthesis in plants.

4.2.3. Downregulation of *UGT87A1* using artificial microRNA technology

No significant metabolic changes were found consistently in two independent *ugt87a2* knockout mutants. One reason could be the existence of redundant genes that compensate for the loss of *UGT87A2*. A putative candidate gene is the highly homologous *UGT87A1*. Artificial amiRNA technology was used to downregulate *UGT87A1* in an *ugt87a2* mutant background using two different amiRNAs. Both amiR-1 and amiR-13 led to *UGT87A1* downregulation, but one of them (amiR*UGT87A1*-1) with much higher efficiency (Figure 41). Several factors are known to influence amiRNA efficiency such as accessibility of the complement amiRNA site, absolute hybridization energy, position of the complementary mRNA region, difficulties reducing steady-state target RNA levels because of negative

feedback regulation. In the case of *UGT87A1*, the plant seemed to tolerate a strong reduction (up to 90%) of *UGT87A1* at the transcriptional level as seen in the case of amiR-1. Therefore factors affecting the hybridization of the amiRNA might be the reasons for the low efficiency of amiR-13. As shown in Fig 40B, the mRNA target site of amiR-13 shows a slightly closer secondary conformation (3 unpaired bases) than the one of amiR-1 (9 unpaired bases). The amiR-13 target site is also located in a loop region. Both could lead to a lower accessibility to the mRNA, thereby reducing the silencing efficiency. Additionally, amiR-13 has a slightly higher hybridization energy (-34.5 kcal/mol) than the optimum (between -35 and -38 kcal/mole). Additionally, although no evidence exists that the position of the target site in the target transcript influences the effectiveness, target sites in most endogenous miRNA targets are found towards the 3' end of the coding regions. amiR-13 is located closer to the 5´ end of the mRNA, which could in part also reduce its efficiency.

Downregulation of *UGT87A1* in *ugt87a2-1* background had no effect on any of the masses that were induced by *UGT87A2* overexpression. Therefore no further information on the involvement of UGT87A2 in ascorbic acid homeostasis or cell wall biosynthesis could be concluded from these results. Certainly, the real substrate could have been missed in the metabolic analysis and the observed metabolic inductions could be only an indirect effect of ectopic *UGT87A2* overexpression. Here a change in the metabolite approach such as measurements covering a broader mass range, using positive ionization mode, or using a different metabolite extraction procedure could give additional hints. But the observed metabolic influences of *UGT87A2* in the overexpression lines strongly suggest an involvement in ascorbic acid homeostasis or in cell wall biosynthesis. Further analyses are needed to confirm such a role of *UGT87A2*. For example analysis of cell wall composition, ascorbic acid 2-O-β-glucoside measurements in different plant organs and further stress exposure analysis of knockout and overexpression lines.

5. MATERIALS AND METHODS

5.1. MATERIALS

5.1.1. Plant materials

Insertion lines and wild-type plants used in this study were *Arabidopsis thaliana* ecotype Col-0, except *ugt76b1-GT5* which was ecotype L*er*. Insertional mutant lines for *UGT76B1* and *UGT87A2* (Table 2) were identified by screening the publicly accessible SIGnAL T-DNA Express database of the SALK Institute (http://signal.salk.edu/cgi-bin/tdnaexpress. Mutant candidates were retrieved from various sources; the SALK (Alonso et al., 2003), the GABI-Kat (Rosso et al., 2003), the JIC SM (Tissier et al., 1999) and the SAIL collections (Sessions et al., 2002). Seeds were purchased from the Nottingham *Arabidopsis* Stock Center (NASC) or from the *Arabidopsis* Biological Resource Center (ABRC, Ohio State University, USA, http://www.biosci.ohio-state.edu/pcmb/Facilities/abrc/abrchome.htm). GABI lines were purchased from GABI-Kat (MPI, Köln, Germany).

Table 2. UGT insertion mutants.

AGI code	Line	Name	Ecotype	Resistance
At2g30140	GABI_686D07	*ugt87a2-1*	Col-0	Sulfadiazine
At2g30140	SALK_124038	*ugt87a2-2*	Col-0	Kanamycin
At3g11340	SAIL_1171A11	*ugt76b1-1*	Col-0	Basta™
At3g11340	GT_5_11976	*ugt76b1-2*	L*er*	Kanamycin

5.1.2.   Bacterial strains

Table 3. Bacterial strains.

Species	Strain
Escherichia coli	DH-5α
	BL21 (DE3) pLys
Pseudomonas syringae	*pv tomato* DC3000, Abbreviation: *Ps-vir*
	pv tomato DC3000 (avrRpt2), Abbreviation: *Ps-avir*
Agrobacterium tumefaciens	GV3101 (pMP90)

5.1.3.   Vectors

Table 4. Vectors.

Name	Application	Source	Reference
pENTR1A	Gateway^{TM} cloning	Invitrogen, Germany	
pRS300	amiRNA cloning	Rebecca Schwab, Germany	http://wmd3.weigelworld.org/ (Schwab et al., 2006)
pBGWFS7	Gateway^{TM} cloning, binary vector	Gent University, Belgium	(Karimi et al., 2002)
pB2GW7	Gateway^{TM} cloning, binary vector	Gent University, Belgium	(Karimi et al., 2002)
pAlligator2	Gateway^{TM} cloning, binary vector	Francois Parcy, France	(Bensmihen et al., 2004)
pDEST15	Gateway^{TM} cloning, binary vector	Invitrogen, Germany	

5.1.3.1. Antibiotics

Table 5. Antibiotic stock and working solutions.

	Source	Stock solution (mg/ ml)	Working concentration (µg/ ml)
Ampicillin	Roche, Mannheim (Germany)	100	100
Rifampicin	Sigma, Deisenhofen (Germany)	10 (in methanol)	25 (for *Pst* DC3000) 100 (for *Agrobacterium*)
Kanamycin	Sigma, Deisenhofen (Germany)	50	50
Gentamicin	Roche, Mannheim (Germany)	50	25
Spectinomycin	Sigma, Deisenhofen (Germany)	10	50-100

All stock solutions were dissolved in water except rifampicin which was dissolved in methanol and kept at -20°C.

5.1.4. Medium and solutions

½ MS (Murashige & Skoog):

	2.2 g/l	Murashige & Skoog Medium including vitamins (Sigma. Germany)
	1-1.5% (w/v)	sucrose
	pH 5.7-5.8	adjusted with KOH
for solid medium:	0.25–5% (w/v)	Gelrite (Duchefa. The Netherlands)

LB (Luria-Bertani):

	2.5 g/l	LB broth high salt
	600 µl	5N NaOH
for solid medium:	15 g/l	Difco Agar

KB (Kings B):

	20 g/l	Tryptone (Difco)
	1.5 g/l	K_2HPO_4
	1.5 g/l	MgSO4
	10 ml/l	Glycerin
	pH 7	Adjusted with HCl/NaOH
for solid medium:	15 g/l	Agar

RB (rich LB medium):

	10 g/l	Tryptone (Difco)
	5 g/l	Yeast extract (Difco)
	5 g/l	NaCl
	2 ml/l	1N NaOH

SOC (Super Optimal broth with Catabolic repressor):

	20 g/l	Trypton
	10 mM	NaCl
	2.5 mM	KCl
	10 mM	$MgCl_2$
	10 mM	$MgSO_4$
	20 mM	Glucose
	pH 7	Adjusted with NaOH

All media were autoclaved for 10 min at 120°C and kept at 4°C.

5.1.5. Primer

Table 6. Primer used for the characterization of transgenic lines (5.2.1.6).

Name	Sequence
AtTUB9 f	gtaccttgaagcttgctaatccta
AtTUB9 r	gttctggacgttcatcatctgttc
76B1_ORF_r	gtctgattatgggaatgcagatta
76B1_f620	aagatccaagatcaggggataag
SAIL_L	ttcataaccaatctcgatacac
Ds5-2mod	cgttttgtatatcccgtttccgt
87A2_F-20	aaatcacacacttcacaagaaac
87A2_R1670	ttgaaacaataaaacctctttga
87A2_r810	tctcgaatggttcttccaatct
LBa1 mod	ggttcacgtagtgggccatc
GABI_LB1	ccaaagatggacccccacccac

Table 7. Primer used for the production of overexpression lines and recombinant UGT expression vectors using Gateway^{TM} recombination.

Name	Sequence
76B1_ORF_GW_f	ggggacaagtttgtacaaaaaagcaggctacacaatggagactagagaaacaaaacca
76B1_ORF_GW_r	ggggaccactttgtacaagaaagctgggtctgattatgggaatgcagatta
87A2_ORF_GW_f	ggggacaagtttgtacaaaaaagcaggcttaacaatggatccaaatgaatctcca
87A2_ORF_GW_r	ggggaccactttgtacaagaaagctgggttgaaacaataaaacctctttgagc

Table 8. Primer used for the production of *UGT*pro:GUS-GFP constructs using Gateway^{TM} recombination.

Name	Sequence
UGT76B1pro_GW_f	ggggacaagtttgtacaaaaaagcaggctcggttaaacataaaccatgt
UGT76B1pro_GW_r	ggggaccactttgtacaagaaagctgggtgtctccattttgttgtgaat
UGT87A2 pro_GW_f	ggggacaagtttgtacaaaaaagca ggctagaaaacatgcaaaagcaat
UGT87A2 pro_GW_r	ggggaccactttgtacaagaaagctgggtggatccataggttgtttctt

Table 9. Primer sequences used for RT-qPCR (5.2.4.7).

Gene	Accession number	Name	Sequence	Citation
UBQ5	At3g62250	AtUBQ5 f	ggtgctaagaagaggaagaat	
		AtUBQ5 r	ctccttcttctggtaaacgt	
S16	At5g18380, At2g09990	S16qRT_f	tttacgccatccgtcagagtat	
		S16qRT_r	tctggtaacgagaacgagcac	
UGT76B1	At3g11340	UGT76B1_f	tggaagatcggattgcatt	
		UGT76B1_r	ccttcatgggcataatcctc	
PR1	At2g14610	PR1_f397	gtgccaaagtgaggtgtaacaa	
		PR1_r495	cgtgtgtatgcatgatcacatc	
PDF1.2	At5g44420	Pdf1.2a _f197	ccaagtgggacatggtcag	(Kumar et al., 2009)
		Pdf1.2a _r 292	acttgtgtgctgggaagaca	
VSP2	At5g24770	VSP2_f1037	ttggcaatatcggagatcaat	
		VSP2_r1136	gggacaatgcgatgaagatag	
SAG13	At2g29350	SAG13_f607	ttgcccacccattgttaaa	
		SAG13_r707	gattcatggctcctttggtt	
SAG12	At5g45890	SAG12_f1154	aatgatgagcaagcactgatg	
		SAG12_r1253	cgtagtgcactctccagtgaa	
LOX2	At3g45140	LOX2_f2794	tgcacgccaaagtcttgtca	(Delker et al., 2007)
		LOX2_r2931	tcagccaaccccctttga	
WRKY70	At3g56400	WRKY70_f1084	ggaagaagacaatcctcatcgt	
		WRKY70_r1187	cgttttcccattgacgtaact	
EDS1	At3g48090	EDS1_f1704	cgaagacacagggccgta	(Straus et al., 2010)
		EDS1_r1893	aagcatgatccgcactcg	
PAD4	At3g52430	PAD4_f1725	ggttctgttcgtctgatgttt	(García et al., 2010)
		PAD4_r1766	gttcctcggtgttttgagtt	
UGT87A2	At2g30140	UGT87A2_f	gaatgagttgttgatagggagaga	
		UGT87A2_r	tcctcgactgatttcactaaggt	
UGT87A1	At2g30150	UGT87A1_f1064	gttttgtgtcatgcggctata	
		UGT87A1_r1142	cagaaactgatcccaaaaaaca	

Table 10. Primer used for *UGT87A1*-amiRNA cloning (5.2.4.8.2)

Name	Sequence
amiRNA-I_87A1_1	gattgacacaaaacacgtagccg tctctcttttgtattcc
amiRNA-II_87A1_1	gacggctacgtgttttgtgtcaatcaaagagaatcaatga
amiRNA-III_87A1_1	gacagctacgtgttatgtgtctatcacaggtcgtgatatg
amiRNA_IV_87A1_1	gatagacacataacacgtagctg tctacatatatattcct
amiRNA_I_87A1_13	gatatgatgtaagtatgggcggt tctctcttttgtattcc
amiRNA_II_87A1_13	gaaccgcccatacttacatcatatcaaagagaatcaatga
amiRNA_III_87A1_13	gaaacgcccatactaacatcatatcacaggtcgtgatatg
amiRNA_IV_87A1_13	gatatgatgttagtatgggcgtt tctacatatatattcct

All primers were obtained from Thermo Electron (Ulm, Germany). Stock solutions were prepared at 200 µM and stored at -20°C.

5.2. METHODS

5.2.1. Plant methods

5.2.1.1. Growth conditions

For infection experiments and RT-qPCR analysis plants were grown on soil under a 14 h light cycle at 45 µmol m^2 s^{-1} of light intensity at 18°C in the dark and 20°C in the light and 75% relative humidity. For metabolic analysis and plant transformation, plants where grown in soil (for analysis of leaf material) or in hydroponic culture (for analysis of root material) at a 12 h light cycle, 120 µmol m^2 s^{-1} light intensity, 20°C and 75% relative humidity.

For UV-B treatment, plants were grown on soil under an 11 h light cycle at 200 µmol m^{-2} s^{-1} light intensity at 18°C in the dark and 23°C in the light and 60% relative humidity. UV-B treatment was started 1 week after germination with approx. 13 kJ/day.

5.2.1.2. Plant growth on soil

For plant breeding, soil (Floraton 1, Floragard) was mixed with silica sand in a ratio of 5:1 and poured in 6-well plant pots. Soil was wetted with water, seeds where placed with a toothpick on wet soil and stratified for 2 days at 4°C (to synchronize germination) before transfer into the plant chamber.

5.2.1.3. Seed surface sterilization

For surface sterilization, seeds were placed in a clean bench on filter paper and submerged in 70% ethanol. Seeds were allowed to dry in the clean bench until complete dryness and the process was repeated a second time.

5.2.1.4. Sterile culture on solid medium

For growth under sterile conditions, seeds were surface sterilized and placed on squared Petri dishes (120 mm x 120 mm x 17 mm Greiner bio-one Germany) containing 50 ml 0.5 x MS medium (1.5% sucrose, 0.5% (w/v) Gelrite). Plates were wrapped with parafilm and kept for 2 days at 4°C for stratification before being transferred into a growth chamber in a vertical orientation.

5.2.1.5.   Hydroponic culture

For analysis of root material seeds where surface sterilized and grown on plates with ½ MS medium (1% sucrose, 0.25% Gelrite). Seedlings were transplanted after 7 days in a floating hydroponic system (Battke et al., 2003) and grown for 10 days in Vitro Vent boxes containing the same medium as described before except with Gelrite. Each box contained 9 plants, 300 ml medium and 250 ml polypropylene (PP) granulate as the floating material.

5.2.1.6.   Production and/or characterization of transgenic lines

After obtaining the T-DNA insertion lines (see 5.1.1 for more information) the position of the T-DNA insert was confirmed by PCR and DNA sequencing. Primers used were 76B1_ORF_r / Sail_L and 76B1_f_620 / Ds5-2mod for SAIL_1171A11 and GT_5_11976 lines and 87A2_r810 / GABI_LB1 and 87A2_r810 / LBa1mod for GABI_686D07 and SALK_ 124038 insertion lines respectively (see Table 6). Lines were then backcrossed once with their respective parental wild-type line and self-pollinated. Homozygous plants were identified by PCR, by amplification of the mutant allele using the same primers used for PCR and sequencing and by the absence of amplification of the wild-type allele using gene specific primers 76B1_f_620 and 76B1_ORF_r for *UGT76B1* and 87A2_F-20 and 87A2_R1670 for *UGT87A2* (see Table 6). Lack of the functional transcript in both knockout lines was confirmed by RT-PCR using the same gene specific primers.

Overexpression lines were produced by *Agrobacterium*-mediated transformation (see 5.2.2.3) using two different plasmid constructs pB2GW7 and pAlligator2 carrying the ORF coupled to a CaMV 35S-derived promoter (Clough and Bent, 1998; Karimi et al., 2002; Bensmihen et al., 2004). The primers used for UGT amplification and cloning using Gateway[TM] (Invitrogen, Germany) recombination are shown in Table 7. After selection of transformants, segregation analysis was used for identification of single insertion lines in the T2 generation. Selection was carried out either by a visible marker using seed coat specifically expressed GFP (pAlligator2) or by resistance to the herbicide Basta[TM] (pB2GW7). Seven independent and homozygous single insertion lines were selected for each vector for further molecular characterization.

5.2.1.7. Backcrossing, seed harvesting and storage

The aim of backcrossing is to to get rid of other unwanted T-DNA-induced mutations in the knockout mutants.

For backcrossing, plants were grown under long light conditions until mature flowers were present. Two to three inflorescences were chosen and all the flowers that were too young (too small), the ones that already showed white petals (opening flowers will tend to have started self-fertilization) as well as all other plant parts in the immediate vicinity were removed to create a free work environment. To prepare the recipient flower (ovary), all the flower parts except the pistil were removed carefully without touching the stigma or style (it is easily damaged). The pollen was obtained from mature flowers from the donor plant. Suitable anthers from a mature flower were dabbed onto the stigma of the emasculated plant. This step was repeated at least twice to ensure proper pollination. When the cross was successful, obvious elongation became visible after 1-2 days to generate a silique. Each pollinated inflorescence was labeled accordingly, ovaries were allowed to develop, and seeds were harvested once siliques were dry. If several crosses were done in a row, forceps were cleaned by dipping them in 95% ethanol (v/v) followed by rinsing with distilled water.

Harvested seeds were transferred to seed packets and allowed to dry for one week in a desiccator before being stored at room temperature.

5.2.1.8. Dark-induced senescence

Excised leaves from five-week-old plants grown under short day photoperiodic conditions were floated with the abaxial side up in a petri dish with deionized water and kept for five days in the dark at room temperature (Oh et al., 1996).

5.2.1.9. Plant wounding experiment

For gene induction analysis and amino acid determination after wounding, leaves were crushed two times across the mid-rip with a hemostat (Koo et al., 2009). For amino acid determination, wounded leaves were harvested 1 h after wounding and immediately frozen in liquid nitrogen.

5.2.2. Microbiological methods

5.2.2.1. Preparation of competent cells

5.2.2.1.1. Competent *E. coli*

A single colony of bacteria was inoculated into 2.5 ml of Rich Broth medium (RB) and cultivated overnight at 37°C and 250 rpm. The culture was then subcultured in 250 ml RB medium containing 20 mM $MgSO_4$ and grown until an OD_{590} of 0.4 to 0.6.

The suspension was centrifuged at 5000 rpm for 5 min at 4°C. The supernatant was discarded and the bacterial pellet resuspended carefully in 100 ml of ice-cold TFB1 and kept on ice for 5 min. The bacterial suspension was then centrifuged again and the new pellet was resuspended gently in 10 ml cold TFB2. After 15-60 min incubation on ice, 100 µl were aliquoted in ice-cold Eppendorf tubes, immediately frozen in liquid nitrogen and stored at -80°C. The expected transformation efficiency should be around 10^6 cfu/µg plasmid DNA.

TFB1:	30 mM	KOAc (potassium acetate)
	100 mM	RbCl
	10 mM	$CaCl_2$
	50 mM	$MnCl_2$
	15%	glycerol
	pH	adjusted to 5.8 with acetic acid

TFB2:	10 mM	MOPS
	75 mM	$CaCl_2$
	10 mM	RbCl
	15%	glycerol
	pH	Adjusted to 6.5 with KOH

Both solutions were filter sterilized using 0.45 µm filter (Millipore Germany) and aliquoted (50 µl) for single use.

5.2.2.1.2. Competent *Agrobacterium tumefaciens*

300 ml LB medium containing appropriate antibiotics were inoculated with 2 ml preculture (overnight, from single colony) and grown at 28°C until OD_{600} 0.5-0.7. After 30 min cooling on ice, the culture was centrifuged at 4°C and 400 rpm for 20 min. After complete removal of the media, the pellet was resuspended in 125 ml ice cold water and incubated on ice for 30 min. The resuspension and centrifugation procedure was repeated with a subsequent incubation on ice for 60 min. After a last centrifugation, the bacterial pellet was resuspendet in 3 ml of ice-cold glycerol (15%), aliquoted in 50 µl portions, immediately frozen in liquid nitrogen and stored at -80°C.

5.2.2.2. Transformation of competent cells

5.2.2.2.1. Heat shock transformation of *E. coli*

Fifty µl competent *E. coli* cells were thawed on ice, mixed with approximately 100 ng plasmid DNA and incubated for 15 min on ice. Incorporation of the plasmid DNA was achieved by a 40 sec heat shock at 42°C (water bath) after which cells were incubated on ice for 5 minutes. After addition of 1 ml LB medium without antibiotics, cells were incubated 1 h at 37°C in order to allow expression of the antibiotic resistance. Cells were then centrifuged and plated on selective LB medium.

5.2.2.2.2. Electroporation of competent *Agrobacterium tumefaciens* cells

For plant transformation, plasmid DNA was transformed to *Agrobacterium tumefaciens* strain GV3101 containing an appropriate helper Ti plasmid (pMP90) by electroporation. For this purpose, the plasmid DNA was precipitated, washed and dissolved in water (low concentration of TE or ½ Quiagen elution buffer also works). Fifty µl electrocompetent cells were thawed on ice and mixed with approximately 20 ng of plasmid DNA (in not more than 1 µl Volume). The mixture was then transferred to a dry, pre-chilled 0.1 cm electroporation cuvette. The electroporation was carried out as recommended for *E. coli* by the electroporator's manufacturer with slight modifications:

Capacitance   25 µF

Voltage   1.25 kV

Resistance   400 Ω

After pulsing the time constant should be larger than 9.1 (optimal would be 9.4 to 9.6) to give a relevant number of transformants. A control without plasmid DNA was always done in parallel. Immediately after the pulse, 1 ml of SOC medium (without antibiotics) was added to the cuvette, gently resuspended and transferred to a 15 ml culture tube. The cuvette was washed with another 1 ml SOC and cells were then incubated at room temperature for 60-90 min with gentle agitation. After collecting the cells by gently centrifuging at 5000 rpm for 2-3 min, a part of the supernatant was discarded and the cells were resuspended by gentle pipetting in the remaining supernatant. 1/4 of total cells were spread onto an LB agar plate with appropriate antibiotic selection (Rifampicin and Gentamicin for agrobacteria and appropriate antibiotic for T-DNA vector) and incubated at 28°C for 2 to 3 days.

5.2.2.3.   *Agrobacterium tumefaciens* mediated plant transformation

The floral dip procedure (Clough and Bent, 1998) was used for transformation of *Arabidopsis thaliana*. *Arabidopsis* plants were grown in a long day light period (16 h, 22°C) in big pots to flowering stage (fertilized). Primary formed bolts were cut to induce the formation of several secondary bolts. Siliques and open flowers were also eliminated before transformation to increase the transformation rate. A single colony of *Agrobacterium tumefaciens* strain GV3101 carrying the construct of interest was used for a 2 ml preculture (overnight, 28°C, 220 rpm). On the next day the agrobacteria were diluted 1:300 in 300 ml LB and appropriate antibiotics (Rifampicin and Gentamicin for agrobacteria and an appropriate antibiotic for the T-DNA vector) and grown overnight (170 rpm) until stationary phase (OD_{600} 1.5-1.6). Cells were harvested by 10 min centrifugation at 4°C and 5500g and the pellet was resuspended in 1 ml infiltration medium and diluted in the same medium to a final OD_{600} of approximately 0.8.

The suspension was then transferred to a beaker and plant inflorescences were dipped for several seconds into it. Care was taken to avoid contact of leaves and soil with the bacterial suspension. Dipped plants were allowed to dry, covered with a transparent plastic bag to maintain humidity and kept in a low light location for one day. Plants were then returned to the growth chamber, fertilized and grown until seed harvest.

Infiltration medium: 5%   sucrose

                                 0.05%   Silwet L-77

The first generation of seeds (T0) was collected and transformants were selected either by GFP fluorescence of the seeds (pAlligator2) before sawing or Basta^{TM} (pB2GW7 or pBGWFS7) resistance one week after sowing on soil.

5.2.2.4. Bacterial infection and determination of bacterial growth in plants

Bacteria were streaked out from a –80°C glycerol stock onto a plate of King's medium with appropriate antibiotics and grown for 1 or 2 days at 28°C. Bacteria from the fresh streak were then transferred to a liquid King's B culture with appropriate antibiotics and grown overnight with shaking at 28°C. When they reached mid to late log phase growth (OD_{600}=0.6 to 1.0), bacteria were diluted to the desired concentration with 10 mM $MgCl_2$ for plant inoculation (OD_{600}=0.2 corresponds to approximately 10^8 cfu ml^{-1}). Plants were grown as described in 5.2.1.1 and covered with a plastic dome 14 h before inoculation to maintain humidity and induce opening of the stomata. Whole leaves of 5- to 6-week-old plants were infiltrated (from the abaxial side) using a 1-ml syringe without a needle. Complete infiltration could be visualized by apparent water-soaking of the leaf. 4 leaves were infiltrated from each plant. Inoculated plants were covered for one more day to maintain high humidity. Leaf discs from control treated and infected plants were harvested at 0 d, 1 d and 3 d after infiltration. 2 leaf discs were cut out per each leaf using a 1.5 ml Eppendorf tube. The bacterial growth was assessed as described by Katagiri et al. (2002) without leaf sterilization. For each time point three samples were prepared by pooling six leaf discs from 3 different treated plants.

5.2.3. Nucleic acid isolation

5.2.3.1. CTAB DNA mini preparation from plant tissue

For quick preparation of genomic DNA (e.g. for genotyping) a small, young plant leaf was squeezed with small pistil (e.g. flamed blue tip) in a 1.5 ml Eppendorf tube. After addition of 250 µl 2x CTAB buffer, the tube was vortexed briefly and placed in a 65°C water bath for at least 10 min (up to two hours). 200 µl of chloroform-isoamylalcohol (24:1) were than added, the tube vortexed vigorously and thoroughly and subsequently centrifuged at full speed for 2

min in a table-top centrifuge. The upper aqueous phase was transferred (care was taken not to touch the interface) into a new Eppendorf tube containing 1 µl of 1% linear polyacrylamide. For DNA precipitation, 3 volumes of absolute Ethanol p.a were added. The tube was mixed and left at -20°C for 20 min or longer for precipitation of the DNA. This step was followed by a 10 min centrifugation at 4°C and full speed in a table-top centrifuge. The DNA pellet was then washed once with 70% Ethanol p.a., allowed to dry on the bench or using a Speed-Vac and dissolved in 100 µl TE buffer. One µl was used for subsequent analyses (e.g. PCR).

2x CTAB Buffer	1.4 M	NaCl
	100 mM	Tris-HCl. pH 8.0
	2% (w/v)	CTAB
	20 mM	EDTA. pH 8.0
	1% (w/v)	polyvinylpyrrolidone
		Mr 40.000 (Sigma PVP-40 or P-0930)

5.2.3.2.   Plasmid DNA preparation

Plasmid DNA from *E. coli* was isolated using the QIAprep Spin Miniprep Kit (Qiagen, Hilden, Germany) according to the manufacturer's instructions. This procedure is based on alkaline lysis of bacterial cells followed by adsorption of the DNA onto a silica membrane in the presence of high salt-binding conditions. Up to 20 µg of high copy plasmid DNA could be obtained from 1 to 5 ml overnight cultures of bacteria in LB medium.

For isolation of plasmid DNA of *Agrobacterium,* the same procedure was used, but 5 independent DNA preps were prepared and eluted in 50 µl total volume to enhance plasmid yield.

5.2.3.3.   RNA extraction

5.2.3.3.1.   Isolation of total RNA for RT-PCR

Total RNA extraction for RT-PCR was performed using a protocol suitable to isolate high quality RNA from a wide range of tissues without the use of toxic and expensive chemicals (Chang S, 1993). Plant material was disrupted with a dismembrator under liquid nitrogen. 500

µl CTAB buffer (prewarmed to 65°C) was added to 50-100 mg ground tissue and samples were homogenized by quick vortexing. Total RNA was extracted with an equal volume of chloroform:isoamyl alcohol and phase separation was achieved by centrifugation, 5 minutes at 10.000 rpm. The extraction was repeated once to increase RNA purity. The supernatant was then transferred to an Eppendorf tube and total RNA precipitated overnight at 4°C by addition of 1/4 volume of 10 M Lithium chloride. The RNA was then harvested by 20 min centrifugation at 14 000 rpm and 4° C and the pellet resuspended in 500 µl of SSTE buffer and dissolved at room temperature for 2 h with agitation. After another extraction with 500 µl chloroform/isoamylalcohol (24:1), the supernatant was transferred to a fresh Eppendorf tube and precipitated with 1/10 volume of 3 M Sodium-Acetate (NaOAc, pH 5.2) and 1 volume of isopropanol for 20 min at -20°C. RNA was then collected again by centrifugation and washed with 70% Ethanol. After drying for 5 min at 37°C, the pellet was resuspended in 500 µl TM buffer. Any traces of DNA were removed by addition of 1 µl DNase and incubation at 37° C for 15 min. DNAse was then extracted with 500 µl chloroform/isoamylalcohol (24:1) and RNA precipitated by addition of 1/10 Volume of 3 M Sodium-Acetate (pH 5.2) and 1 volume of isopropanol and incubation for 30 min at -20° C. After centrifugation and washing with 75% ethanol as mentioned above, the pellet was allowed to dry and resuspended in 20 µl DEPC-treated sterile water.

Quality and concentration of the RNA samples were assessed by measuring the absorption at 260 nm in a spectrophotometer and RNA integrity was analyzed in a 1% agarose gel electrophoresis (5.2.3.4 and 5.2.4.2).

All buffers and solutions were prepared with DEPC treated sterile water and RNase free tubes and tips were used for all procedures.

CTAB RNA Extraction buffer	2%	CTAB
	2%	PVP-40
	100 mM	Tris/HCl pH 8.0
	25 mM	EDTA
	2 M	NaCl
	0.5 g/l	Spermidine
added just before use:	2%	beta-mercaptoethanol

SSTE Buffer	1 M	NaCl
	0.5%	SDS
	10 mM	Tris/HCl pH 8.0
	1 mM	EDTA
TM Buffer	40 mM	Tris/HCl pH 7.5
	6 mM	$MgCl_2$

5.2.3.3.2. Isolation of total RNA using Qiagen RNeasy Plant Mini Kit

For RT-qPCR experiments, total RNA was extracted using RNeasy Plant Mini Kit (Qiagen, Hilden, Germany). Plant material was disrupted with a dismembrator and 30-100 mg were used for RNA extraction according to the manufacturer's instructions. DNAse treatment was performed on the column as recommended.

5.2.3.4. Determination of nucleic acids concentration

DNA and RNA concentrations were determined measuring the absorption at 260 nm and 280 nm using the Nanodrop ND-1000 spectrophotometer (Kisker-biotech, Germany). Water or buffer was used to zero the spectrophotometer and a volume of 1.5 µl was used for each measurement. The A_{260}/A_{280} ratio was used to assess the purity of total DNA or RNA and to detect the presence of protein, phenolics or other contaminants that absorb at or near 280nm. A ratio of approximately 1.8 or 2.0 is generally accepted for pure DNA and RNA, respectively. The $A_{260}/_{230}$ ratio is a second purity measure, which should commonly be in the range of 2.0-2.2. An appreciably lower ratio may indicate the presence of contaminants absorbing at 230 nm.

5.2.4. **Molecular biology methods**

5.2.4.1. **PCR (Polymerase Chain Reaction)**

Polymerase chain reaction (PCR) is a method that allows exponential amplification of short DNA sequences within a longer double stranded DNA molecule *in vitro*. This is achieved through repeated cycles of denaturation (melting double stranded DNA) at high temperature, primer annealing (temperature depends on the primer sequence) and elongation (72°C, polymerase adds dNTPs from 5' to 3', reading the template from 3' to 5' end). The annealing temperature depends on the length and base pair composition of the primers used for amplification and is one of the most important parameters that needs adjustment in the PCR reaction. Moreover, the flexibility of this parameter allows optimization of the reaction in the presence of variable amounts of other ingredients (especially template DNA).

The PCR mix was prepared as followed:

1 μl genomic DNA (CTAB preparation) or 20 ng plasmid DNA	Template DNA
2 μl	10X reaction buffer
0.2 μl	20 mM dNTPs
1 μl	10 μM forward primer
1 μl	10 μM reverse primer
0.1 μl (5 U/ μl)	Taq polymerase (Agrobiogen, 6805-P)
to an end volume of 20 μl	Sterile ddH$_2$O

PCR reaction was performed in an automated Multicycler PTC-200 (Biozym, Germany) as followed:

95°C	2 min	1 cycle
95°C (denaturation)	30 sec	
X°C (annealing)	30 sec	30-40 cycles
72°C (extension)	1 min/1kb	
72°C	5 min	1 cycle
Cool down to 4°C	∞	

Resulting PCR products were separated and visualized on agarose gel (5.2.4.2).

5.2.4.2. Separation and visualization of nucleic acids on agarose gel electrophoresis

Nucleic acids were separated on 0.5-2% (depending on their size) agarose gels (in 1x TAE buffer) containing 0.5 μg/ml ethidium bromide. Samples were mixed with 5X DNA loading buffer and separated on the gel in parallel to an appropriate standard size marker. Gels were run at 5-10 V/cm for up to 1 h. DNA fragments were visualized under UV light and recorded with Bio-Rad Gel Doc 2000 (Bio-Rad, Munich, Germany).

Loading buffer	36%	Glycerin
	1x	TAE
	2.5 mg/ml	Orange G
	in	ddH$_2$O

5.2.4.3. Purification of PCR product and DNA gel extraction

Before sequencing, DNA fragments were purified from primers, nucleotides, polymerase and salts from previous enzymatic reactions. Purification was performed with the QIAquick® PCR Purification Kit (Qiagen, Hilden, Germany) according to manufacturer's instructions.

To purify target DNA fragments from unspecific fragments out of standard or low melting agarose (e.g. after restriction), the corresponding DNA bands were cut out of the gel with a scalpel and transferred into a sterile Eppendorf tube. The isolation procedure was performed with the Qiaquick® Gel Extraction Kit (Qiagen, Hilden, Germany) according to the manufacturer's manual.

5.2.4.4. DNA sequencing

PCR-amplified sequences from T-DNA insertion lines or plasmid DNA from cloned vectors were purified as described in methods 5.2.3.2 and 5.2.4.3, prepared according to the manufacturer's instructions and processed by Eurofins MWG GmbH (Ebersberg, Germany).

5.2.4.5. **Digestion by restriction endonucleases and ligation**

Restriction digests were performed with restriction enzymes from New England Biolabs (Frankfurt am Main, Germany), using the appropriate buffer and temperature as recommended by the manufacturer. Digest contained about 0.5 µg plasmid DNA or PCR products, 1X reaction buffer and approx. 5 units of restriction endonuclease(s); ddH$_2$O was added to a final volume of 20 µl. The mixture was incubated at 37°C for about 2-4 h in a thermoblock or waterbath. Afterwards the enzymes were deactivated for 10 min at 65°C and fragment sizes were checked by agarose gel electrophoresis. For cloning the digestion mix was directly loaded on an agarose gel electrophoresis (5.2.4.2) without prior enzyme inactivation and purified as described in 5.2.4.3.

Ligation of restricted DNA fragments was performed using T4 ligase (Fermentas 5 U/µl) overnight at 16°C followed by enzyme inactivation for 10 min at 65°C. The optimal molar ratio for the ligation reaction is 3:1 (insert:vector).

5.2.4.6. **Reverse Transcription Polymerase Chain Reaction (RT-PCR)**

To confirm lack of the corresponding transcript in the knockout lines and to quantify transcript amounts of several marker genes, RNA was prepared as described above and used for cDNA synthesis. 0.5-1 µg of total RNA was reverse transcribed using the SuperScript II First Strand synthesis system of the reverse transcription-PCR kit (Invitrogen) according to the manufacturer's instructions. For each sample a negative RT reaction without enzyme (-RT) was prepared to check afterwards for contaminations with genomic DNA.

Reactions were prepared as follows:

1 µg	total RNA
1X	5X first-strand-synthesis buffer (Invitrogen, Germany)
1 mM	dNTP Mix (MBI Fermentas, Germany)
0.01 M	DTT
40 units	RNase Inhibitor (MBI Fermentas, Germany)
0.34 µl	oligo (dT)$_{15}$ (Promega), 0.5µg/µl
to a final volume of 20 µL	DEPC-treated water

After 10 min incubation at room temperature, 1 µl Reverse transcriptase Superscript II (diluted 1:1 in 1X first-strand synthesis buffer, 67 U; Invitrogen, Germany) was added to the positive reactions (+RT).

The cDNA was then synthesized as follows in a Multicycler PTC-200 (Biozym, Germany):

42°C	30 min
50°C	40 min
95°C	5 min
cool down to 4°C	∞

A PCR reaction with *TUBULIN* primers (Table 6) was then performed in a Multicycler PTC-200 (Biozym, Germany) using 1 µl cDNA to make sure that the RT-PCR was successful and to check the –RT control for contamination with genomic DNA. Polymerized fragments were then separated and visualized on agarose gel (5.2.4.2). A successful RNA isolation and cDNA synthesis yielded a positive band for the +RT reaction and no band in the negative control (-RT).

5.2.4.7.   Quantitative real time polymerase chain reaction (qRT-PCR)

Plant material of the indicated organ and age was collected. Total RNA was isolated as described in 5.2.3.3.2; cDNA prepared as described in 5.2.4.7 and diluted 1:15 with HPLC grade water (Merck).
Gene-specific primer pairs were designed using the Primer Express 3.0 software, trying to get intron spanning primers and an approximate amplicon of 150 bp. Primer pairs are listed in

Table 9. All primer pairs were checked for amplification specificity and an efficiency superior to 80% using a serial cDNA dilution. Real time quantification was performed using a 7500 real time PCR system (Applied Biosystems, Germany).

Individual PCR reaction mixtures contained the following:

4 µl	diluted cDNA
0.5 µl	10 µM forward primer
0.5 µl	10 µM reverse primer
5 µl	HPLC water
10 µl	2 X Sybr Green Mastermix (Thermo Scientific)

And the RT-qPCR program used was:

95°C	15 min	1 cycle for enzyme activation
95°C	15 sec	
55°C	35 sec	40 cycles
72°C	45 sec	
95°C	15 sec	
60°C	1 min	1 cycle, dissociation stage
95°C	15 sec	

The amount of target gene was normalized over the abundance of the constitutive *UBQ5* (At3g62250) and *S16* (At5g18380, At2g09990) genes. The stability of the reference genes was tested and normalization was performed using GeNorm (Vandesompele et al., 2002).

For molecular analysis of the overexpression lines one biological and two technical (PCR) replicates were performed and the results confirmed in the subsequent generation. In all other experiments three biological replicates of each sample and two technical (PCR) replicates were performed.

For RT-qPCR of infected material, plants were infected as described in 5.2.2.4. Three biological replicates were analyzed; each consisting of six individually infected leaves. Plant material was harvested before infection and mock treatments (time point 0) and at the indicated time points after treatment. Each experiment was repeated with similar results.

For marker gene analysis on uninfected material and senescent leaves, methods for paired or grouped data were applied for statistical analysis, namely the paired t-test and repeated-

measurements ANOVA (linear mixed-effects models), in order to check for interplate variation (each replicate was measured on a different qPCR plate). Two-way ANOVA was used to join results from two independent analyses (three replicates each). First a model with interaction was fitted. If the interaction effect was significant, one-way ANOVAs were performed for the single experiments; otherwise a two-way ANOVA without interaction effect was fitted. All analyses (p-value, arithmetic mean) were performed on $\log_{10}$-transformed data as recommended in literature (Rieu and Powers, 2009). For all calculations, the R software with the nlme package was used (Pinheiro et al., 2009; R-Development-Core-Team, 2009).

5.2.4.8. Molecular cloning of artificial microRNA using the Gateway[TM] recombination technology

5.2.4.8.1. Design of artificial micro RNAs

For cloning of *UGT87A1* microRNAs, amiRNA candidate sequences were designed with the artificial microRNA designer WMD2 (Ossowski et al., 2008), http://wmd2.weigelworld.org/cgi-bin/mirnatools.pl), using default settings and the AGI At2g30150 to target *UGT87A1*. To check the mRNA conformation of the target region, a publicly accessible RNAfold web server (http://rna.tbi.univie.ac.at/cgi-bin/RNAfold.cgi) was used to predict the secondary structure of *UGT87A1* mRNA.

Two amiRNA sequences were designed to specifically silence *UGT87A1* targeting different regions of the target gene. No potential off targets were reported by the WMD2 program for the two selected amiRNAs. Selection of correct target sides was based on several selection criteria as described in the protocol. Further, amiRNA targets were selected preferentially, the target region of which laid in a somewhat open secondary structure conformation to facilitate the access of the miRNA to its target sequence.

5.2.4.8.2. Cloning of amiRNA

Artificial microRNAs were cloned according to the protocol available at http://wmd2.weigelworld.org/cgi-bin/mirnatools.pl (Schwab et al., 2006).

The plasmid pRS300 (courtesy of Regina Schwab, MPI Tübingen), containing the miR319a precursor in pBSK (cloned via SmaI site), was used as a template for the following PCRs. The

artificial microRNA designer WMD2 delivered 4 specific oligonucleotide sequences (I to IV, Table 10) for each selected miRNA which were used to clone the artificial microRNA into the endogenous miR319a precursor by site-directed mutagenesis. Additionally two more oligonucleotides A and B were used for cloning. They were based on the template plasmid sequence and located outside of the multiple cloning site of pBSK to generate bigger PCR products. The amiRNA containing precursor was generated by overlapping PCR using the iProof High-Fidelity Taq polymerase (Bio-Rad) and 1x Iproof HF buffer. A first round amplified fragments (a) to (c) which are listed in Table 11. These were subsequently fused in PCR (d). PCRs were performed as described in the cloning protocol for *Arabidopsis* downloaded from the microRNA designer WMD2 website. For more details see Schwab et al. (2006).

Table 11. PCR reactions performed for amiRNA cloning.

PCR	forward oligo	reverse oligo	template
(a)	A	IV	pRS300
(b)	III	II	pRS300
(c)	I	B	pRS300
(d)	A	B	(a) + (b) + (c)

PCR fragments were purified as described in 5.2.4.3. and eluted in 15 µl double distilled water. AmiRNA precursor fragments were cloned into Gateway^{TM} vector pENTR1A using restriction enzymes EcoRI and NotI and transformed into *E. coli* DH5α. Transformed cells were selected on kanamycin and insertion of the fragment confirmed by plasmid preparation and restriction analysis (EcoRI/NotI). The integrity of the insert was confirmed by sequencing according to 5.2.4.4 using primer pENTattL2rev (Eurofins).

The new vector carrying the insert was then used for Gateway^{TM} recombination (LR reaction) according to the manufactures instructions to transfer the insert into the final destination vector (pAlligator). Using heat shock, the new plasmid was again used to transform *E. coli*, amplified, purified, and the recombination confirmed using restriction analysis with EcoRI.

As destination vectors such as pAlligator are binary vectors, the new plasmid could directly be used to transform *Agrobacterium tumefaciens* (5.2.2.2.2), which was then used for plant transformation using the floral dip method (5.2.2.3). To get *ugt87a2* and *ugt87a1* double knockouts, the amiRNA constructs were transformed into *ugt87a2-1* lines.

5.2.5. Protein methods

5.2.5.1. GST tagged protein expression and purification

The open reading frame of the corresponding *UGT* was amplified using the same primers as for the construction of the over-expression lines (Table 7). The glutathione-S-transferase (GST)–UGT expression plasmid was constructed using the pDEST15 expression vector and transformed into *E. coli* strain BL21 (DE3). Bacteria were grown in 100 ml at 37°C to an OD_{600} of 0.4, cooled on ice and induced with 0,5 mM IPTG (Isopropyl β-D-1-thiogalactopyranoside, stock solution 0,1M). After 6 h growth at 30°C (alternatively they can be grown at 20°C overnight), cells were pelleted and the recombinant protein was affinity-purified using glutathione-coupled sepharose beads according to the manufacturer's instructions (GE Healthcare). The eluted fusion proteins were concentrated by membrane filtration (Amicon Ultra-4; Millipore) and supplemented with 20% glycerol for storage at -20°C (Messner et al., 2003).

5.2.5.2. *In vitro* analysis of the recombinant protein

To analyze the UGT enzyme activity assay mixtures contained 0.1 M Tris–HCl (pH 7.5), 5 mM UDP-glucose, 0.5 mM aglycon and about 1 µg GST-UGT fusion protein in a final volume of 50 µl. After incubation for 1 hour at 30°C the reaction was stopped by addition of 200 µl methanol and cleared by centrifugation (15,000 g, 2 min). Reactions were diluted 1:50 in 70% methanol and analyzed on an API4000 mass spectrometer using direct injection into the electrospray source at a flow rate of 30 µl min^{-1}. 150 scans were accumulated for each measurement in dual ion monitoring mode, which was adjusted to monitor ions at nominal m/z ratios of the substrate and expected product with a mass range of ± 5 Da.

5.2.6. Histochemical localization of gene expression

Genomic fragments upstream of the start codon were amplified from genomic DNA (accession Columbia) by PCR using the following primer pairs; *UGT76B1*pro_GW_f and *UGT76B1*pro_GW_r for *UGT76B1* and *UGT87A2*pro_GW_f and *UGT87A2*pro_GW_r for *UGT87A2*. Fragments were introduced into vector pBGWFS7 (Invitrogen) using Gateway™ recombination. The resulting UGT promoter:GUS-GFP fusion, was then transformed into Col-O *Arabidopsis* plants using floral dip transformation (Clough and Bent, 1998). After

selection of transformants, segregation analysis was used for the identification of single insertion lines in the T2 generation. Two independent segregating lines were selected for each gene for further analysis. Transgenic lines were selected on the basis of Basta[TM] resistance.

Histochemical analysis of the GUS reporter gene was performed at different developmental stages according to a protocol described by Lagarde et al. (1996), using 1 mM hexacyanoferrat II/III. After staining, plant material was rinsed several times in 70% ethanol at 80ºC, until complete destaining of chlorophyll.

To gain more detailed information about *UGT* expression in roots, the same *UGT*pro:GUS-GFP fusion lines were analyzed with a Confocal Laser Scanning microscope (LSM 510 Axiovert 100 M; Carl Zeiss, Jena). For cell wall staining, 1-week-old seedlings grown on vertically orientated plates were immerged in 50 µg ml^{-1} propidium iodide (PI, Sigma, Germany, cat. no. P4170, in water) for 30 min, washed twice with double-distilled water and observed thereafter. Stainings were performed on two independent single insertion lines showing consistent results.

5.2.7. Metabolic analysis

5.2.7.1. Non-targeted metabolome analysis using FT-ICR-MS

A wide range of analytical methods—mainly based on mass spectrometry—have been developed recently to separate, detect and identify the host of small molecules present in biological samples. The high-capacity Fourier Transform Ion Cyclotron Mass Spectrometry (FT-ICR-MS) is suitable for rapid and non-targeted screening of similarities and dissimilarities in large collections of biological samples such as plant mutant populations. Separation of the metabolites can be achieved solely by its ultra-high mass resolution. Additionally, the high mass accuracy of the instrument enables us to achieve a good separation of the metabolites present in complex mixtures through direct injection and to calculate possible elemental compositions of each ion and its precursor molecule.

5.2.7.1.1. Metabolite extraction

A 12 Tesla FT-ICR-MS was used to compare the metabolic profile of *UGT* mutant and overexpression lines with their respective wild type. Different extraction methods and measuring conditions (e.g. extract dilution and ion accumulation) were compared. Considering reproducibility, optimal peak intensities and possible reduction of matrix effects

(mutual interference of ions present in the mass spectrometer), 6 replicates (3 biological replicates and 2 technical replicates each) were performed for each genotype.

Frozen root tissue was individually grounded using a dismembrator. Metabolite extraction was performed as described previously (Weckwerth et al., 2004) with slight modifications (Figure 43). Forty four µg ml^{-1} loganin and 3 µg ml^{-1} nitrophenol were added to the extraction buffer (methanol/chloroform/water 2.5:1:1 v/v/v) as internal standards. Two ml of a single phase solvent mixture of methanol/chloroform/water 2.5:1:1 v/v/v (kept at -20°C) was added to 100 mg plant material and mixed at 4°C for 30 min. After centrifugation (10 min, 14.000 rpm, 4°C) 1 ml of the supernatant (supernatant A) was transferred into a fresh Eppendorf tube and the remaining pellet was extracted in a second step with 1 ml methanol/chloroform 1:1 v/v (kept at 4°C). After a second centrifugation round, 500 µl supernatant (supernatant B) were mixed with supernatant A. The chloroform phase was then separated from the water/methanol phase by adding 250 µl of HPLC grade water (4°C, Merck). The aqueous phase was divided into several 200 µl aliquots and dried completely using a SpeedVac.
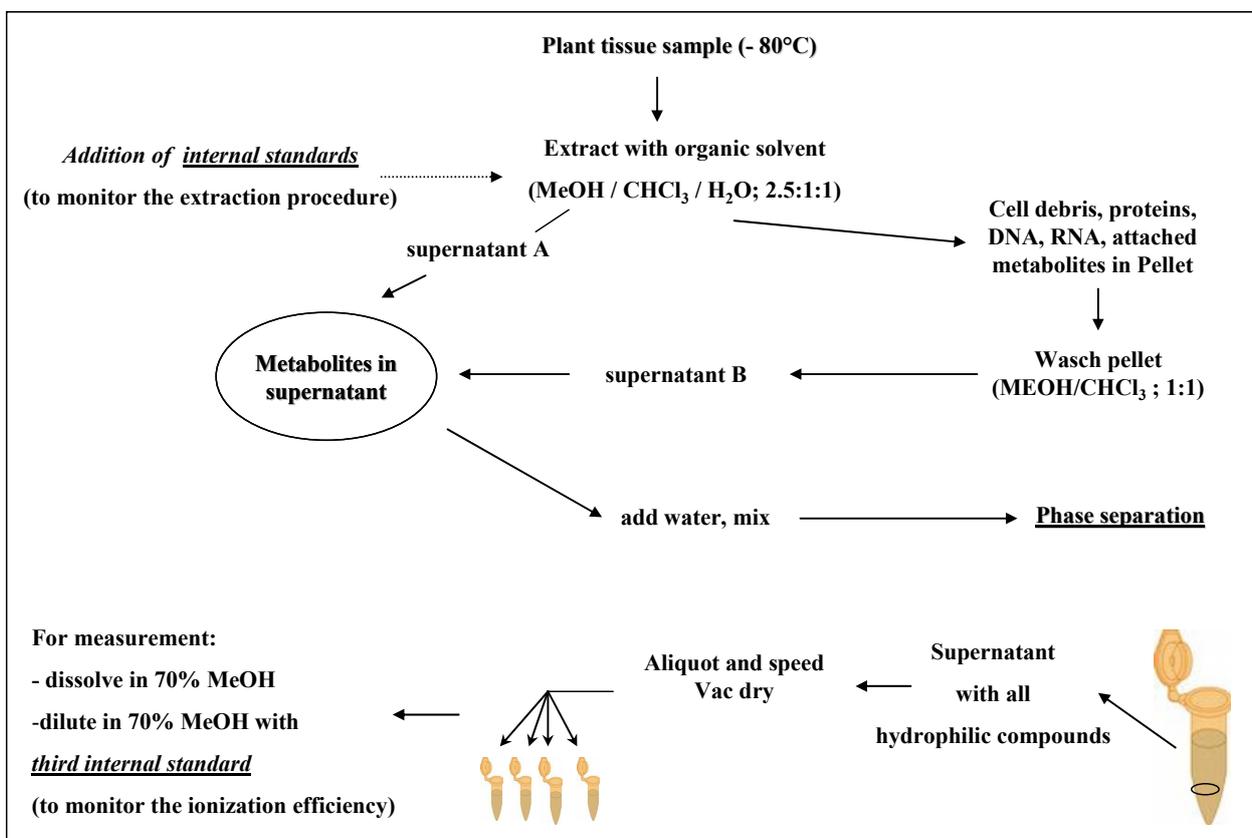
Figure 43. Metabolite extraction procedure for metabolome analysis.

5.2.7.1.2. FT-ICR-MS measurements

For FT-ICR-MS analysis one dried aliquot of each sample was redissolved in 70% methanol and diluted 1:25 or 1:50 for roots and leaf material, respectively, in 70% methanol containing 35 pmol ml^{-1} di-alanin. High-resolution mass spectra were acquired on a Bruker APEX Qe Fourier transform ion cyclotron resonance mass spectrometer FT-ICR-MS (Brukers, Bremen, Germany) equipped with a 12 Tesla superconducting magnet and an APOLLO II Electrospray ionization source. Measurements were performed in the negative ionization mode. Samples were introduced into the electrospray source at a flow rate of 120 µl/h with a nebulizer gas pressure of 20 psi and a drying gas pressure of 15 psi (at 200°C). Spectra were externally calibrated based on arginine cluster ions (10 ppm). The spectra were acquired with a time domain of 1 MW over a mass range between 147 and 2000 amu. Three hundred scans were accumulated for each spectrum. Internal mass calibration was performed using the internal standards (nitrophenol, loganin, dialanin) in addition to endogenous plant metabolites with calibration accuracy smaller than 0.01 ppm. For detailed information on compounds and masses used for calibration see Table 12. Internal standards were also used to detect variation in the extraction procedure, matrix effects and variation in the ionization efficiency in the Electrospray source. Mass lists were calibrated using the Data Analysis program (Bruker, Germany) and exported to ascii files. The signal to noise ratio for mass list extraction was set to 2. Mass list matrices for statistical analysis were produced using a custom-made program with a window width of 4 ppm (M. Frommberger, Helmholtz Zentrum München).

Table 12. Mass list used for internal mass calibration of each measurement.

Compound	Formula [M-H]	m/z [M-H]
Nitrophenol	$C_6H_4NO_3^-$	138.019664
Dialanin	$C_6H_{11}N_2O_3^-$	159.07752
Glucose	$C_6H_{11}O_6^-$	179.056114
SA-Glucoside	$C_{13}H_{15}O_8^-$	299.077244
Dialanin Clusterion	$C_{12}H_{23}N_4O_6^-$	319.162308
Ascorbic acid glucoside	$C_{12}H_{17}O_{11}^-$	337.077639
Sucrose	$C_{12}H_{21}O_{11}^-$	341.108939
1-O-Sinapoyl-beta-D-glucose	$C_{17}H_{21}O_{10}^-$	385.114024
Loganin	$C_{17}H_{25}O_{10}^-$	389.145324
Glucoraphanin	$C_{12}H_{22}NO_{10}S_3^-$	436.041135
Neoglucobrassicin	$C_{17}H_{21}N_2O_{10}S_2^-$	477.064308
Glucobrassicin	$C_{16}H_{19}N_2O_9S_2^-$	447.053743
Kaempferol di-rhamnoside	$C_{27}H_{29}O_{14}^-$	577.156284
Kaempferol glucoside-rhamnoside	$C_{27}H_{29}O_{15}^-$	593.151199
Kaempferol di-glucoside-rhamnoside	$C_{33}H_{39}O_{20}^-$	755.204024

5.2.7.1.3.   Reproducibility and statistical analysis

As a general reproducibility check, the intensity of the internal standards and the sum of total peak intensities was monitored to detect variation in the ionization efficiency (in addition to internal standards). Measurements with more than 20% deviation from the mean of total intensities among one experiment were repeated. Detailed reproducibility check and statistical analysis was performed in R (R-Development-Core-Team, 2009). The R script for statistical analysis was written by Theresa Faus-Kessler (Helmholtz Zentrum München). First, masses which were detected in only two or less out of 6 measurements in both genotypes were deleted. Remaining zero values were replaced by 200,000 counts, the value considered as detection limit. Figures 43-45 show examples of statistical analysis performed in R. Pairwise xy-plots and a Pearson correlation analysis of all peak intensities (excluding missing values) were used to check extract reproducibility (correlation $r^2 > 0.9$). As shown by the single plots in Figure 45, high reproducibility between measurements could be achieved. As expected, technical replicates show higher extract reproducibilities than biological replicates. Principal component analysis (Figure 46) also shows no separation between different genotypes when

observing the first and the second principal components. This is not surprising as only few metabolites were found to be significantly different (in the Wilcoxon test, see results section 3.1.10); instead it shows a high reproducibility among the different extracts. However, a clear separation could be observed in some cases by plotting principal component 2 and 3, the third component might account for the significant metabolite changes found.

A two sample Wilcoxon rank sum test was performed for each mass separately to detect significant peak intensity differences between wild-type and mutant plants. Significance level was set to 1%. The Wilcoxon test can be used as an alternative to the paired Student's t-test when the population cannot be assumed to be normally distributed. However, a T-Test was performed in parallel (see Supplemental Table 1). Experiments were repeated twice to filter for reproducible metabolite variations. Mass matrices from indepent experiments were joined setting a mass precision of three decimal places.
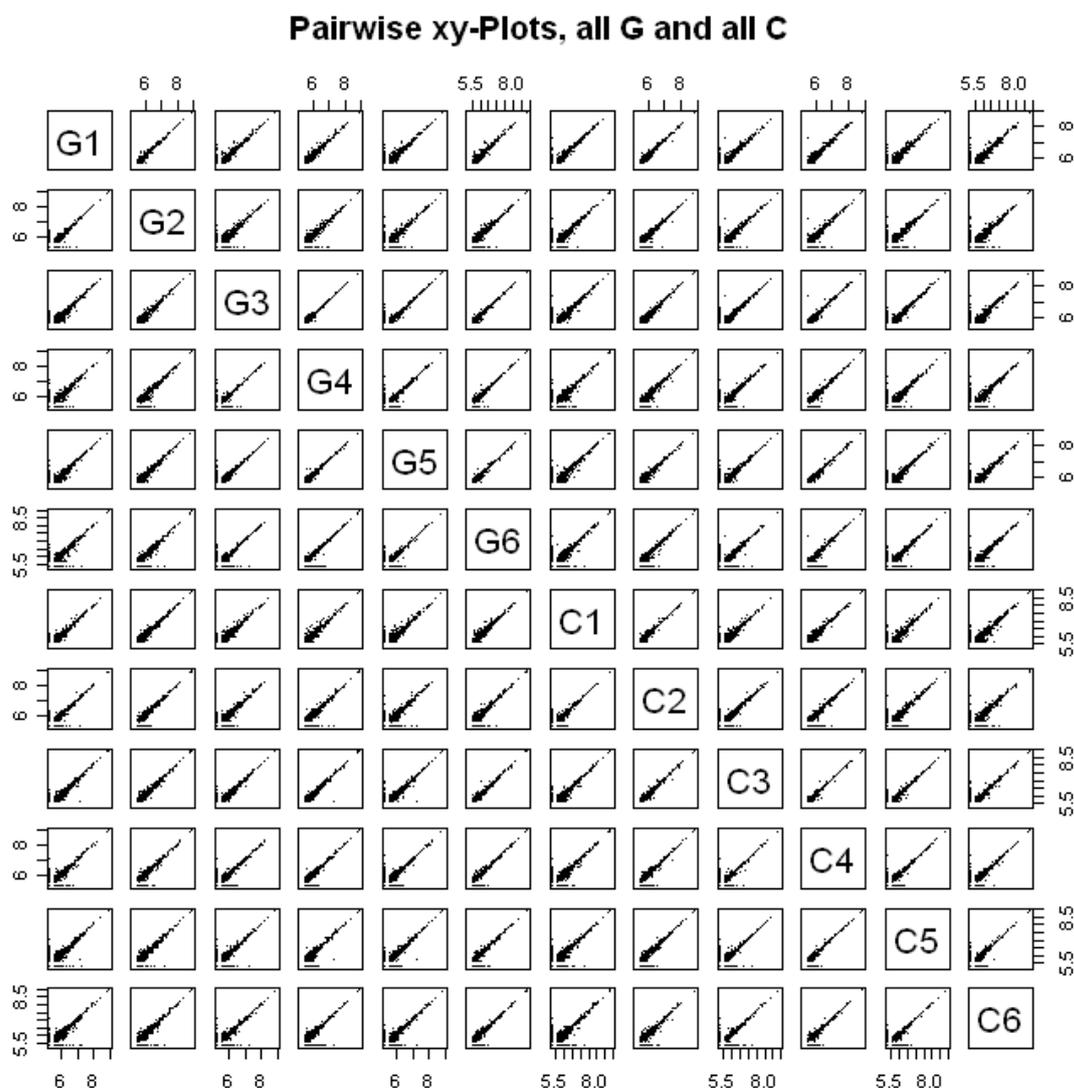

Figure 44. Pairwise xy-plots of Col-0 and *ugt76b1-1* extract measurements.

Comparison of peak intensities between two extracts. G1-G6: *ugt76b1-1*. C1-C6: Col-0.

A

technical replicate

biological replicate

G1 vs. G2

$R^2 = 0.985$

G1 vs. G3

$R^2 = 0.970$

C1 vs.C2

$R^2 = 0.982$

C1 vs. C3

$R^2 = 0.972$
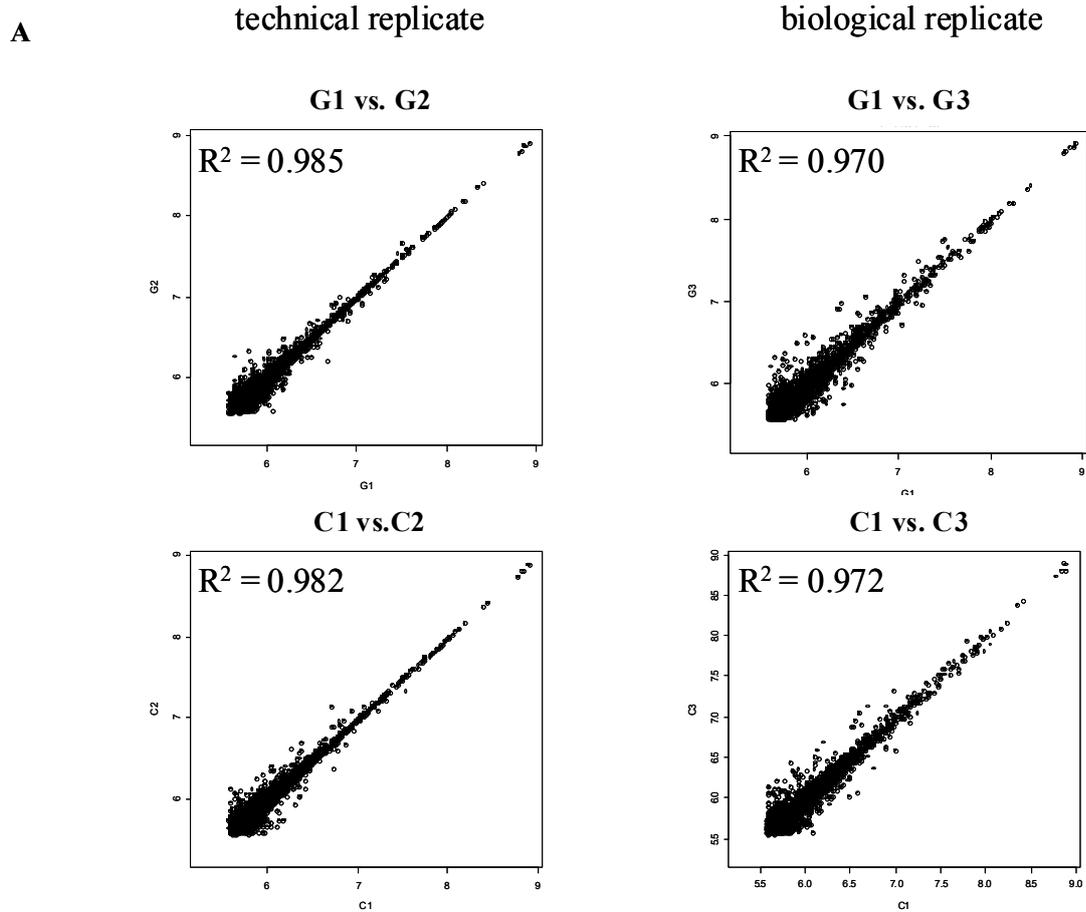
B

	G1	G2	G3	G4	G5	G6	C1	C2	C3	C4	C5	C6
G1	1.0000000	**0.9850933**	**0.9700915**	**0.9707289**	**0.9721189**	**0.9735935**	0.9781447	0.9810893	0.9709693	0.9705301	0.9678126	0.9669827
G2	0.9850933	1.0000000	**0.9693960**	**0.9696757**	**0.9726348**	**0.9740321**	0.9697248	0.9794211	0.9702688	0.9704048	0.9682114	0.9693554
G3	0.9700915	0.9693960	1.0000000	**0.9874743**	**0.9835660**	**0.9841153**	0.9633859	0.9738440	0.9764210	0.9777054	0.9731238	0.9734704
G4	0.9707289	0.9696757	0.9874743	1.0000000	**0.9818372**	**0.9834928**	0.9628362	0.9731227	0.9763778	0.9777040	0.9725524	0.9748592
G5	0.9721189	0.9726348	0.9835660	0.9818372	1.0000000	**0.9856208**	0.9624628	0.9750912	0.9747092	0.9779231	0.9728272	0.9749964
G6	0.9735935	0.9740321	0.9841153	0.9834928	0.9856208	1.0000000	0.9652248	0.9758458	0.9779758	0.9782019	0.9745114	0.9780539
C1	0.9781447	0.9697248	0.9633859	0.9628362	0.9624628	0.9652248	1.0000000	0.9819615	0.9720080	0.9708751	0.9692474	0.9609378
C2	0.9810893	0.9794211	0.9738440	0.9731227	0.9750912	0.9758458	0.9819615	1.0000000	0.9803575	0.9804754	0.9770491	0.9706496
C3	0.9709693	0.9702688	0.9764210	0.9763778	0.9747092	0.9779758	**0.9720080**	**0.9803575**	1.0000000	0.9855631	0.9838342	0.9819521
C4	0.9705301	0.9704048	0.9777054	0.9777040	0.9779231	0.9782019	**0.9708751**	**0.9804754**	0.9855631	1.0000000	0.9852777	0.9816664
C5	0.9678126	0.9682114	0.9731238	0.9725524	0.9728272	0.9745114	**0.9692474**	**0.9770491**	0.9838342	0.9852777	1.0000000	0.9838267
C6	0.9669827	0.9693554	0.9734704	0.9748592	0.9749964	0.9780539	**0.9609378**	**0.9706496**	0.9819521	0.9816664	**0.9838267**	1.0000000

Figure 45. Pairwise correlation analysis between extracts.

Pearson correlation excluded zero values is used for reproducibility analysis.

G1-G6: *ugt76b1-1*, G1 vs. G2, G3 vs. G4 and G5 vs. G6 are technical replicates.

C1-C6: Col-0, C1 vs. C2, C3 vs. C4 and C5 vs. C6 are technical replicates.

(A) Correlations between technical and biological replicates show good extract reproducibility.

(B) Matrix of Pearson correlations between all extracts. Correlation between technical replicates is marked in red; correlation between biological replicates is shown in black and bold.

107
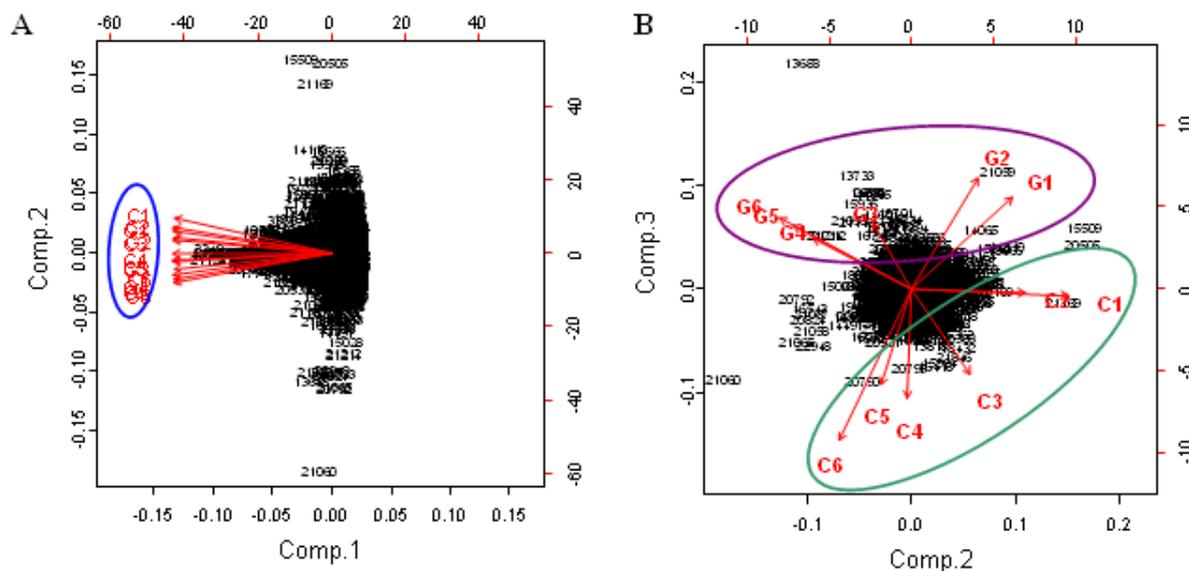
Figure 46. Principal component analysis of *ugt76b1-1* and Col-0 metabolome analyses.

Figure shows biplots from principal component analysis including observations and variables.

5.2.7.1.4.   Molecular formula generation and compound identification

Putative molecular formulas were generated using the Data Analysis program (Bruker, Germany) or Masstrix (http://metabolomics.helmholtz-muenchen.de/masstrix2/run.cgi? TASK=LIST) and confirmed if possible by the $^{12}C/^{13}C$ peak ratios. Putative compounds were identified using several databases such as:

-   PMN (http://plantcyc.org/)
-   KEGG (http://www.genome.jp/kegg/ligand.html)
-   ChemSpider (http://www.chemspider.com/)
-   ChemIDplus Advanced (http://chem.sis.nlm.nih.gov/chemidplus/)
-   ChEBI (http://www.ebi.ac.uk/chebi/advancedSearchFT.do)
-   KNApSAcK (http://prime.psc.riken.jp/?action=metabolites_index)

5.2.7.1.5.   Fragmentation studies

For fragmentation studies, the plant extract was partially cleaned and concentrated using a Strata NH2 column (3 ml, Phenomenex). Dried extracts were redissolved in 90% acetonitrile and loaded on the column (preconditioned with acetonitrile). Elution was performed with decreasing acetonitrile concentrations in 20% steps. Glucosides were accumulated in the fraction eluted with 20% acetonitrile. This fraction was SpeedVac dried and redissolved in 70% methanol for further analysis. Standards were dissolved in 70% methanol and diluted to

50 ppm for fragmentation. For MS/MS fragmentation studies, the targeted ions were trapped in a first hexapole for 200 ms prior to their mass selection inside a quadrupole mass filter. Once isolated, the targeted ions were then accelerated and were let to collide with argon atoms inside a second hexapole which served as a collision cell. The second hexapole had a relatively high pressure of 5 x 10^{-3} mbar. As a result of the collisions between the accelerated isolated ions and argon atoms in the second hexapole, product ions were produced and they were forwarded to the ICR cell via a couple of accelerating and decelerating lenses. The ion accumulation time inside the collision cell was 500 ms.

For those targeted ions with m/z < 200 amu, no quadrupole MS/MS fragmentation was done. Instead, the ions were forwarded as normal to the ICR cell and then they were isolated inside the cell by applying a frequency sweep to eject all ions except for those that should be selected for further fragmentation events. Once isolated inside the ICR cell, the targeted ions can then be excited in the radial plane which is perpendicular to the magnetic field lines by applying an on-resonance radial single shot excitation pulse with a duration of 400 μs and a power of 4.5 Vp-p. A pulsed valve opens at the same time for 5 ms to inject argon atoms inside the ICR cell for collisional induced dissociation experiments. The produced fragment ions are then allowed to thermalize inside the cell before accelerating them in the radial plane for detection.

A suitable database to search for fragmentation patterns of several compounds is the High Resolution Mass Spectral Database MassBank (http://www.massbank.jp/QuickSearch.html).

5.2.7.2.   HPLC analysis

5.2.7.2.1.   Ascorbic acid and conjugates

Ascorbic acid and its glucoside contents in plants were analyzed by a similar method as described previously (Tai and Gohda, 2007).

100 mg ground plant material was extracted with 1 ml extraction buffer for 30 min at 4°C. The extract was then centrifuged for 10 min at 14.000 rpm and 4°C. The supernatant was filtered through a 0.45 μm filter to avoid clogging of the HPLC column.

For HPLC analysis the extract was diluted 1:3 with dilution buffer and again centrifuged. 25 μg/ml Ascorbic acid, 50 μg/ml Ascorbic acid-2-O-α-glucoside (Hayashibara Biochemical Laboratories, Inc., Okayama, Japan) and Goji berries (*Lycium Barbarum* L) were used as

standards. For spiking experiments, *Lycium* extract was added to *UGT87A2-OE-19* plant extract at a final dilution of 1:30.

HPLC conditions (HILIC):

Column: Inertsil Diol (4.6 i.d. ×250 mm, 5 μm, GL Sciences)

Precolumn: LUNA Hilic (4 x 3.0 mm, Phenomenex)

Mobile phase: Isocratic 86:14 (v/v) (Acetonitrile: 66.7 mM Ammonium acetate)

Flow rate: 0.7 ml/min

Detection: UV 260 nm

Extraction buffer:	30:70 (v/v)	Acetonitrile:water
	200 mg/ml	DTT
Dilution buffer:	86:14 (v/v)	Acetonitrile:66.7 mM Ammonium acetate
	50 mg/ml	DTT

For semi-quantification of ascorbic acid (Supplemental Figure 7) a slightly modified mobile phase was used, for earlier elution of ascorbic acid:

Isocratic 85:15 (v/v) (Acetonitrile: 66.7 mM Ammonium acetate)

5.2.7.2.2. Salicylic acid and conjugates

Rosette leaves from four to six individual five-week-old plants (snap-frozen in liquid nitrogen and stored at -80°C) were pooled and used for metabolite extraction. Approximately 200 mg ground plant material was extracted with 3.5 ml of a 1 + 2 mixture of methanol and 2% (v/v) formic acid containing 25 μl o-Anisic acid (500 μg/ ml) as an internal standard. The extract was split into three aliquots of 3 ml, 1 ml and 2 ml for separate determination of free SA, SA glucosides, and SA esters, respectively. For determination of the SA conjugates, the extract was digested overnight with β-glucosidase (Roth, Karsruhe, Germany, cat. no. 7512.2) or with esterase (Sigma, Germany, cat. no. E2884). SA from undigested and digested samples was extracted under acidic conditions using reversed-phase sorbent cartridges (Oasis HLB 1cc, Waters, cat. no. WAT094225), recovered under basic conditions, and subsequently analyzed via HPLC. Quantification was based on SA fluorescence (excitation 305 nm/ emission 400 nm) with o-anisic acid added as an internal standard during metabolite extraction and

authentic SA standards. Thus, the content in free SA, in free SA plus glucose-conjugated SA, and in free SA plus esterified SA could be acquired.

5.2.7.3. Data mining of public expression data

A complete collection of 122 *UGT* genes from *Arabidopsis thaliana* was extracted via the CAZY database (www.cazy.org). No AGI locus was associated with two pseudogenes listed (*UGT85A6P* and *UGT90A3P*); *UGT89B1* (At1g73880) was not represented on the Affymetrix array which has been used for the expression analyses compiled in Figure 4. Among the residual 119 probe sets, 105 targeted individual members specifically, whereas seven did not discriminate two highly homologous isoforms each. Normalized microarray data for all 119 probe sets comprising abiotic and biotic (without elicitors) stressors applied to Col-0 wild-type seedling were downloaded from the BAR database (bbc.botany.utoronto.ca).

For a number of treatments two or more time points had been deposited. In cases, where both up- and downregulations had been recorded, the difference between the total number of significant inductions (> 1.5 fold) and repressions (< 0.67) was calculated. A specific gene was assigned *induced* when inductions were present in at least two time points and the number of inductions exceeded repressions in at least two consecutive time points. In cases, where the number of inductions equalled repressions, genes were nevertheless assigned *induced*, if clear induction kinetics had been observed. In cases of only two experimental time points, induction in one instance was sufficient as long no repression had been observed in the second time point. For final classification, the maximal induction among different time points was selected for each treatment. The total number of significant stress inductions was separately indicated for abiotic and biotic stress cues and a mutual rank [$MR = (\text{rank abiotic} \times \text{rank biotic})^{0.5}$, (Obayashi et al., 2009)] for both biotic and abiotic stress inductions was calculated for each *UGT* isoform to sort genes from highest to lowest combined stress inducibility.

6. REFERENCES

Achnine, L., Huhman, D.V., Farag, M.A., Sumner, L.W., Blount, J.W., and Dixon, R.A. (2005). Genomics-based selection and functional characterization of triterpene glycosyltransferases from the model legume *Medicago truncatula*. Plant J **41:** 875-887.

Aga, H., Yoneyama, M., Sakai, S., and Yamamoto, I. (1991). Synthesis of 2-O-α-glucopyranosyl L-ascorbic acid by cyclomaltodextrin glucanotransferase from *Bacillus stearothermophilus*. Agric Biol Chem **55:** 1751-1756.

Ahmed, A., Peters, N.R., Fitzgerald, M.K., Watson, J.A., Jr., Hoffmann, F.M., and Thorson, J.S. (2006). Colchicine glycorandomization influences cytotoxicity and mechanism of action. J Am Chem Soc **128:** 14224-14225.

Arrigoni, O., and De Tullio, M.C. (2002). Ascorbic acid: much more than just an antioxidant. Biochim Biophys Acta General Subjects **1569:** 1-9.

Bajguz, A. (2007). Metabolism of brassinosteroids in plants. Plant Physiol Biochem **45:** 95-107.

Balague, C., Lin, B., Alcon, C., Flottes, G., Malmstrom, S., Kohler, C., Neuhaus, G., Pelletier, G., Gaymard, F., and Roby, D. (2003). HLM1, an essential signaling component in the hypersensitive response, is a member of the cyclic nucleotide-gated channel ion channel family. Plant Cell **15:** 365-379.

Bandu, M.L., Grubbs, T., Kater, M., and Desaire, H. (2006). Collision induced dissociation of alpha hydroxy acids: Evidence of an ion-neutral complex intermediate. Int J Mass Spectrom **251:** 40-46.

Barth, C., De Tullio, M., and Conklin, P.L. (2006). The role of ascorbic acid in the control of flowering time and the onset of senescence. J Exp Bot **57:** 1657-1665.

Barth, C., Moeder, W., Klessig, D.F., and Conklin, P.L. (2004). The timing of senescence and response to pathogens is altered in the ascorbate-deficient *Arabidopsis* mutant vitamin c-1. Plant Physiol **134:** 1784-1792.

Battke, F., Schramel, P., and Ernst, D. (2003). A novel method for *in vitro* culture of plants: Cultivation of barley in a floating hydroponic system. Plant Mol Biol Rep **21:** 405-409.

Bell, E., Creelman, R.A., and Mullet, J.E. (1995). A chloroplast lipoxygenase is required for wound-induced jasmonic acid accumulation in *Arabidopsis*. Proc Natl Acad Sci USA **92:** 8675-8679.

Bensmihen, S., To, A., Lambert, G., Kroj, T., Giraudat, J., and Parcy, F. (2004). Analysis of an activated ABI5 allele using a new selection method for transgenic *Arabidopsis* seeds. FEBS Lett **561:** 127-131.

Berger, S., Bell, E., and Mullet, J.E. (1996). Two Methyl Jasmonate-Insensitive Mutants Show Altered Expression of AtVsp in Response to Methyl Jasmonate and Wounding. Plant Physiol **111:** 525-531.

Binder, S., Knill, T., and Schuster, J. (2007). Branched-chain amino acid metabolism in higher plants. Physiol Plant **129:** 68-78.

Blanco, F., Salinas, P., Cecchini, N.M., Jordana, X., Van Hummelen, P., Alvarez, M.E., and Holuigue, L. (2009). Early genomic responses to salicylic acid in *Arabidopsis*. Plant Mol Biol **70:** 79-102.

Bolton, M.D. (2009). Primary metabolism and plant defense--fuel for the fire. Mol Plant Microbe Interact **22:** 487-497.

Bowles, D., Isayenkova, J., Lim, E.K., and Poppenberger, B. (2005). Glycosyltransferases: managers of small molecules. Curr Opin Plant Biol **8:** 254-263.

Bowles, D., Lim, E.K., Poppenberger, B., and Vaistij, F.E. (2006). Glycosyltransferases of lipophilic small molecules. Ann Rev Plant Biol **57:** 567-597.

Bowling, S.A., Clarke, J.D., Liu, Y., Klessig, D.F., and Dong, X. (1997). The *cpr5* mutant of *Arabidopsis* expresses both NPR1-dependent and NPR1-independent resistance. Plant Cell **9:** 1573-1584.

Bowling, S.A., Guo, A., Cao, H., Gordon, A.S., Klessig, D.F., and Dong, X. (1994). A mutation in *Arabidopsis* that leads to constitutive expression of systemic acquired resistance. Plant Cell **6:** 1845-1857.

Brazier-Hicks, M., and Edwards, R. (2005). Functional importance of the family 1 glucosyltransferase *UGT72B1* in the metabolism of xenobiotics in *Arabidopsis thaliana*. Plant J **42:** 556-566.

Brazier, M., Cole, D.J., and Edwards, R. (2002). O-Glucosyltransferase activities toward phenolic natural products and xenobiotics in wheat and herbicide-resistant and herbicide-susceptible black-grass (*Alopecurus myosuroides*). Phytochemistry **59:** 149-156.

Brazier, M., Cole, D.J., and Edwards, R. (2003). Partial purification and characterisation of a 2,4,5-trichlorophenol detoxifying O-glucosyltransferase from wheat. Phytochemistry **64:** 419-424.

Brodersen, P., Petersen, M., Bjorn Nielsen, H., Zhu, S., Newman, M.A., Shokat, K.M., Rietz, S., Parker, J., and Mundy, J. (2006). *Arabidopsis* MAP kinase 4 regulates salicylic acid- and jasmonic acid/ethylene-dependent responses via EDS1 and PAD4. Plant J **47:** 532-546.

Buchanan-Wollaston, V., Page, T., Harrison, E., Breeze, E., Lim, P.O., Nam, H.G., Lin, J.F., Wu, S.H., Swidzinski, J., Ishizaki, K., and Leaver, C.J. (2005). Comparative transcriptome analysis reveals significant differences in gene expression and signalling pathways between developmental and dark/starvation-induced senescence in *Arabidopsis*. Plant J **42:** 567-585.

Campbell, J.A., Davies, G.J., Bulone, V., and Henrissat, B. (1997). A classification of nucleotide-diphospho-sugar glycosyltransferases based on amino acid sequence similarities. Biochem J **326 (Pt 3):** 929-939.

Cantarel, B.L., Coutinho, P.M., Rancurel, C., Bernard, T., Lombard, V., and Henrissat, B. (2009). The Carbohydrate-Active EnZymes database (CAZy): an expert resource for Glycogenomics. Nucleic Acids Res **37:** D233-D238.

Cao, H., Glazebrook, J., Clarke, J.D., Volko, S., and Dong, X. (1997). The *Arabidopsis NPR1* gene that controls systemic acquired resistance encodes a novel protein containing ankyrin repeats. Cell **88:** 57-63.

Casella, L., Monzani, E., Santagostini, L., de Gioia, L., Gullotti, M., Fantucci, P., Beringhelli, T., and Marchesini, A. (1999). Inhibitor binding studies on ascorbate oxidase. Coord Chem Rev **186:** 619-628.

Chang S, P.J., Cairney J (1993). A simple and efficient method for isolating RNA from pine trees. Plant Mol Biol Rep **11:** 113-116.

Chapple, C. (1998). Molecular-Genetic Analysis of Plant Cytochrome P450-Dependent Monooxygenases. Annu Rev Plant Physiol Plant Mol Biol **49:** 311-343.

Charnock, S.J., Henrissat, B., and Davies, G.J. (2001). Three-dimensional structures of UDP-sugar glycosyltransferases illuminate the biosynthesis of plant polysaccharides. Plant Physiol **125:** 527-531.

Chong, J., Baltz, R., Schmitt, C., Beffa, R., Fritig, B., and Saindrenan, P. (2002). Downregulation of a pathogen-responsive tobacco UDP-Glc:phenylpropanoid glucosyltransferase reduces scopoletin glucoside accumulation, enhances oxidative stress, and weakens virus resistance. Plant Cell **14:** 1093-1107.

Cicek, M., Blanchard, D., Bevan, D.R., and Esen, A. (2000). The aglycone specificity-determining sites are different in 2,4-dihydroxy-7-methoxy-1,4-benzoxazin-3-one

(DIMBOA)-glucosidase (maize beta-glucosidase) and dhurrinase (sorghum beta-glucosidase). J Biol Chem **275:** 20002-20011.

Clough, S.J., and Bent, A.F. (1998). Floral dip: a simplified method for *Agrobacterium*-mediated transformation of *Arabidopsis thaliana*. Plant J **16:** 735-743.

Conklin, P.L., and Barth, C. (2004). Ascorbic acid, a familiar small molecule intertwined in the response of plants to ozone, pathogens, and the onset of senescence. Plant Cell and Environ **27:** 959-970.

Conklin, P.L., Norris, S.R., Wheeler, G.L., Williams, E.H., Smirnoff, N., and Last, R.L. (1999). Genetic evidence for the role of GDP-mannose in plant ascorbic acid (vitamin C) biosynthesis. Proc Natl Acad Sci USA **96:** 4198-4203.

Consonni, C., Humphry, M.E., Hartmann, H.A., Livaja, M., Durner, J., Westphal, L., Vogel, J., Lipka, V., Kemmerling, B., Schulze-Lefert, P., Somerville, S.C., and Panstruga, R. (2006). Conserved requirement for a plant host cell protein in powdery mildew pathogenesis. Nat Genet **38:** 716-720.

Cordoba-Pedregosa, M.D., Cordoba, F., Villalba, J.M., and Gonzalez-Reyes, J.A. (2003). Zonal changes in ascorbate and hydrogen peroxide contents, peroxidase, and ascorbate-related enzyme activities in onion roots. Plant Physiol **131:** 697-706.

Cosgrove, D.J. (2005). Growth of the plant cell wall. Nat Rev Mol Cell Biol **6:** 850-861.

Coutinho, P.M., Deleury, E., Davies, G.J., and Henrissat, B. (2003). An evolving hierarchical family classification for glycosyltransferases. J Mol Biol **328:** 307-317.

Dean, J.V., and Delaney, S.P. (2008). Metabolism of salicylic acid in wild-type, *ugt74f1* and *ugt74f2* glucosyltransferase mutants of *Arabidopsis thaliana*. Physiol Plant **132:** 417-425.

Devadas, S.K., Enyedi, A., and Raina, R. (2002). The *Arabidopsis hrl1* mutation reveals novel overlapping roles for salicylic acid, jasmonic acid and ethylene signalling in cell death and defence against pathogens. Plant J **30:** 467-480.

Diaz, C., Purdy, S., Christ, A., Morot-Gaudry, J.F., Wingler, A., and Masclaux-Daubresse, C.L. (2005). Characterization of markers to determine the extent and variability of leaf senescence in *Arabidopsis*. A metabolic profiling approach. Plant Physiol **138:** 898-908.

Dooner, H.K., and Nelson, O.E. (1977). Controlling element-induced alterations in UDPglucose:flavonoid glucosyltransferase, the enzyme specified by the bronze locus in maize. Proc Natl Acad Sci USA **74:** 5623-5627.

Ehlting, J., Sauveplane, V., Olry, A., Ginglinger, J.F., Provart, N.J., and Werck-Reichhart, D. (2008). An extensive (co-)expression analysis tool for the cytochrome P450 superfamily in *Arabidopsis thaliana*. BMC Plant Biol **8:** 47.

Fahey, J.W., Zalcmann, A.T., and Talalay, P. (2001). The chemical diversity and distribution of glucosinolates and isothiocyanates among plants. Phytochemistry **56:** 5-51.

Fedoroff, N.V., Furtek, D.B., and Nelson, O.E. (1984). Cloning of the bronze locus in maize by a simple and generalizable procedure using the transposable controlling element Activator (Ac). Proc Natl Acad Sci USA **81:** 3825-3829.

Feys, B., Benedetti, C.E., Penfold, C.N., and Turner, J.G. (1994). *Arabidopsis* Mutants Selected for Resistance to the Phytotoxin Coronatine Are Male Sterile, Insensitive to Methyl Jasmonate, and Resistant to a Bacterial Pathogen. Plant Cell **6:** 751-759.

Feys, B.J., Moisan, L.J., Newman, M.A., and Parker, J.E. (2001). Direct interaction between the *Arabidopsis* disease resistance signaling proteins, EDS1 and PAD4. EMBO J **20:** 5400-5411.

Fonseca, S., Chini, A., Hamberg, M., Adie, B., Porzel, A., Kramell, R., Miersch, O., Wasternack, C., and Solano, R. (2009). (+)-7-iso-Jasmonoyl-L-isoleucine is the endogenous bioactive jasmonate. Nat Chem Biol **5:** 344-350.

Ford, C.M., Boss, P.K., and Hoj, P.B. (1998). Cloning and characterization of *Vitis vinifera* UDP-glucose:flavonoid 3-O-glucosyltransferase, a homologue of the enzyme encoded by the maize Bronze-1 locus that may primarily serve to glucosylate anthocyanidins in vivo. J Biol Chem **273:** 9224-9233.

Frick, S., and Kutchan, T.M. (1999). Molecular cloning and functional expression of O-methyltransferases common to isoquinoline alkaloid and phenylpropanoid biosynthesis. Plant J **17:** 329-339.

Fridman, E., and Pichersky, E. (2005). Metabolomics, genomics, proteomics, and the identification of enzymes and their substrates and products. Curr Opin Plant Biol **8:** 242-248.

Frydman, A., Weisshaus, O., Bar-Peled, M., Huhman, D.V., Sumner, L.W., Marin, F.R., Lewinsohn, E., Fluhr, R., Gressel, J., and Eyal, Y. (2004). Citrus fruit bitter flavors: isolation and functional characterization of the gene *Cm1,2RhaT* encoding a 1,2 rhamnosyltransferase, a key enzyme in the biosynthesis of the bitter flavonoids of citrus. Plant J **40:** 88-100.

Fujioka, S., and Yokota, T. (2003). Biosynthesis and metabolism of brassinosteroids. Ann Rev Plant Biol **54:** 137-164.

Fujita, M., Fujita, Y., Noutoshi, Y., Takahashi, F., Narusaka, Y., Yamaguchi-Shinozaki, K., and Shinozaki, K. (2006). Crosstalk between abiotic and biotic stress responses: a current view from the points of convergence in the stress signaling networks. Curr Opin Plant Biol **9:** 436-442.

Gachon, C., Baltz, R., and Saindrenan, P. (2004). Over-expression of a scopoletin glucosyltransferase in Nicotiana tabacum leads to precocious lesion formation during the hypersensitive response to tobacco mosaic virus but does not affect virus resistance. Plant Mol Biol **54:** 137-146.

Gachon, C.M.M., Langlois-Meurinne, M., and Saindrenan, P. (2005). Plant secondary metabolism glycosyltransferases: the emerging functional analysis. Trends Plant Sci **10:** 542-549.

Genger, R.K., Jurkowski, G.I., McDowell, J.M., Lu, H., Jung, H.W., Greenberg, J.T., and Bent, A.F. (2008). Signaling pathways that regulate the enhanced disease resistance of *Arabidopsis* "defense, no death" mutants. Mol Plant Microbe Interact **21:** 1285-1296.

Gilbert, L., Alhagdow, M., Nunes-Nesi, A., Quemener, B., Guillon, F., Bouchet, B., Faurobert, M., Gouble, B., Page, D., Garcia, V., Petit, J., Stevens, R., Causse, M., Fernie, A.R., Lahaye, M., Rothan, C., and Baldet, P. (2009). GDP-D-mannose 3,5-epimerase (GME) plays a key role at the intersection of ascorbate and non-cellulosic cell-wall biosynthesis in tomato. Plant J **60:** 499-508.

Glauser, G., Boccard, J., Rudaz, S., and Wolfender, J.L. (2010). Mass Spectrometry-based Metabolomics Oriented by Correlation Analysis for Wound-induced Molecule Discovery: Identification of a Novel Jasmonate Glucoside. Phytochem Anal **21:** 95-101.

Glazebrook, J. (2005). Contrasting mechanisms of defense against biotrophic and necrotrophic pathogens. Ann Rev Phytopathol **43:** 205-227.

Glazebrook, J., Rogers, E.E., and Ausubel, F.M. (1996). Isolation of *Arabidopsis* mutants with enhanced disease susceptibility by direct screening. Genetics **143:** 973-982.

Goggin, F.L., Avila, C.A., and Lorence, A. (2010). Vitamin C content in plants is modified by insects and influences susceptibility to herbivory. Bioessays **32**: 777-790.

Gou, M., Su, N., Zheng, J., Huai, J., Wu, G., Zhao, J., He, J., Tang, D., Yang, S., and Wang, G. (2009). An F-box gene, *CPR30*, functions as a negative regulator of the defense response in *Arabidopsis*. Plant J **60:** 757-770.

Greenberg, J.T., Guo, A., Klessig, D.F., and Ausubel, F.M. (1994). Programmed cell death in plants: a pathogen-triggered response activated coordinately with multiple defense functions. Cell **77:** 551-563.

Gruber, A.R., Lorenz, R., Bernhart, S.H., Neubock, R., and Hofacker, I.L. (2008). The Vienna RNA websuite. Nucleic Acids Res **36:** W70-74.

Hancock, R.D., and Viola, R. (2005). Biosynthesis and catabolism of L-ascorbic acid in plants. Crit Rev Plant Sci **24:** 167-188.

Hancock, R.D., Chudek, J.A., Walker, P.G., Pont, S.D., and Viola, R. (2008). Ascorbic acid conjugates isolated from the phloem of Cucurbitaceae. Phytochemistry **69:** 1850-1858.

Hanson, A.D., Pribat, A., Waller, J.C., and de Crecy-Lagard, V. (2010). 'Unknown' proteins and 'orphan' enzymes: the missing half of the engineering parts list - and how to find it. Biochem J **425:** 1-11.

Hefner, T., Arend, J., Warzecha, H., Siems, K., and Stockigt, J. (2002). Arbutin synthase, a novel member of the NRD1beta glycosyltransferase family, is a unique multifunctional enzyme converting various natural products and xenobiotics. Bioorg Med Chem **10:** 1731-1741.

Heidel, A.J., Clarke, J.D., Antonovics, J., and Dong, X.N. (2004). Fitness costs of mutations affecting the systemic acquired resistance pathway in *Arabidopsis thaliana*. Genetics **168:** 2197-2206.

Heil, M., and Baldwin, I.T. (2002). Fitness costs of induced resistance: emerging experimental support for a slippery concept. Trends Plant Sci **7:** 61-67.

Hematy, K., Cherk, C., and Somerville, S. (2009). Host-pathogen warfare at the plant cell wall. Curr Op Plant Biol **12:** 406-413.

Hemavathi, Upadhyaya, C.P., Akula, N., Young, K.E., Chun, S.C., Kim, D.H., and Park, S.W. (2010). Enhanced ascorbic acid accumulation in transgenic potato confers tolerance to various abiotic stresses. Biotechnol Lett **32:** 321-330.

Hirai, M.Y., Klein, M., Fujikawa, Y., Yano, M., Goodenowe, D.B., Yamazaki, Y., Kanaya, S., Nakamura, Y., Kitayama, M., Suzuki, H., Sakurai, N., Shibata, D., Tokuhisa, J., Reichelt, M., Gershenzon, J., Papenbrock, J., and Saito, K. (2005).

Elucidation of gene-to-gene and metabolite-to-gene networks in *Arabidopsis* by integration of metabolomics and transcriptomics. J Biol Chem **280:** 25590-25595.

Hou, B., Lim, E.K., Higgins, G.S., and Bowles, D.J. (2004). N-glucosylation of cytokinins by glycosyltransferases of *Arabidopsis thaliana*. J Biol Chem **279:** 47822-47832.

Hughes J, H.M. (1994). Multiple secondary plant product UDP-glucose glucosyltransferase genes expressed in cassava (*Manihot esculenta* Crantz) cotyledons. DNA sequ **5:** 41-49.

Hugouvieux, V., Barber, C.E., and Daniels, M.J. (1998). Entry of *Xanthomonas campestris* pv. *campestris* into hydathodes of *Arabidopsis thaliana* leaves: A system for studying early infection events in bacterial pathogenesis. Mol Plant Microbe Interact **11:** 537-543.

Isbell, H.S., and Frush, H.L. (1979). Oxidation of L-ascorbic acid by hydrogen peroxide: preparation of L-threonic acid. Carbohydr Res **72:** 301-304.

Jackson, R.G., Kowalczyk, M., Li, Y., Higgins, G., Ross, J., Sandberg, G., and Bowles, D.J. (2002). Over-expression of an *Arabidopsis* gene encoding a glucosyltransferase of indole-3-acetic acid: phenotypic characterisation of transgenic lines. Plant J **32:** 573-583.

Jackson, R.G., Lim, E.K., Li, Y., Kowalczyk, M., Sandberg, G., Hoggett, J., Ashford, D.A., and Bowles, D.J. (2001). Identification and biochemical characterization of an *Arabidopsis* indole-3-acetic acid glucosyltransferase. J Biol Chem **276:** 4350-4356.

Jiang, K., and Feldman, L.J. (2005). Regulation of root apical meristem development. Annu Rev Cell Dev Biol **21:** 485-509.

Jones, J.D., and Dangl, J.L. (2006). The plant immune system. Nature **444:** 323-329.

Jones, P., and Vogt, T. (2001). Glycosyltransferases in secondary plant metabolism: tranquilizers and stimulant controllers. Planta **213:** 164-174.

Jones, P., Messner, B., Nakajima, J., Schäffner, A.R., and Saito, K. (2003). UGT73C6 and UGT78D1, glycosyltransferases involved in flavonol glycoside biosynthesis in *Arabidopsis thaliana*. J Biol Chem **278:** 43910-43918.

Jones, P.R., Moller, B.L., and Hoj, P.B. (1999). The UDP-glucose : p-hydroxymandelonitrile-O-glucosyltransferase that catalyzes the last step in synthesis of the cyanogenic glucoside dhurrin in *Sorghum bicolor* - Isolation, cloning, heterologous expression, and substrate specificity. J Biol Chem **274:** 35483-35491.

Jorgensen, K., Rasmussen, A.V., Morant, M., Nielsen, A.H., Bjarnholt, N., Zagrobelny, M., Bak, S., and Moller, B.L. (2005). Metabolon formation and metabolic channeling in the biosynthesis of plant natural products. Curr Opin Plant Biol **8:** 280-291.

Journot-Catalino, N., Somssich, I.E., Roby, D., and Kroj, T. (2006). The transcription factors WRKY11 and WRKY17 act as negative regulators of basal resistance in *Arabidopsis thaliana*. Plant Cell **18:** 3289-3302.

Karimi, M., Inze, D., and Depicker, A. (2002). GATEWAY((TM)) vectors for *Agrobacterium*-mediated plant transformation. Trends Plant Sci **7:** 193-195.

Karlovsky, P. (1999). Biological detoxification of fungal toxins and its use in plant breeding, feed and food production. Nat Toxins **7:** 1-23.

Katagiri, F., Thilmony, R., and He, S. (2002). The *Arabidopsis thaliana–Pseudomonas syringae* interaction. In The *Arabidopsis* Book, C.R. Somerville, Meyerowitz, E. M. Rockville, M.D.: Am Soc Plant Biol ed, pp. 1–35.

Kazan, K., and Manners, J.M. (2008). Jasmonate signaling: toward an integrated view. Plant Physiol **146:** 1459-1468.

Kloek, A.P., Verbsky, M.L., Sharma, S.B., Schoelz, J.E., Vogel, J., Klessig, D.F., and Kunkel, B.N. (2001). Resistance to *Pseudomonas syringae* conferred by an *Arabidopsis thaliana* coronatine-insensitive (coi1) mutation occurs through two distinct mechanisms. Plant J **26:** 509-522.

Knill, T., Schuster, J., Reichelt, M., Gershenzon, J., and Binder, S. (2008). *Arabidopsis* branched-chain aminotransferase 3 functions in both amino acid and glucosinolate biosynthesis. Plant Physiol **146:** 1028-1039.

Koo, A.J., Gao, X., Jones, A.D., and Howe, G.A. (2009). A rapid wound signal activates the systemic synthesis of bioactive jasmonates in *Arabidopsis*. Plant J **59:** 974-986.

Koornneef, A., and Pieterse, C.M. (2008). Cross talk in defense signaling. Plant Physiol **146:** 839-844.

Kristensen, C., Morant, M., Olsen, C.E., Ekstrom, C.T., Galbraith, D.W., Moller, B.L., and Bak, S. (2005). Metabolic engineering of dhurrin in transgenic *Arabidopsis* plants with marginal inadvertent effects on the metabolome and transcriptome. Proc Natl Acad Sci USA **102:** 1779-1784.

Kus, J.V., Zaton, K., Sarkar, R., and Cameron, R.K. (2002). Age-related resistance in *Arabidopsis* is a developmentally regulated defense response to *Pseudomonas syringae*. Plant Cell **14:** 479-490.

Lagarde, D., Basset, M., Lepetit, M., Conejero, G., Gaymard, F., Astruc, S., and Grignon, C. (1996). Tissue-specific expression of *Arabidopsis AKT1* gene is consistent with a role in K+ nutrition. Plant J **9:** 195-203.

Lairson, L.L., Henrissat, B., Davies, G.J., and Withers, S.G. (2008). Glycosyltransferases: structures, functions, and mechanisms. Annu Rev Biochem **77:** 521-555.

Langlois-Meurinne, M., Gachon, C.M.M., and Saindrenan, P. (2005). Pathogen-responsive expression of glycosyltransferase genes *UGT73B3* and *UGT73B5* is necessary for resistance to *Pseudomonas syringae* pv tomato in *Arabidopsis*. Plant Physiol **139:** 1890-1901.

Lao, S.H., Loutre, C., Brazier, M., Coleman, J.O., Cole, D.J., Edwards, R., and Theodoulou, F.L. (2003). 3,4-Dichloroaniline is detoxified and exported via different pathways in *Arabidopsis* and soybean. Phytochemistry **63:** 653-661.

Larkindale, J., Hall, J.D., Knight, M.R., and Vierling, E. (2005). Heat stress phenotypes of *Arabidopsis* mutants implicate multiple signaling pathways in the acquisition of thermotolerance. Plant Physiol **138:** 882-897.

Li, J., Brader, G., and Palva, E.T. (2004). The WRKY70 transcription factor: a node of convergence for jasmonate-mediated and salicylate-mediated signals in plant defense. Plant Cell **16:** 319-331.

Li, L., Modolo, L.V., Escamilla-Trevino, L.L., Achnine, L., Dixon, R.A., and Wang, X. (2007). Crystal structure of Medicago truncatula UGT85H2--insights into the structural basis of a multifunctional (iso)flavonoid glycosyltransferase. J Mol Biol **370:** 951-963.

Li, X., Zhang, Y., Clarke, J.D., Li, Y., and Dong, X. (1999). Identification and cloning of a negative regulator of systemic acquired resistance, SNI1, through a screen for suppressors of *npr1-1*. Cell **98:** 329-339.

Li, Y., Baldauf, S., Lim, E.K., and Bowles, D.J. (2001). Phylogenetic analysis of the UDP-glycosyltransferase multigene family of *Arabidopsis thaliana*. J Biol Chem **276:** 4338-4343.

Lim, E.K., and Bowles, D.J. (2004). A class of plant glycosyltransferases involved in cellular homeostasis. EMBO J **23:** 2915-2922.

Lim, E.K., Ashford, D.A., Hou, B.K., Jackson, R.G., and Bowles, D.J. (2004). *Arabidopsis* glycosyltransferases as biocatalysts in fermentation for regioselective synthesis of diverse quercetin glucosides. Biotechnol Bioeng **87:** 623-631.

Lim, E.K., Doucet, C.J., Hou, B., Jackson, R.G., Abrams, S.R., and Bowles, D.J. (2005). Resolution of (+)-abscisic acid using an *Arabidopsis* glycosyltransferase. Tetrahedron-Asym **16:** 143-147.

Lim, E.K., Doucet, C.J., Li, Y., Elias, L., Worrall, D., Spencer, S.P., Ross, J., and Bowles, D.J. (2002). The activity of *Arabidopsis* glycosyltransferases toward salicylic acid, 4-hydroxybenzoic acid, and other benzoates. J Biol Chem **277:** 586-592.

Lim, E.K., Baldauf, S., Li, Y., Elias, L., Worrall, D., Spencer, S.P., Jackson, R.G., Taguchi, G., Ross, J., and Bowles, D.J. (2003). Evolution of substrate recognition across a multigene family of glycosyltransferases in *Arabidopsis*. Glycobiology **13:** 139-145.

Lim, P.O., Kim, H.J., and Nam, H.G. (2007). Leaf senescence. Annu Rev Plant Biol **58:** 115-136.

Linster, C.L., and Clarke, S.G. (2008). L-Ascorbate biosynthesis in higher plants: the role of VTC2. Trends Plant Sci **13:** 567-573.

Lorrain, S., Vailleau, F., Balaque, C., and Roby, D. (2003). Lesion mimic mutants: keys for deciphering cell death and defense pathways in plants? Trends Plant Sci **8:** 263-271.

Loutre, C., Dixon, D.P., Brazier, M., Slater, M., Cole, D.J., and Edwards, R. (2003). Isolation of a glucosyltransferase from *Arabidopsis thaliana* active in the metabolism of the persistent pollutant 3,4-dichloroaniline. Plant J **34:** 485-493.

Lukowitz, W., Nickle, T.C., Meinke, D.W., Last, R.L., Conklin, P.L., and Somerville, C.R. (2001). *Arabidopsis cyt1* mutants are deficient in a mannose-1-phosphate guanylyltransferase and point to a requirement of N-linked glycosylation for cellulose biosynthesis. Proc Natl Acad Sci USA **98:** 2262-2267.

Mackenzie, P.I., Owens, I.S., Burchell, B., Bock, K.W., Bairoch, A., Belanger, A., Fournel-Gigleux, S., Green, M., Hum, D.W., Iyanagi, T., Lancet, D., Louisot, P., Magdalou, J., Chowdhury, J.R., Ritter, J.K., Schachter, H., Tephly, T.R., Tipton, K.F., and Nebert, D.W. (1997). The UDP glycosyltransferase gene superfamily: recommended nomenclature update based on evolutionary divergence. Pharmacogenetics **7:** 255-269.

Mamer, O.A., and Reimer, M.L. (1992). On the mechanisms of the formation of L-alloisoleucine and the 2-hydroxy-3-methylvaleric acid stereoisomers from L-isoleucine in maple syrup urine disease patients and in normal humans. J Biol Chem **267:** 22141-22147.

Mandai, T., Yoneyama, M., Sakai, S., Muto, N., and Yamamoto, I. (1992). The crystal structure and physicochemical properties of L-ascorbic acid 2-glucoside. Carbohydr Res **232:** 197-205.

Martin, R.C., Mok, M.C., and Mok, D.W. (1999a). A gene encoding the cytokinin enzyme zeatin O-xylosyltransferase of *Phaseolus vulgaris*. Plant Physiol **120:** 553-558.

Martin, R.C., Mok, M.C., and Mok, D.W. (1999b). Isolation of a cytokinin gene, *ZOG1*, encoding zeatin O-glucosyltransferase from *Phaseolus lunatus*. Proc Natl Acad Sci USA **96:** 284-289.

Martin, R.C., Mok, M.C., Habben, J.E., and Mok, D.W. (2001). A maize cytokinin gene encoding an O-glucosyltransferase specific to cis-zeatin. Proc Natl Acad Sci USA **98:** 5922-5926.

Masada, S., Terasaka, K., Oguchi, Y., Okazaki, S., Mizushima, T., and Mizukami, H. (2009). Functional and Structural Characterization of a Flavonoid Glucoside 1,6-Glucosyltransferase from *Catharanthus roseus*. Plant Cell Physiol **50:** 1401-1415.

Matsuda, F., Yonekura-Sakakibara, K., Niida, R., Kuromori, T., Shinozaki, K., and Saito, K. (2009). MS/MS spectral tag-based annotation of non-targeted profile of plant secondary metabolites. Plant J **57:** 555-577.

Mazel, A., and Levine, A. (2002). Induction of glucosyltransferase transcription and activity during superoxide-dependent cell death in *Arabidopsis* plants. Plant Physiol Biochem **40:** 133-140.

Meissner, D., Albert, A., Bottcher, C., Strack, D., and Milkowski, C. (2008). The role of UDP-glucose : hydroxycinnamate glucosyltransferases in phenylpropanoid metabolism and the response to UV-B radiation in *Arabidopsis thaliana*. Planta **228:** 663-674.

Messner, B., Thulke, O., and Schäffner, A.R. (2003). *Arabidopsis* glucosyltransferases with activities toward both endogenous and xenobiotic substrates. Planta **217:** 138-146.

Miller, K.D., Guyon, V., Evans, J.N., Shuttleworth, W.A., and Taylor, L.P. (1999). Purification, cloning, and heterologous expression of a catalytically efficient flavonol 3-O-galactosyltransferase expressed in the male gametophyte of *Petunia hybrida*. J Biol Chem **274:** 34011-34019.

Mo, Y., Nagel, C., and Taylor, L.P. (1992). Biochemical complementation of chalcone synthase mutants defines a role for flavonols in functional pollen. Proc Natl Acad Sci USA **89:** 7213-7217.

124

Modolo, L.V., Blount, J.W., Achnine, L., Naoumkina, M.A., Wang, X.Q., and Dixon, R.A. (2007). A functional genomics approach to (iso)flavonoid glycosylation in the model legume *Medicago truncatula*. Plant Mol Biol **64:** 499-518.

Moehs, C.P., Allen, P.V., Friedman, M., and Belknap, W.R. (1997). Cloning and expression of solanidine UDP-glucose glucosyltransferase from potato. Plant J **11:** 227-236.

Mok, D.W.S., and Mok, M.C. (2001). Cytokinin metabolism and action. Annual Review of Plant Physiol Plant Mol Biol **52:** 89-118.

Mok, D.W.S., Martin, R.C., Shan, X., and Mok, M.C. (2000). Genes encoding zeatin O-glycosyltransferases. Plant Growth Regul **32:** 285-287.

Mol, J., Grotewold, E., and Koes, R. (1998). How genes paint flowers and seeds. Trends Plant Sci **3:** 212-217.

Moraga, A., Nohales, P., Perez, J., and Gomez-Gomez, L. (2004). Glucosylation of the saffron apocarotenoid crocetin by a glucosyltransferase isolated from *Crocus sativus* stigmas. Planta **219:** 955-966.

Morris, K., Mackerness, S.A.H., Page, T., John, C.F., Murphy, A.M., Carr, J.P., and Buchanan-Wollaston, V. (2000). Salicylic acid has a role in regulating gene expression during leaf senescence. Plant J **23:** 677-685.

Müller-Moulé, P. (2008). An expression analysis of the ascorbate biosynthesis enzyme VTC2. Plant Mol Biol **68:** 31-41.

Nakamura, S., and Oku, T. (2009). Bioavailability of 2-O-alpha-D-glucopyranosyl-L-ascorbic acid as ascorbic acid in healthy humans. Nutrition **25:** 686-691.

Nambara, E., and Marion-Poll, A. (2005). Abscisic acid biosynthesis and catabolism. Ann Rev Plant Biol **56:** 165-185.

Nielsen, K.A., Tattersall, D.B., Jones, P.R., and Moller, B.L. (2008). Metabolon formation in dhurrin biosynthesis. Phytochemistry **69:** 88-98.

Noctor, G. (2006). Metabolic signalling in defence and stress: the central roles of soluble redox couples. Plant Cell Environ **29:** 409-425.

Obayashi, T., Hayashi, S., Saeki, M., Ohta, H., and Kinoshita, K. (2009). ATTED-II provides coexpressed gene networks for *Arabidopsis*. Nucleic Acids Res **37:** D987-991.

Oh, S.A., Lee, S.Y., Chung, I.K., Lee, C.H., and Nam, H.G. (1996). A senescence-associated gene of *Arabidopsis thaliana* is distinctively regulated during natural and artificially induced leaf senescence. Plant Mol Biol **30:** 739-754.

Ohta, D., Kanaya, S., and Suzuki, H. (2010). Application of Fourier-transform ion cyclotron resonance mass spectrometry to metabolic profiling and metabolite identification. Curr Opin Biotechnol **21:** 35-44.

Olmos, E., Kiddle, G., Pellny, T.K., Kumar, S., and Foyer, C.H. (2006). Modulation of plant morphology, root architecture, and cell structure by low vitamin C in *Arabidopsis thaliana*. J Exp Bot **57:** 1645-1655.

Osbourn, A.E. (2003). Saponins in cereals. Phytochemistry **62:** 1-4.

Osmani, S.A., Bak, S., Imberty, A., Olsen, C.E., and Moller, B.L. (2008). Catalytic key amino acids and UDP-sugar donor specificity of a plant glucuronosyltransferase, UGT94B1: molecular modeling substantiated by site-specific mutagenesis and biochemical analyses. Plant Physiol **148:** 1295-1308.

Ossowski, S., Schwab, R., and Weigel, D. (2008). Gene silencing in plants using artificial microRNAs and other small RNAs. Plant J **53:** 674-690.

Paquette, S., Moller, B.L., and Bak, S. (2003). On the origin of family 1 plant glycosyltransferases. Phytochemistry **62:** 399-413.

Park, J.E., Park, J.Y., Kim, Y.S., Staswick, P.E., Jeon, J., Yun, J., Kim, S.Y., Kim, J., Lee, Y.H., and Park, C.M. (2007). GH3-mediated auxin homeostasis links growth regulation with stress adaptation response in *Arabidopsis*. J Biol Chem **282:** 10036-10046.

Pavet, V., Olmos, E., Kiddle, G., Mowla, S., Kumar, S., Antoniw, J., Alvarez, M.E., and Foyer, C.H. (2005). Ascorbic acid deficiency activates cell death and disease resistance responses in *Arabidopsis*. Plant Physiol **139:** 1291-1303.

Pedras, M.S.C., Zaharia, I.L., Gai, Y., Zhou, Y., and Ward, D.E. (2001). *In planta* sequential hydroxylation and glycosylation of a fungal phytotoxin: Avoiding cell death and overcoming the fungal invader. Proc Natl Acad Sci USA **98:** 747-752.

Peer, W.A. and Murphy, A.S. (2007). Flavonoids and auxin transport: modulators or regulators? Trends Plant Sci. **12:** 556-563.

Petersen, B.L., Chen, S., Hansen, C.H., Olsen, C.E., and Halkier, B.A. (2002). Composition and content of glucosinolates in developing *Arabidopsis thaliana*. Planta **214:** 562-571.

Petersen, M., Brodersen, P., Naested, H., Andreasson, E., Lindhart, U., Johansen, B., Nielsen, H.B., Lacy, M., Austin, M.J., Parker, J.E., Sharma, S.B., Klessig, D.F., Martienssen, R., Mattsson, O., Jensen, A.B., and Mundy, J. (2000). *Arabidopsis* map kinase 4 negatively regulates systemic acquired resistance. Cell **103:** 1111-1120.

Pflugmacher, S., and Sandermann, H. (1998). Taxonomic distribution of plant glucosyltransferases acting on xenobiotics. Phytochemistry **49:** 507-511.

Pieterse, C.M., Leon-Reyes, A., Van der Ent, S., and Van Wees, S.C. (2009). Networking by small-molecule hormones in plant immunity. Nat Chem Biol **5:** 308-316.

Pignocchi, C., and Foyer, C.H. (2003). Apoplastic ascorbate metabolism and its role in the regulation of cell signalling. Curr Opin Plant Biol **6:** 379-389.

Pinheiro, J., Bates, D., DebRoy, S., Sarkar, D., and team., t.R.C. (2009). nlme: Linear and Nonlinear Mixed Effects Models. R package version 3.1-94.

Pitzschke, A., Djamei, A., Bitton, F., and Hirt, H. (2009). A major role of the MEKK1-MKK1/2-MPK4 pathway in ROS signalling. Mol Plant **2:** 120-137.

Podebrad, F., Heil, M., Leib, S., Geier, B., Beck, T., Mosandl, A., Sewell, A.C., and Bohles, H. (1997). Analytical approach in diagnosis of inherited metabolic diseases: Maple syrup urine disease (MSUD) - Simultaneous analysis of metabolites in urine by enantioselective multidimensional capillary gas chromatography mass spectrometry (enantio-MDGC-MS). Hrc-J High Res Chrom **20:** 355-362.

Poppenberger, B., Berthiller, F., Lucyshyn, D., Sieberer, T., Schuhmacher, R., Krska, R., Kuchler, K., Glossl, J., Luschnig, C., and Adam, G. (2003). Detoxification of the *Fusarium* mycotoxin deoxynivalenol by a UDP-glucosyltransferase from *Arabidopsis thaliana*. J Biol Chem **278:** 47905-47914.

Poppenberger, B., Fujioka, S., Soeno, K., George, G.L., Vaistij, F.E., Hiranuma, S., Seto, H., Takatsuto, S., Adam, G., Yoshida, S., and Bowles, D. (2005). The UGT73C5 of *Arabidopsis thaliana* glucosylates brassinosteroids. Proc Natl Acad Sci USA **102:** 15253-15258.

Poulton, J.E. (1988). Localization and catabolism of cyanogenic glycosides. Ciba Found Symp **140:** 67-91.

Priest, D.M., Jackson, R.G., Ashford, D.A., Abrams, S.R., and Bowles, D.J. (2005). The use of abscisic acid analogues to analyse the substrate selectivity of UGT71B6, a UDP-glycosyltransferase of *Arabidopsis thaliana*. FEBS Lett **579:** 4454-4458.

Prince, R.C., and Gunson, D.E. (1994). Just plain vanilla? Trends Biochem Sci **19:** 521.

Quirino, B.F., Normanly, J., and Amasino, R.M. (1999). Diverse range of gene activity during *Arabidopsis thaliana* leaf senescence includes pathogen-independent induction of defense-related genes. Plant Mol Biol **40:** 267-278.

R-Development-Core-Team. (2009). R: A Language and Environment for Statistical Computing. R Foundation for Statistical Computing, Vienna, Austria. http://www.R-project.org.

Rao, T.S., Kale, N.R., and Dalvi, S.P. (1987). Kinetics and mechanism of the oxidation of L-ascorbic acid by 2,6-dichlorophenol-indophenol in aqueous solution. React Kinet Catal Lett **34:** 179-184.

Ren, C.M., Zhu, Q., Gao, B.D., Ke, S.Y., Yu, W.C., Xie, D.X., and Peng, W. (2008). Transcription factor WRKY70 displays important but no indispensable roles in jasmonate and salicylic acid signaling. J Integr Plant Biol **50:** 630-637.

Rieu, I., and Powers, S.J. (2009). Real-Time Quantitative RT-PCR: Design, Calculations, and Statistics. Plant Cell **21:** 1031-1033.

Ross, J., Li, Y., Lim, E., and Bowles, D.J. (2001). Higher plant glycosyltransferases. Genome Biol **2:** REVIEWS3004.

Rusterucci, C., Aviv, D.H., Holt, B.F., Dangl, J.L., and Parker, J.E. (2001). The disease resistance signaling components EDS1 and PAD4 are essential regulators of the cell death pathway controlled by LSD1 in *Arabidopsis*. Plant Cell **13:** 2211-2224.

Saito, K., Hirai, M.Y., and Yonekura-Sakakibara, K. (2008). Decoding genes with coexpression networks and metabolomics - 'majority report by precogs'. Trends Plant Sci **13:** 36-43.

Sasaki, Y., Asamizu, E., Shibata, D., Nakamura, Y., Kaneko, T., Awai, K., Amagai, M., Kuwata, C., Tsugane, T., Masuda, T., Shimada, H., Takamiya, K., Ohta, H., and Tabata, S. (2001). Monitoring of methyl jasmonate-responsive genes in *Arabidopsis* by cDNA macroarray: self-activation of jasmonic acid biosynthesis and crosstalk with other phytohormone signaling pathways. DNA Res **8:** 153-161.

Sawada, S., Suzuki, H., Ichimaida, F., Yamaguchi, M., Iwashita, T., Fukui, Y., Hemmi, H., Nishino, T., and Nakayama, T. (2005). UDP-glucuronic acid : anthocyanin glucuronosyltransferase from red daisy (*Bellis perennis*) flowers - Enzymology and phylogenetics of a novel glucuronosyltransferase involved in flower pigment biosynthesis. J Biol Chem **280:** 899-906.

Scholl, R.L., May, S.T., and Ware, D.H. (2000). Seed and molecular resources for *Arabidopsis*. Plant Physiol **124:** 1477-1480.

Schwab, R., Ossowski, S., Riester, M., Warthmann, N., and Weigel, D. (2006). Highly specific gene silencing by artificial microRNAs in *Arabidopsis*. Plant Cell **18:** 1121-1133.

Seveno, M., Seveno-Carpentier, E., Voxeur, A., Menu-Bouaouiche, L., Rihouey, C., Delmas, F., Chevalier, C., Driouich, A., and Lerouge, P. (2010). Characterization of a putative 3-deoxy-d-manno-2-octulosonic acid (Kdo) transferase gene from *Arabidopsis thaliana*. Glycobiology **20:** 617-628.

Shah, J., Kachroo, P., and Klessig, D.F. (1999). The *Arabidopsis ssi1* mutation restores pathogenesis-related gene expression in *npr1* plants and renders defensin gene expression salicylic acid dependent. Plant Cell **11:** 191-206.

Shao, H., He, X.Z., Achnine, L., Blount, J.W., Dixon, R.A., and Wang, X.Q. (2005). Crystal structures of a multifunctional triterpene/flavonoid glycosyltransferase from *Medicago truncatula*. Plant Cell **17:** 3141-3154.

Silva, H., Yoshioka, K., Dooner, H.K., and Klessig, D.F. (1999). Characterization of a new *Arabidopsis* mutant exhibiting enhanced disease resistance. Mol Plant Microbe Interact **12:** 1053-1063.

Sinnot, M.L. (1990). **Catalytic Mechanisms of Enzymic Glycosyl Transfer**. Chem Rev **90:** 1171-1202.

Smirnoff, N., Conklin, P.L., and Loewus, F.A. (2001). BIOSYNTHESIS OF ASCORBIC ACID IN PLANTS: A Renaissance. Ann Rev Plant Physiol Plant Mol Biol **52:** 437-467.

Song, J.T. (2005). Biochemical characterization of an *Arabidopsis* glucosyltransferase with high activity toward jasmonic acid. J Plant Biol **48:** 422-428.

Song, J.T., Lu, H., and Greenberg, J.T. (2004). Divergent roles in *Arabidopsis thaliana* development and defense of two homologous genes, *aberrant growth and death2* and *AGD2-LIKE DEFENSE RESPONSE PROTEIN1*, encoding novel aminotransferases. Plant Cell **16:** 353-366.

Song, J.T., Koo, Y.J., Seo, H.S., Kim, M.C., Choi, Y.D., and Kim, J.H. (2008). Overexpression of AtSGT1, an *Arabidopsis* salicylic acid glucosyltransferase, leads to increased susceptibility to *Pseudomonas syringae*. Phytochemistry **69:** 1128-1134.

Spoel, S.H., Johnson, J.S., and Dong, X. (2007). Regulation of tradeoffs between plant defenses against pathogens with different lifestyles. Proc Natl Acad Sci USA **104:** 18842-18847.

Spoel, S.H., Koornneef, A., Claessens, S.M.C., Korzelius, J.P., Van Pelt, J.A., Mueller, M.J., Buchala, A.J., Metraux, J.P., Brown, R., Kazan, K., Van Loon, L.C., Dong, X.N., and Pieterse, C.M.J. (2003). NPR1 modulates cross-talk between salicylate-

and jasmonate-dependent defense pathways through a novel function in the cytosol. Plant Cell **15:** 760-770.

Sprague, S.J., Watt, M., Kirkegaard, J.A., and Howlett, B.J. (2007). Pathways of infection of *Brassica napus* roots by *Leptosphaeria maculans*. New Phytol **176:** 211-222.

Staswick, P.E., and Tiryaki, I. (2004). The oxylipin signal jasmonic acid is activated by an enzyme that conjugates it to isoleucine in *Arabidopsis*. Plant Cell **16:** 2117-2127.

Staswick, P.E., Su, W., and Howell, S.H. (1992). Methyl jasmonate inhibition of root growth and induction of a leaf protein are decreased in an *Arabidopsis thaliana* mutant. Proc Natl Acad Sci USA **89:** 6837-6840.

Szerszen, J.B., Szczyglowski, K., and Bandurski, R.S. (1994). *iaglu*, a gene from *Zea mays* involved in conjugation of growth hormone indole-3-acetic acid. Science **265:** 1699-1701.

Taguchi, G., Yazawa, T., Hayashida, N., and Okazaki, M. (2001). Molecular cloning and heterologous expression of novel glucosyltransferases from tobacco cultured cells that have broad substrate specificity and are induced by salicylic acid and auxin. Eur J Biochem **268:** 4086-4094.

Tai, A., and Gohda, E. (2007). Determination of ascorbic acid and its related compounds in foods and beverages by hydrophilic interaction liquid chromatography. J Chromatogr B Analyt Technol Biomed Life Sci **853:** 214-220.

Tattersall, D.B., Bak, S., Jones, P.R., Olsen, C.E., Nielsen, J.K., Hansen, M.L., Hoj, P.B., and Møller, B.L. (2001). Resistance to an herbivore through engineered cyanogenic glucoside synthesis. Science **293:** 1826-1828.

The-*Arabidopsis*-Genome-Initiative. (2000). Analysis of the genome sequence of the flowering plant *Arabidopsis thaliana*. Nature **408:** 796-815.

Tognetti, V.B., Van Aken, O., Morreel, K., Vandenbroucke, K., van de Cotte, B., De Clercq, I., Chiwocha, S., Fenske, R., Prinsen, E., Boerjan, W., Genty, B., Stubbs, K.A., Inze, D., and Van Breusegem, F. (2010). Perturbation of Indole-3-Butyric Acid Homeostasis by the UDP-Glucosyltransferase *UGT74E2* Modulates *Arabidopsis* Architecture and Water Stress Tolerance. Plant Cell **22:** 2660-2679

Tohge, T., Nishiyama, Y., Hirai, M.Y., Yano, M., Nakajima, J., Awazuhara, M., Inoue, E., Takahashi, H., Goodenowe, D.B., Kitayama, M., Noji, M., Yamazaki, M., and Saito, K. (2005). Functional genomics by integrated analysis of metabolome and transcriptome of *Arabidopsis* plants over-expressing an MYB transcription factor. Plant J **42:** 218-235.

Toufighi, K., Brady, S.M., Austin, R., Ly, E., and Provart, N.J. (2005). The Botany Array Resource: e-Northerns, Expression Angling, and promoter analyses. Plant J **43:** 153-163.

Toyoda-Ono, Y., Maeda, M., Nakao, M., Yoshimura, M., Sugiura-Tomimori, N., and Fukami, H. (2004). 2-O-(beta-D-glucopyranosyl)ascorbic acid, a novel ascorbic acid analogue isolated from *Lycium* fruit. J Agr Food Chem **52:** 2092-2096.

Uknes, S., Mauch-Mani, B., Moyer, M., Potter, S., Williams, S., Dincher, S., Chandler, D., Slusarenko, A., Ward, E., and Ryals, J. (1992). Acquired resistance in *Arabidopsis*. Plant Cell **4:** 645-656.

Ülker, B., Shahid Mukhtar, M., and Somssich, I.E. (2007). The WRKY70 transcription factor of *Arabidopsis* influences both the plant senescence and defense signaling pathways. Planta **226:** 125-137.

Vandesompele, J., De Preter, K., Pattyn, F., Poppe, B., Van Roy, N., De Paepe, A., and Speleman, F. (2002). Accurate normalization of real-time quantitative RT-PCR data by geometric averaging of multiple internal control genes. Genome Biol **3:** RESEARCH0034.

Vlot, A.C., Dempsey, D.A., and Klessig, D.F. (2009). Salicylic Acid, a multifaceted hormone to combat disease. Annu Rev Phytopathol **47:** 177-206.

Vogt, T., and Jones, P. (2000). Glycosyltransferases in plant natural product synthesis: characterization of a supergene family. Trends Plant Sci **5:** 380-386.

Walley, J.W., Coughlan, S., Hudson, M.E., Covington, M.F., Kaspi, R., Banu, G., Harmer, S.L., and Dehesh, K. (2007). Mechanical stress induces biotic and abiotic stress responses via a novel cis-element. PLoS Genet **3:** 1800-1812.

Wang, D., Amornsiripanitch, N., and Dong, X. (2006). A genomic approach to identify regulatory nodes in the transcriptional network of systemic acquired resistance in plants. PLoS Pathog **2:** e123.

Wang, Z., Xiao, Y., Chen, W., Tang, K., and Zhang, L. (2010). Increased vitamin C content accompanied by an enhanced recycling pathway confers oxidative stress tolerance in *Arabidopsis*. J Integr Plant Biol **52:** 400-409.

Warzecha, H., Obitz, P., and Stockigt, J. (1999). Purification, partial amino acid sequence and structure of the product of raucaffricine-O-beta-D-glucosidase from plant cell cultures of *Rauwolfia serpentina*. Phytochemistry **50:** 1099-1109.

Wasternack, C. (2007). Jasmonates: An update on biosynthesis, signal transduction and action in plant stress response, growth and development. Ann Bot **100:** 681-697.

Weaver, L.M., Gan, S., Quirino, B., and Amasino, R.M. (1998). A comparison of the expression patterns of several senescence-associated genes in response to stress and hormone treatment. Plant Mol Biol **37:** 455-469.

Weckwerth, W., Wenzel, K., and Fiehn, O. (2004). Process for the integrated extraction identification, and quantification of metabolites, proteins and RNA to reveal their co-regulation in biochemical networks. Proteomics **4:** 78-83.

Weymouth-Wilson, A.C. (1997). The role of carbohydrates in biologically active natural products. Nat Prod Rep **14:** 99-110.

Wheeler, G.L., Jones, M.A., and Smirnoff, N. (1998). The biosynthetic pathway of vitamin C in higher plants. Nature **393:** 365-369.

Wildermuth, M.C., Dewdney, J., Wu, G., and Ausubel, F.M. (2001). Isochorismate synthase is required to synthesize salicylic acid for plant defence. Nature **414:** 562-565.

Williams, C.A., and Grayer, R.J. (2004). Anthocyanins and other flavonoids. Nat Prod Rep **21:** 539-573.

Winkel-Shirley, B. (1999). Evidence for enzyme complexes in the phenylpropanoid and flavonoid pathways. Physiol Plant **107:** 142-149.

Wolucka, B.A., and Van Montagu, M. (2007). The VTC2 cycle and the de novo biosynthesis pathways for vitamin C in plants: an opinion. Phytochemistry **68:** 2602-2613.

Yamamoto, I., Muto, N., Nagata, E., Nakamura, T., and Suzuki, Y. (1990a). Formation of a stable L-ascorbic acid alpha-glucoside by mammalian alpha-glucosidase-catalyzed transglucosylation. Biochim Biophys Acta **1035:** 44-50.

Yamamoto, I., Muto, N., Murakami, K., Suga, S., and Yamaguchi, H. (1990b). L-ascorbic acid alpha-glucoside formed by regioselective transglucosylation with rat intestinal and rice seed alpha-glucosidases: its improved stability and structure determination. Chem Pharm Bull (Tokyo) **38:** 3020-3023.

Yonekura-Sakakibara, K., Tohge, T., Niida, R., and Saito, K. (2007). Identification of a flavonol 7-O-rhamnosyltransferase gene determining flavonoid pattern in *Arabidopsis* by transcriptome coexpression analysis and reverse genetics. J Biol Chem **282:** 14932-14941.

Yonekura-Sakakibara, K., Tohge, T., Matsuda, F., Nakabayashi, R., Takayama, H., Niida, R., Watanabe-Takahashi, A., Inoue, E., and Saito, K. (2008).

Comprehensive flavonol profiling and transcriptome coexpression analysis leading to decoding gene-metabolite correlations in *Arabidopsis*. Plant Cell **20:** 2160-2176.

Zablackis, E., Huang, J., Muller, B., Darvill, A.G., and Albersheim, P. (1995). Characterization of the cell-wall polysaccharides of *Arabidopsis thaliana* leaves. Plant Physiol **107:** 1129-1138.

Zeleny, R., Kolarich, D., Strasser, R., and Altmann, F. (2006). Sialic acid concentrations in plants are in the range of inadvertent contamination. Planta **224:** 222-227.

Zhang, C.S., Griffith, B.R., Fu, Q., Albermann, C., Fu, X., Lee, I.K., Li, L.J., and Thorson, J.S. (2006). Exploiting the reversibility of natural product glycosyltransferase-catalyzed reactions. Science **313:** 1291-1294.

Zhou, N., Tootle, T.L., Tsui, F., Klessig, D.F., and Glazebrook, J. (1998). *PAD4* functions upstream from salicylic acid to control defense responses in *Arabidopsis*. Plant Cell **10:** 1021-1030.

Zimmermann, P., Hennig, L., and Gruissem, W. (2005). Gene-expression analysis and network discovery using Genevestigator. Trends Plant Sci **10:** 407-409.

7. SUPPLEMENTAL MATERIAL

7.1. SUPPLEMENTAL FIGURES
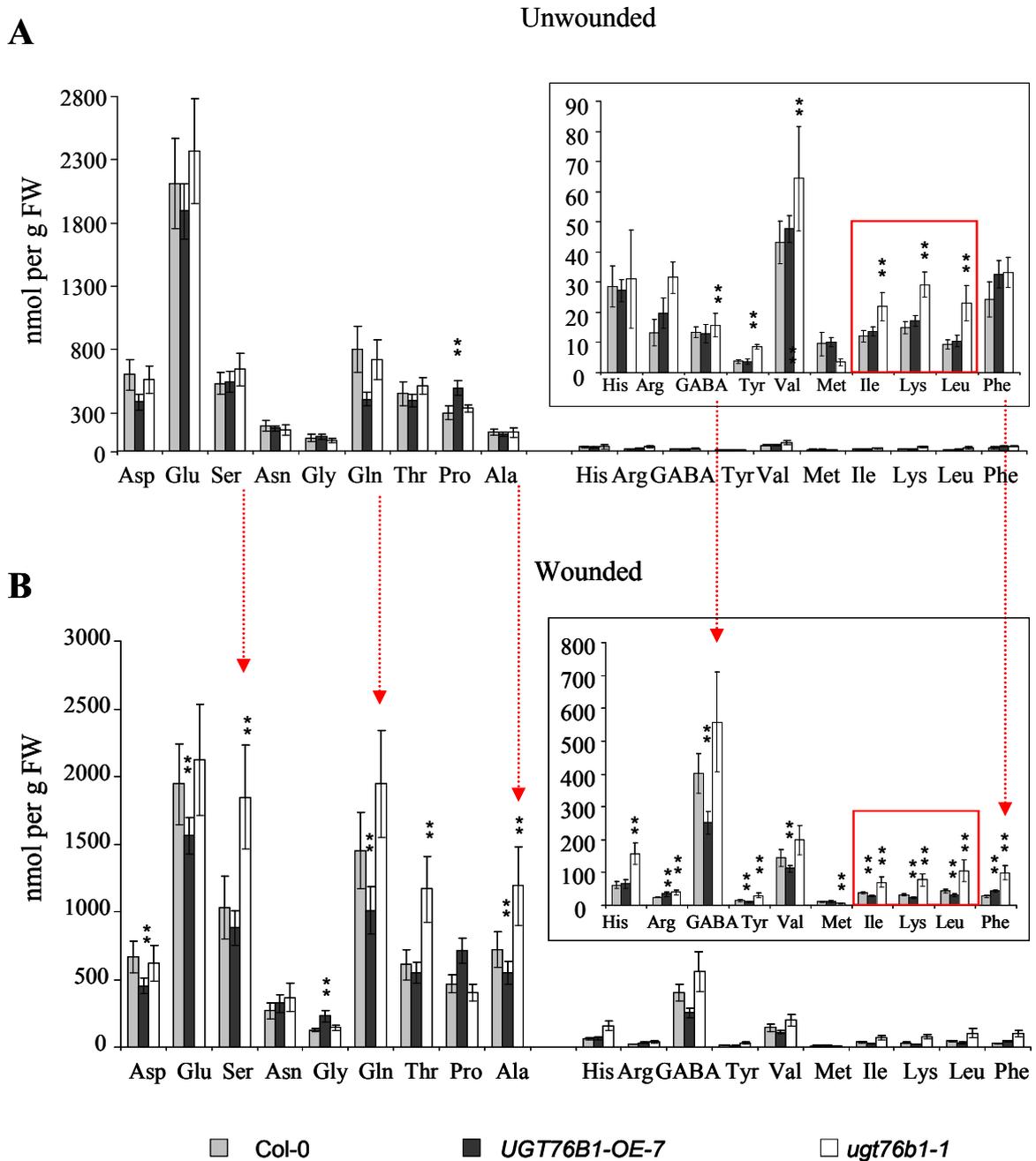
Supplemental Figure 1. Amino acid determination in *ugt76b1-1* and *UGT76B1-OE-7* compared to wild type.

Amino acid concentrations were determined in leaves of 4-week-old seedlings **(A)** before and **(B)** 1 h after mechanical wounding (see methods 3.2.1.9). Stars indicate significance of the difference to the wild-type line: ** p-value < 0.01. Measurement **(A)** was repeated and stars indicate significance detected in both independent experiments. Each measurement includes 8-10 biological replicates. The analysis has been performed by Mohamed Hajirezaei, IPK Gatersleben.

135
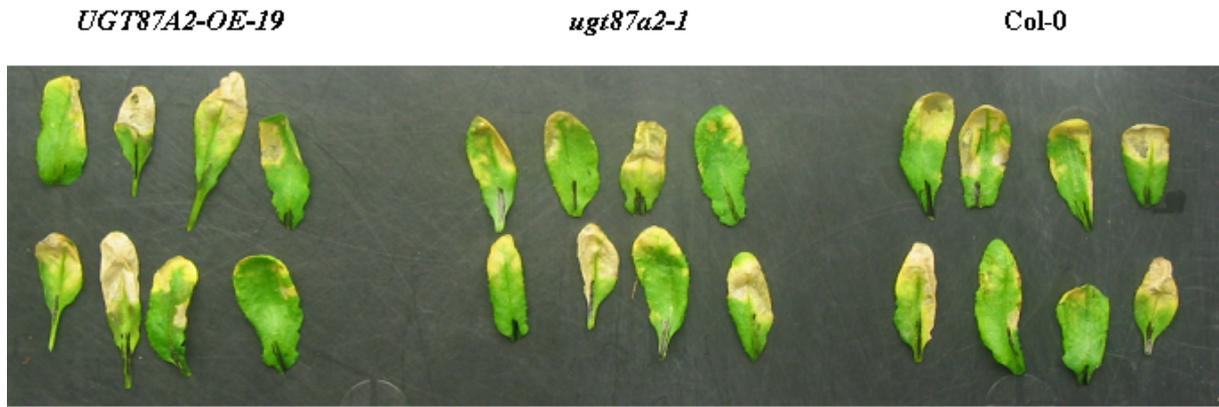
Supplemental Figure 2. Susceptibility of *UGT87A2-OE-19* and *ugt87a2-1* lines to *Ps-vir*.

5-week-old plants were inoculated with 2 10^6 cfu/ml Ps-vir. Pictures were taken 1 week after inoculation.
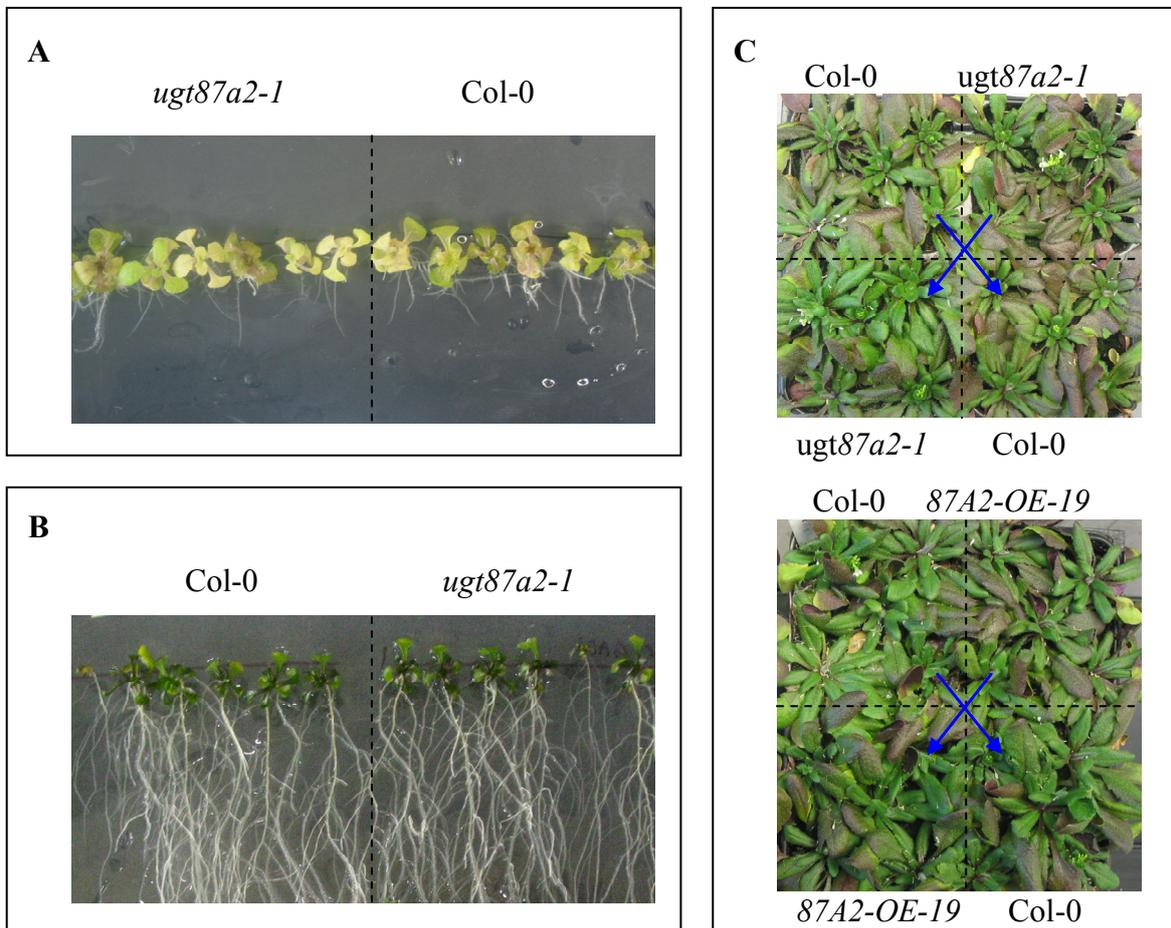
Supplemental Figure 3. Susceptibility of *UGT87A2-OE* and *ugt87a2-1* lines to abiotic stress cues.

(A) 50 mM NaCl (since germination). A slight tendency for a higher susceptibility could be observed in *ugt87a2-1*, but the results were not clearly reproducible. **(B)** 200 μM Mannitol (since germination). **(C)** UV-B irradiation (par/UV= 200 μmol m^{-2} s^{-1} / ca. 13 kJ/day, for details see 5.2.1.1).
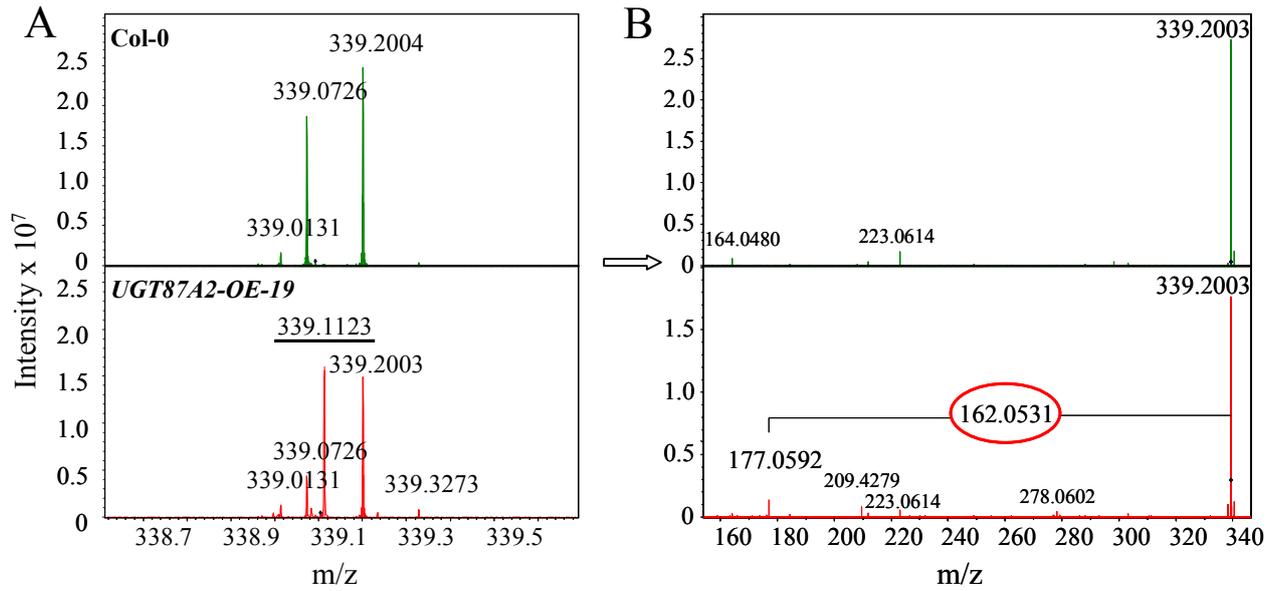
Supplemental Figure 4. Fragmentation of signal peak m/z 339 revealing a glucoside.

As it was not possible to completely isolate m/z 339.111 from other peaks with same nominal mass, a wild-type extract was fragmented in parallel to assure that m/z 177 originates from m/z 339.111, which is missing in Col-0.

(A) Isolated peaks with nominal mass 339 at 0 eV. **(B)** Fragmentation pattern of m/z 339 in Col-0 (upper) and *87A2-OE-19* (lower panel).

```
>AT2G30150.1AT2G30150.1 | Symbols:  | UDP-glucoronosyl/UDP-glucosyl transferase
             family protein | chr2:12874706-12876122 FORWARD
          Length = 440

 Score =  688 bits (1775), Expect = 0.0,   Method: Composition-based stats.
 Identities = 335/439 (76%), Positives = 373/439 (84%), Gaps = 5/439 (1%)

Query: 17   MPYPGRGHINPMMNLCKRLVRRYPNLHVTFVVTEEWLGFIGPDPKPDRIHFSTLPNLIPS 76
            MP+PGRGHINPM+NLCK LVRR PNL VTFVVTEEWLGFIG DPKP+RIHF+TLPN+IPS
Sbjct: 1    MPWPGRGHINPMLNLCKSLVRRDPNLTVTFVVTEEWLGFIGSDPKPNRIHFATLPNIIPS 60

Query: 77   ELVRAKDFIGFIDAVYTRLEEPFEKLLDSLNSPPPSVIFADTYVIWAVRVGRKRNIPVVS 136
            ELVRA DFI FIDAV TRLEEPFE+LLD LNSPP ++I ADTY+IWAVRVG KRNIPV S
Sbjct: 61   ELVRANDFIAFIDAVLTRLEEPFEQLLDRLNSPPTAII-ADTYIIWAVRVGTKRNIPVAS 119

Query: 137  LWTMSATILSFFLHSDLLISHGHALFEPSE---EEVVDYVPGLSPTKLRDLPPIFDGYSD 193
             WT SATILS F++SDLL SHGH   EPSE   +E+VDY+PGLSPT+L DL  I  GYS
Sbjct: 120  FWTTSATILSLFINSDLLASHGHFPIEPSESKLDEIVDYIPGLSPTRLSDLQ-ILHGYSH 178

Query: 194  RVFKTAKLCFDELPGARSLLFTTAYELEHKAIDAFTSKLDIPVYAIGPLIPFEELSVQND 253
            +VF   K F EL  A+ LLF +AYELE KAID FTSK D PVY+ GPLIP EELSV N+
Sbjct: 179  QVFNIFKKSFGELYKAKYLLFPSAYELEPKAIDFFTSKFDFPVYSTGPLIPLEELSVGNE 238

Query: 254  NKEPNYIQWLEEQPEGSVLYISQGSFLSVSEAQMEEIVKGLRESGVRFLWVARGGELKLK 313
            N+E +Y +WL+EQPE SVLYISQGSFLSVSEAQMEEIV G+RE+GV+F WVARGGELKLK
Sbjct: 239  NRELDYFKWLDEQPESSVLYISQGSFLSVSEAQMEEIVVGVREAGVKFFWVARGGELKLK 298

Query: 314  EALEGSLGVVVSWCDQLRVLCHKAVGGFWTHCGFNSTLEGIYSGVPMLAFPLFWDQILNA 373
            EALEGSLGVVVSWCDQLRVLCH A+GGFWTHCG+NSTLEGI SGVP+L FP+FWDQ LNA
Sbjct: 299  EALEGSLGVVVSWCDQLRVLCHAAIGGFWTHCGYNSTLEGICSGVPLLTFPVFWDQFLNA 358

Query: 374  KMIVEDWRVGMRIERTKKNELLIGREEIKEVVKRFMDRESEEGKEMRRRACDLSEISRGA 433
            KMIVE+WRVGM IER K+ ELLI  +EIKE+VKRFMD ESEEGKEMRRR CDLSEI RGA
Sbjct: 359  KMIVEEWRVGMGIERKKQMELLIVSDEIKELVKRFMDGESEEGKEMRRRTCDLSEICRGA 418

Query: 434  VAKSGSSNVNIDEFVRHIT 452
            VAK GSS+ NID F++ IT
Sbjct: 419  VAKGGSSDANIDAFIKDIT 437
```

Supplemental Figure 5. Alignment between UGT87A2 (query) and UGT87A1 proteins.

The protein alignment was performed at the TAIR website (http://www.arabidopsis.org/) using the BLASTP tool.
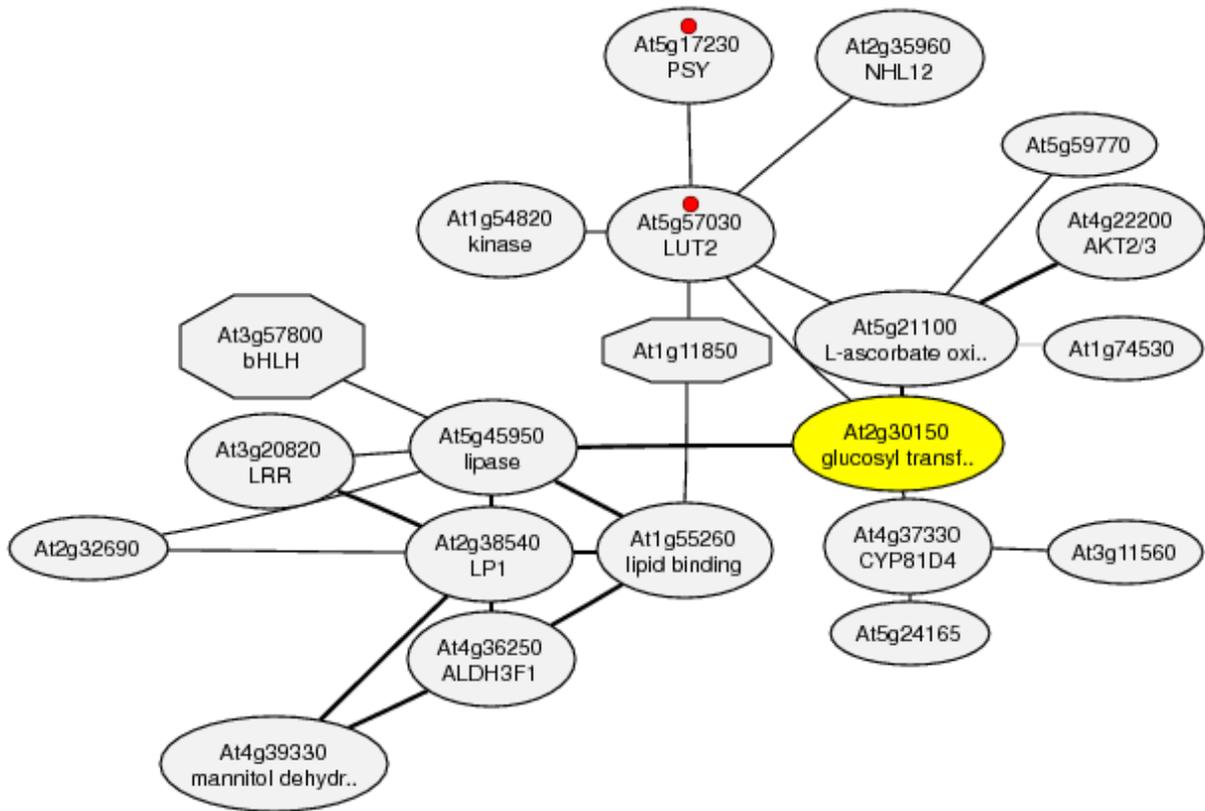
Supplemental Figure 6. Gene co-expression network for *UGT87A1* (At2g30150).

Co-expression analysis was performed using the ATTED co-expression tool (http://atted.jp/). Co-regulated gene relationships are based on co-expressed genes deduced from microarray data (tissue, light, abiotic and biotic stress treatment). Coexpressed gene networks are drawn based on rank of correlation (mutual rank). Solid edges (lines) indicate gene coexpression and the edge thickness indicates the strength of coexpression. Octagon-shaped nodes indicate transcription factor genes whereas circular nodes indicate other types of genes. Common KEGG pathways in the network are denoted by color-coded dots in the nodes (red dot: genes involved in the Carotenoid biosynthesis).
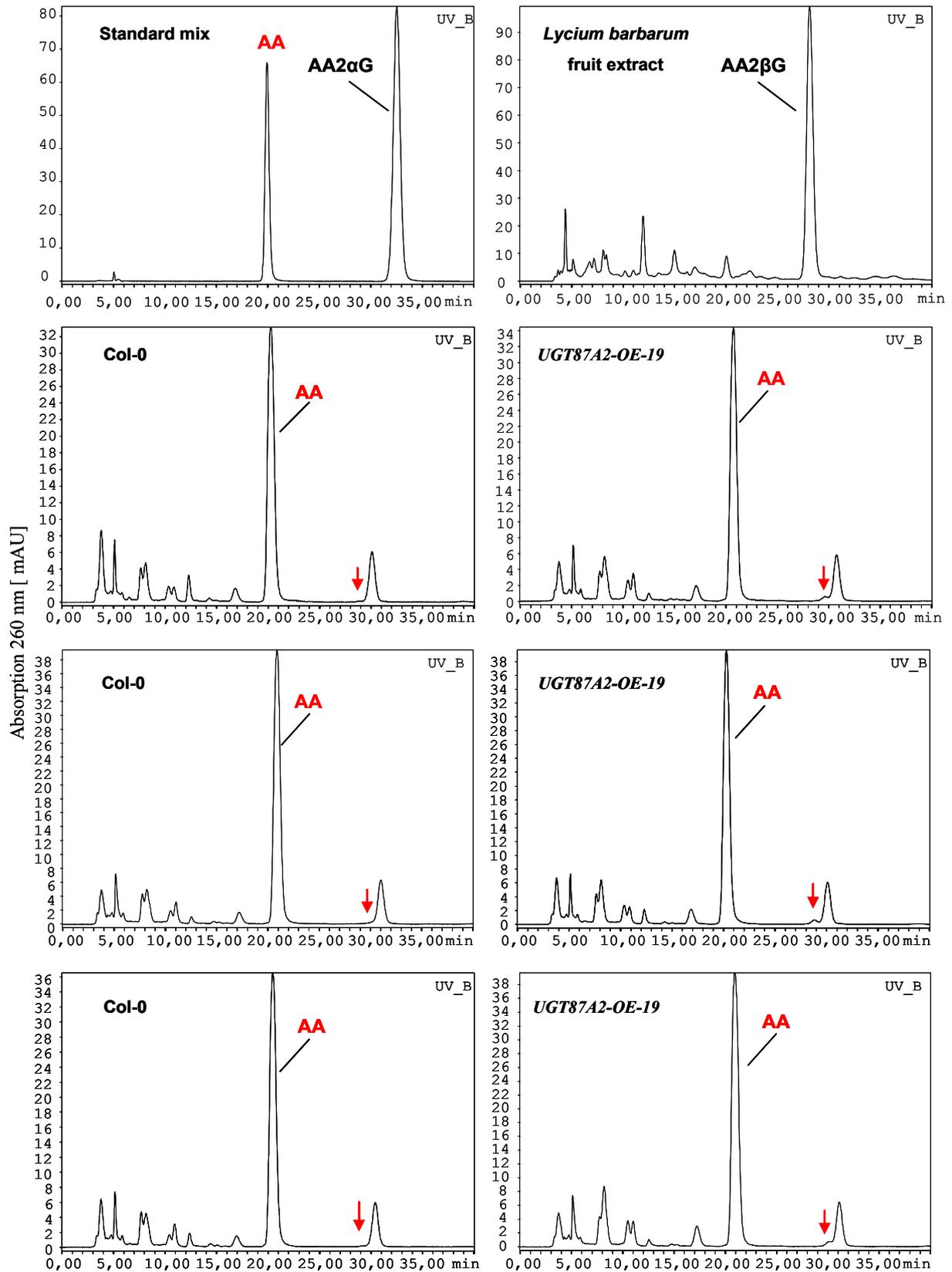
Supplemental Figure 7. Semi-quantification of ascorbic acid in *UGT87A2-OE-19* plants compared to Col-0.

No significant changes in ascorbic acid levels could be found in leaves of *UGT87A2-OE-19* compared to Col-0 (3 independent biological replicates). The red arrow indicates ascorbic acid-2-β-O-glucoside.

7.2. SUPPLEMENTAL TABLES

The following tables contain the mass lists from the non-targeted metabolome analyses. Significant metabolic changes between genotypes (p-Value ≤ 0.01) in one experiment are shaded in grey. Significant metabolic changes confirmed in two experiments are marked in red. Zero values were replaced by 200,000 counts, the value considered as detection limit (see 5.2.7.1.3). Fold changes were calculated based on the geometrical means.

Supplemental Table 1. *UGT76B1-OE* vs. Col-0							
Mass [M-H]	**T-Test p-value**	**Wilcoxon p-value**	**Median Col**	**Median UGT76B1-OE-7**	**Median UGT76B1-A-5**	**Fold UGT76B1-OE-7 vs. Col**	**Fold UGT76B1-A-5 vs. Col**
207.0874	0.0039	0.0022	2,137,078	1,354,049	1,749,048	0.68	0.72
251.0773	0.0151	0.0022	2,224,915	16,622,036	3,233,089	7.65	1.57
281.0878	0.0250	0.0022	1,527,539	6,814,391	2,082,229	5.03	1.32
293.1242	0.0002	0.0022	2,505,041	4,592,730	3,361,901	1.82	1.41
295.1035	0.0112	0.0022	1,599,354	3,876,759	2,021,751	2.65	1.32
297.1530	0.0001	0.0022	9,310,235	5,117,946	6,059,604	0.58	0.62
298.1564	0.0002	0.0022	1,634,768	860,435	905,080	0.56	0.60
311.1686	0.0000	0.0022	36,586,575	20,617,144	22,206,309	0.53	0.55
312.1720	0.0001	0.0022	6,666,521	3,624,586	4,163,797	0.54	0.58
313.1644	0.0003	0.0022	1,532,364	782,753	1,014,305	0.51	0.63
325.1843	0.0003	0.0022	37,517,272	19,788,586	22,815,373	0.52	0.54
326.1877	0.0006	0.0022	7,303,073	3,916,662	4,393,425	0.52	0.53
327.1800	0.0006	0.0022	1,573,238	861,840	855,056	0.55	0.56
339.1999	0.0003	0.0022	23,903,668	13,137,773	13,798,422	0.52	0.53
340.2033	0.0003	0.0022	4,784,186	2,631,103	2,957,518	0.52	0.52
341.1090	0.0040	0.0022	54,017,935	65,885,463	75,421,375	1.26	1.38
342.1123	0.0059	0.0022	7,151,042	8,459,972	9,992,938	1.25	1.40
343.1132	0.0020	0.0022	1,137,585	1,457,750	1,632,715	1.35	1.43
439.0857	0.0036	0.0022	24,118,582	30,438,915	29,310,920	1.32	1.35
449.1088*	0.0055	0.0022	605,658	942,410	1,453,330	2.21	2.54
577.2248	0.0151	0.0022	1,797,648	2,176,620	2,547,759	1.25	1.60
341.2066	0.0000	0.0028	475,338	200,000	200,000	0.40	0.40
327.1909	0.0001	0.0037	660,800	200,000	200,000	0.31	0.40
212.0692	0.0147	0.0043	2,948,633	3,199,604	3,398,717	1.09	1.21
327.0932	0.0297	0.0043	608,500	2,853,973	783,494	5.54	1.28
404.1279	0.0073	0.0043	1,914,790	3,024,427	4,162,284	1.47	1.93
440.0891	0.0132	0.0043	3,395,797	4,191,977	3,839,883	1.31	1.28
476.0939	0.0208	0.0043	10,175,445	7,353,656	3,383,776	0.76	0.33
476.1087	0.0193	0.0043	504,787,080	394,463,410	178,148,830	0.76	0.32
477.0933	0.0225	0.0043	3,131,851	3,507,189	4,478,494	1.20	1.43
477.1065	0.0142	0.0043	14,190,837	10,489,377	5,243,986	0.75	0.35
502.1969	0.0048	0.0043	9,794,490	11,629,523	11,593,365	1.19	1.21
431.0949	0.0117	0.0043	200,000	755,404	739,065	2.53	2.59
238.0650	0.0054	0.0048	282,326	663,126	609,456	2.35	2.10
341.1957	0.0305	0.0050	1,036,192	594,293	710,729	0.41	0.48
337.1842	0.0006	0.0062	495,914	200,000	200,000	0.40	0.51
494.0670	0.0047	0.0072	709,169	482,959	200,000	0.55	0.30
313.1755	0.0153	0.0078	553,790	405,564	200,000	0.61	0.47
168.0244	0.0184	0.0078	302,167	568,481	514,167	2.07	1.74

477.0109	0.0319	0.0078	513,286	1,103,920	1,138,665	2.69	2.76
476.1376	0.0445	0.0081	2,093,027	1,818,486	925,146	0.40	0.25
188.9080	0.0026	0.0087	5,765,344	6,206,770	6,306,183	1.06	1.08
216.9190	0.0197	0.0087	471,396	684,786	725,643	1.33	1.78
279.1086	0.0074	0.0087	860,206	1,673,344	1,143,820	2.09	1.32
293.1065	0.0091	0.0087	799,444	616,722	510,341	0.81	0.64
341.0913	0.0057	0.0087	2,388,921	3,326,931	3,091,418	1.50	1.28
476.0791	0.0376	0.0087	5,238,027	4,203,578	2,270,039	0.79	0.33
476.1307	0.0228	0.0087	2,495,492	2,008,498	813,531	0.76	0.35
477.1120	0.0197	0.0087	86,926,324	68,468,768	30,798,673	0.77	0.33
478.1044	0.0196	0.0087	67,488,092	52,863,877	23,904,959	0.77	0.33
479.1078	0.0201	0.0087	11,789,626	9,463,520	4,053,349	0.78	0.34
480.1002	0.0292	0.0087	3,284,084	2,651,511	2,225,478	0.78	0.61
481.2037	0.0115	0.0087	3,624,495	3,254,611	2,535,342	0.89	0.69
501.1936	0.0044	0.0087	50,856,386	59,904,727	62,118,300	1.18	1.24
597.3490	0.0201	0.0087	1,076,719	1,232,479	1,363,499	1.17	1.32
197.0292	0.0049	0.0096	435,090	200,000	200,000	0.51	0.51
438.0857	0.0043	0.0096	627,933	200,000	200,000	0.37	0.37
161.9153	0.0018	0.0101	401,680	200,000	200,000	0.48	0.60
162.6737	0.0050	0.0115	613,875	200,000	200,000	0.43	0.48
478.1167	0.0476	0.0124	4,634,394	3,680,195	200,000	0.76	0.04
311.0984	0.0068	0.0124	288,945	1,742,720	472,234	6.38	1.74
212.0656	0.0131	0.0152	529,381	653,464	688,773	1.31	1.56
212.0721	0.0097	0.0152	5,358,939	5,711,210	6,081,503	1.07	1.14
212.0788	0.0470	0.0152	1,815,698	2,440,394	2,581,393	1.45	1.53
262.0569	0.0307	0.0152	4,201,266	3,610,288	3,099,455	0.92	0.78
272.9571	0.0078	0.0152	463,539	626,844	588,103	1.31	1.28
341.1014	0.0097	0.0152	1,262,567	1,495,200	1,470,269	1.19	1.21
399.1660	0.0196	0.0152	1,204,928	1,910,274	1,868,144	1.79	1.36
440.0797	0.0166	0.0152	1,321,036	1,440,759	1,841,434	1.12	1.45
448.0774	0.0545	0.0152	16,478,124	15,379,200	3,244,544	0.89	0.19
451.0703	0.1294	0.0152	1,031,568	816,326	653,822	0.82	0.49
464.2217	0.0189	0.0152	723,548	863,178	874,956	1.30	1.17
467.1880	0.0143	0.0152	1,051,073	884,212	717,922	0.88	0.68
488.1621	0.0093	0.0152	3,689,619	5,284,168	6,500,822	1.38	1.49
503.1974	0.1757	0.0152	1,279,180	1,548,551	1,688,941	1.65	1.69
462.1069	0.0145	0.0167	1,516,661	200,000	200,000	0.34	0.18
389.2181	0.0118	0.0181	200,000	695,364	533,287	2.44	2.03
833.5179	0.0172	0.0181	200,000	506,292	513,357	1.86	2.05
436.0860	0.0355	0.0194	746,985	661,333	200,000	0.61	0.38
465.0922	0.0610	0.0194	2,648,359	2,322,756	200,000	0.90	0.08
466.0846	0.0285	0.0194	748,684	593,553	200,000	0.82	0.28
482.2071	0.0338	0.0194	919,861	737,587	200,000	0.58	0.32
578.2280	0.0241	0.0194	345,389	660,832	784,367	2.02	2.15
899.2931	0.0348	0.0194	344,528	535,053	525,876	1.94	1.68

Only one experiment was performed for both *UGT76B1-OE* lines vs. Col-0. m/z peaks marked in green were also found to be significantly changed in *ugt76b1* lines.

142

Supplemental Table 2. ugt76b1 knockout lines

Mean mass [M-H]	ugt76b1-2 vs. Ler					ugt76b1-1 vs. Col				
	Mass [M-H]	Median Ler	Median ugt76b1-2	Wilcoxon p-value	Fold ugt76b1-2 vs. Ler	Mass	Median Col	Median ugt76b1-1	Wilcoxon p-value	Fold ugt76b1-1 vs. Col
293.1242	293.1242	2,756,766	1,117,106	0.0022	0.38	293.1242	2,492,343	680,045	0.0022	0.28
279.1085	279.1085	627,188	200,000	0.0037	0.37	279.1086	693,926	200,000	0.0028	0.29
449.1087*	449.1087	898,697	1,292,510	0.0022	1.44	449.1087	1,451,797	1,682,888	0.0043	1.21
209.0819	209.0819	3,424,504	4,697,846	0.0022	1.28	209.0820	7,505,018	8,884,358	0.0087	1.15
380.0986	380.0985	828,994	1,131,944	0.0152	1.43	380.0987	2,649,492	3,424,056	0.0022	1.27
161.0608	161.0608	1,994,851	2,314,790	0.0649	1.13	161.0608	3,000,962	3,631,587	0.0022	1.22
164.0479	164.0479	4,943,087	5,376,176	0.0649	1.11	164.0479	7,104,986	7,967,365	0.0022	1.14
404.1198	404.1198	200,000	326,897	0.0740	1.56	404.1198	2,867,745	3,362,812	0.0022	1.28
179.0714	179.0714	52,215,122	56,795,835	0.0931	1.11	179.0714	67,540,170	79,742,918	0.0022	1.18
180.0747	180.0747	5,575,862	6,239,922	0.1320	1.12	180.0747	7,320,094	8,708,618	0.0022	1.19
423.1871	423.1871	10,095,922	12,396,682	0.1320	1.17	423.1871	12,518,470	14,381,963	0.0022	1.12
486.1381	486.1380	616,031	536,642	0.1320	0.78	486.1381	655,021	1,087,865	0.0022	1.61

* m/z 449.1087 was induced in both *UGT76B1* overexpression and knockout lines and was therefore not selected for further analyses.

143

Supplemental Table 3. *UGT87A2*-OE lines vs. Col-0

	First Experiment							Second experiment						
Mass [M-H]	Median intensity Col	Median intensity OE-6	Median intensity OE-19	P-value	Fold OE-6 vs. Col	Fold OE-19 vs. Col	Mass	Median intensity Col	Median intensity OE-6	Median intensity OE-19	Wilcoxon p-value	Fold OE-6 vs. Col	Fold OE-19 vs. Col
337.07764	1,797,029	4,571,283	9,473,414	0.0022	2.32	4.97	337.07764	5,840,167	7,732,621	21,115,854	0.0022	1.48	3.54
237.06156	338,401	2,136,286	3,926,815	0.0048	6.10	12.19	237.06160	717,627	1,547,253	3,941,925	0.0022	2.27	5.71
267.07220	491,916	1,477,587	2,951,772	0.0050	3.80	7.69	267.07219	882,538	1,690,093	5,262,776	0.0022	2.36	6.07
339.11182	200,000	1,472,446	1,890,459	0.0028	6.35	7.35	339.11193	200,000	5,445,271	10,860,319	0.0028	26.55	56.27
355.10681	200,000	2,721,508	4,964,675	0.0028	11.18	24.02	355.10686	200,000	1,613,328	2,946,891	0.0028	7.31	13.12
775.18582	794,884	1,566,104	1,587,935	0.0087	1.80	2.01	775.18573	6,370,926	12,626,933	10,725,685	0.0043	1.74	1.66
338.08105*	200,000	705,556	1,463,642	0.0028	3.23	7.10	338.08109	674,917	1,288,506	2,382,496	0.0087	1.53	3.50
422.01211	200,000	633,734	585,201	0.0096	2.26	3.08	422.01195	2,062,581	1,812,558	1,205,411	0.0260	0.84	0.61
336.19627	1,138,587	934,463	632,302	0.0022	0.77	0.56	336.19553	347,367	200,000	200,000	0.1823	0.78	0.58
803.20809	1,644,253	2,442,729	2,877,989	0.0087	1.47	1.56	803.20821	200,000	667,546	200,000	0.2530	1.99	1.46
337.95963	601,818	515,788	200,000	0.0124	0.62	0.44	337.95970	1,289,848	1,534,644	1,142,132	0.6991	1.29	0.99
378.08897	2,475,498	2,971,661	3,469,798	0.0087	1.22	1.42	378.08900	8,252,104	8,322,876	7,604,906	0.9372	0.91	0.91
395.02969	745,866	200,000	200,000	0.0115	0.42	0.39	395.02961	364,463	587,805	200,000	1.0000	1.23	0.79
270.01058	518,334	621,355	833,860	0.0152	1.24	1.44	270.01065	814,250	1,447,936	1,227,015	0.0649	1.66	1.33
629.12785	490,574	1,219,734	1,017,230	0.0194	2.78	2.88	629.12786	7,131,008	16,589,694	14,552,724	0.0152	1.94	1.79

Supplemental Table 4. *ugt87a2*-KO lines vs. Col-0

Mean mass [M-H]	First Experiment							Second experiment						
	Mass [M-H]	Median intensity Col	Median intensity ugt87a2-1	Median intensity ugt87a2-2	Wilcoxon p-value	Fold ugt87a2-1 vs. Col	Fold ugt87a2-2 vs. Col	Mass	Median intensity Col	Median intensity ugt87a2-1	Median intensity ugt87a2-2	Wilcoxon p-value	Fold ugt87a2-1 vs. Col	Fold ugt87a2-2 vs. Col
505.078	505.0784	1,339.310	787.113	998.863	0.0022	0.53	0.76	505.0784	1,284.664	601.882	998.402	0.0931	0.51	0.91
390.111	390.1117	1,398.903	795.953	1,046.278	0.0022	0.54	0.76	390.1118	1,094.008	905.259	1,246.109	0.8182	0.86	1.16
509.973	509.9737	588.961	1,039.454	1,101.205	0.0043	2.11	1.86	509.9736	1,304.518	973.569	1,077.651	0.1320	0.69	0.88
260.029	260.0290	7,183.571	5,551.018	6,338.275	0.0043	0.75	0.89	260.0291	6,955.340	6,144.557	7,195.558	0.2403	0.81	0.99
308.039	308.0390	3,599.604	1,557.705	2,743.320	0.0043	0.40	0.77	308.0390	2,357.980	1,652.444	2,349.503	0.3095	0.63	1.02
334.908	334.9084	2,757.021	1,750.176	2,306.777	0.0043	0.55	0.80	334.9083	1,851.945	1,542.902	2,057.755	0.4848	0.69	1.02
766.105	766.1063	757.709	200.000	526.386	0.0043	0.26	0.50	766.1056	433.287	200.000	533.819	0.3261	0.52	1.01
211.946	211.9466	1,604.780	200.000	1,025.643	0.0050	0.20	0.66	211.9466	1,869.440	675.685	1,825.319	0.2403	0.30	1.00
339.091	339.0914	364.460	722.632	816.709	0.0078	2.05	2.30	339.0913	499.624	547.230	717.345	0.2946	1.04	1.68
209.949	209.9491	10,771.889	3,417.640	6,753.652	0.0087	0.29	0.70	209.9491	11,879.056	5,655.354	10,705.126	0.0152	0.37	0.88
222.073	222.0732	2,963.946	1,913.378	2,219.125	0.0087	0.62	0.80	222.0732	7,311.080	4,483.395	5,955.761	0.0649	0.60	0.85
262.964	262.9644	4,728.145	3,433.816	3,612.902	0.0087	0.69	0.81	262.9644	3,970.195	2,915.384	3,628.266	0.0649	0.73	0.92
225.926	225.9266	10,815.136	3,963.398	7,620.521	0.0087	0.37	0.77	225.9266	10,716.577	7,399.601	9,338.332	0.1797	0.53	0.95
244.042	244.0426	4,793.477	2,208.192	3,722.092	0.0087	0.52	0.83	244.0426	4,026.911	2,510.231	3,477.999	0.1797	0.64	0.95
233.956	233.9568	10,434.647	7,007.791	8,773.339	0.0087	0.69	0.88	233.9569	12,565.162	10,089.230	10,918.778	0.3095	0.75	0.95
309.000	309.0001	2,290.523	1,200.143	1,731.585	0.0087	0.46	0.78	309.0001	1,945.151	1,764.502	1,691.646	0.5887	0.75	1.02
606.029	606.0296	624.685	502.445	487.715	0.0129	0.58	0.60	606.0299	593.873	200.000	711.418	0.1705	0.44	0.75
307.038	307.0382	27,367.053	13,259.068	20,470.399	0.0152	0.45	0.80	307.0382	18,699.065	12,732.186	17,724.516	0.1320	0.59	1.00
210.949	210.9498	1,410.186	490.736	757.536	0.0152	0.30	0.65	210.9498	1,478.942	787.687	1,466.238	0.1797	0.36	0.99
309.035	309.0358	3,991.054	1,880.152	3,024.498	0.0152	0.45	0.80	309.0358	2,616.416	1,839.717	2,642.652	0.1797	0.58	0.99
315.072	315.0721	8,585.489	10,721.362	9,462.505	0.0152	1.27	1.12	315.0722	6,810.806	9,848.188	7,973.769	0.2403	1.37	1.07
452.141	452.1410	63,931.621	41,423.394	41,903.068	0.0152	0.65	0.76	452.1410	7,252.188	5,809.493	6,954.277	0.2403	0.60	0.91
217.979	217.9793	2,704.685	1,684.694	2,213.120	0.0152	0.62	0.84	217.9793	3,258.120	3,034.430	3,214.093	0.3095	0.84	0.98
346.993	346.9932	614.418	684.188	812.019	0.0152	1.33	1.58	346.9934	512.116	731.442	567.473	0.3751	1.71	0.98
424.037	424.0373	3,112.578	2,084.156	2,622.960	0.0152	0.66	0.83	424.0373	2,077.570	1,897.852	2,319.921	0.3939	0.84	1.00
300.003	300.0038	3,538.442	4,799.751	4,250.569	0.0152	1.43	1.17	300.0038	2,752.508	3,390.778	3,033.449	0.4848	1.23	0.97

Mass [M-H]	T-Test p-value	Wilcoxon p-value	Median Col	Median *1-6*	Median *1-9*	Fold *1-6* vs. Col	Fold *1-9* vs. Col
			Supplemental Table 5. *ugt87a2* amiR*UGT87A1* vs. Col-0				
216.0514	0.0006	0.0022	9,184,419	14,606,289	13,570,108	1.68	1.54
242.0783	0.0055	0.0022	7,291,606	10,964,897	10,323,495	1.59	1.49
304.9827	0.0019	0.0022	7,127,051	12,064,406	11,422,034	1.60	1.49
339.1086	0.0033	0.0022	72,862,896	125,218,190	86,975,717	1.68	1.22
340.1119	0.0100	0.0022	12,126,151	22,406,738	14,369,227	1.66	1.20
347.1249	0.0019	0.0022	12,163,438	23,487,905	18,255,391	1.82	1.61
384.0569	0.1780	0.0022	5,460,407	8,407,334	8,585,912	2.49	2.57
419.0919	0.0039	0.0022	44,622,887	96,331,562	76,878,484	2.01	1.63
469.2079	0.0007	0.0022	15,578,909	29,488,759	21,430,811	1.85	1.41
475.1722	0.0028	0.0022	5,968,430	12,475,272	9,273,734	1.71	1.56
300.0806	0.0103	0.0043	9,029,864	15,426,607	14,045,980	1.72	1.52
333.1456	0.0011	0.0043	6,445,065	12,515,770	12,469,358	1.94	1.91
385.1505	0.0079	0.0043	15,972,869	25,449,897	25,181,612	1.57	1.61
645.2567	0.1502	0.0043	12,208,052	23,039,101	23,072,604	3.71	3.31
646.2604	0.0121	0.0043	200,000	10,532,398	7,459,360	16.48	12.89
245.0429	0.0150	0.0087	40,293,539	55,046,890	53,099,777	1.41	1.44
263.0772	0.0033	0.0087	7,263,416	10,704,461	10,935,037	1.47	1.40
299.0771	0.0075	0.0087	63,070,658	97,196,865	101,445,640	1.60	1.54
306.1194	0.0038	0.0087	11,841,960	24,894,301	26,709,404	2.20	2.06
329.1143	0.1723	0.0087	7,163,900	11,024,393	11,008,718	2.76	2.73
375.1198	0.0193	0.0087	10,112,683	15,127,773	14,979,269	1.50	1.54
427.1974	0.0087	0.0087	15,315,015	24,556,303	24,439,599	1.64	1.78
437.0482	0.2276	0.0087	9,475,198	7,639,671	6,604,723	0.25	0.72
469.0988	0.2070	0.0087	6,171,167	10,259,008	7,292,394	2.63	2.15
686.0825	0.0089	0.0087	11,616,454	23,388,793	29,072,914	1.51	1.91
339.2020	0.0052	0.0096	200,000	4,691,846	5,013,472	12.55	32.73
223.0976	0.0081	0.0152	7,786,061	15,600,601	11,540,383	1.70	1.48
259.0224	0.0285	0.0152	31,653,146	50,557,759	43,396,627	1.50	1.39
333.0592	0.0197	0.0152	88,774,497	135,171,910	109,200,850	1.46	1.34
414.0501	0.0202	0.0152	7,366,142	12,312,983	13,073,333	1.43	1.50
420.0953	0.0075	0.0152	7,237,649	19,083,433	13,072,465	2.31	1.69
425.0835	0.0028	0.0152	6,566,180	10,550,257	9,963,986	1.41	1.50
617.2619	0.0076	0.0152	15,869,774	39,527,738	24,470,021	2.10	1.53
633.2567	0.0035	0.0161	200,000	6,544,986	5,125,128	18.28	15.34
431.1712	0.0127	0.0167	5,468,737	200,000	200,000	0.06	0.15
471.2237	0.0131	0.0167	200,000	6,838,391	5,917,093	6.62	16.71
483.1542	0.0147	0.0167	200,000	5,299,669	4,882,710	5.81	14.57
283.0548	0.0464	0.0194	2,398,493	7,037,141	7,599,885	5.99	8.01
557.1878	0.1052	0.0200	4,999,175	8,539,473	6,180,224	4.80	3.50

Only one experiment was performed for analysis of *ugt87a2* amiR*UGT87A1* vs. Col-0.

146

CURRICULUM VITAE

Name: Veronica v. Saint Paul

Date/place of birth: 12th April 1983, Bad Harzburg

Nationality: German

EDUCATION

02/2007-today	Graduate student in Biochemistry at the Ludwig-Maximilians Universität München (Germany) Title: *Stress inducible glycosyltransferases in Arabidopsis thaliana and their impact on plant metabolism and defense mechanisms*. Advisor: PD Dr. Anton R. Schäffner, Helmholtz Zentrum München, Institute for Biochemical Plant Pathology
09/2001-07/2006	Master in Biotechnology Universidad Autónoma de Barcelona (Spain) and Technische Universität Braunschweig (Germany)
1993-2001	German School Barcelona (Spain), A-levels in life sciences

PROFESSIONAL EXPERIENCE

10/2006 - 12/2006	Research assistant at the Technische Universität Braunschweig, Germany
09/2005 - 06/2006	Master thesis Title: *PVX-vermittelte Expression der Cre-Rekombinase in der Kartoffel.* Biologische Bundesanstalt für Land- und Forstwirtschaft Braunschweig and Technische Universität Braunschweig Advisors: Prof. Dr. Joachim Schiemann and Prof Dr. Reinhard Hehl
07/2005 - 09/2005	Internship at the Department of Biology, Virginia Commonwealth University (USA) Topic: *A signaling network that regulates plant cell proliferation and differentiation.* Advisor: Dr. Wan Ling-Chiu

FELLOWSHIP

Kekulé-Fellowship of the ´Verband der Chemischen Industrie´

PUBLICATIONS

von Saint Paul V, Kanawati B, Zhang W, Geist B, Faus-Kessler T, Schmitt-Kopplin P, Schäffner AR. The *Arabidopsis* glucosyltransferase UGT76B1 conjugates isoleucic acid and suppresses plant defense and senescence. Plant Cell (In Revision)

Kanawati B, von Saint Paul V, Herrmann C, Schäffner AR, Schmitt-Kopplin P. (2011) Mass spectrometric differentiation between α and β ascorbic acid 2-glucosides. Experimental and DFT study. Rapid Communications in Mass Spectrometry, **25**: 806-814

Yin R, Meßner B, Faus-Kessler T, Hoffmann T, Schwab W, Hajirezaei MR, von Saint Paul V, Heller W, and Schäffner AR. Feedback inhibition of phenylpropanoid and flavonol-biosynthetic pathways upon a compromised flavonol-3-O-glycosylation. Journal of Experimental Botany (Submitted)

CONTRIBUTIONS TO SCIENTIFIC CONFERENCES (*Poster Presentations*)

von Saint Paul V, Kanawati B, Zhang W, Geist B, Faus-Kessler T, Schmitt-Kopplin P, Schäffner AR. Glucosyltransferase UGT76B1 impacts on plant defense and senescence in *Arabidopsis thaliana*. 7th Tri-National *Arabidopsis* Meeting, Salzburg (Austria), September 2010

von Saint Paul V, Kanawati B, Faus-Kessler T, Schmitt-Kopplin P, Schäffner AR. Towards a function of a stress inducible glycosyltransferase using non-targeted metabolome analysis. 20th International Conference on *Arabidopsis* research, Edinburgh (Scotland), July 2009

von Saint Paul V, Kanawati B, Faus-Kessler T, Schmitt-Kopplin P, Schäffner AR. Towards a function of a stress inducible glycosyltransferase. 22. Pflanzenmolekularbiologie-Tagung Dabringhausen (Germany), February 2009

von Saint Paul V, Kanawati B, Faus-Kessler T, Schmitt-Kopplin P, Schäffner AR. Towards a function of stress inducible glycosyltransferases. 5th Tri-National *Arabidopsis* Meeting, Zürich (Switzerland), September 2008

von Saint Paul V, Kanawati B, Yin R, Messner B, Faus-Kessler T, Welzl G, Schmitt-Kopplin P, Schäffner AR. Non targeted metabolome analysis of mutant *Arabidopsis* plants affected in flavonol glycosylation using FT-ICR Mass Spectrometry. 41. Jahrestagung der Deutschen Gesellschaft für Massenspektrometrie, Gießen (Germany), March 2008